ΕΘΝΙΚΟ ΜΕΤΣΟΒΙΟ ΠΟΛΥΤΕΧΝΕΙΟ
Σχολή Πολιτικών Μηχανικών
Τομέας Γεωτεχνικής

National Technical University of Athens
School of Civil Engineering
Geotechnical Department

Rotational Inertia Effect on Seismic Performance of Highway Bridges Considering Soil–Structure Interaction

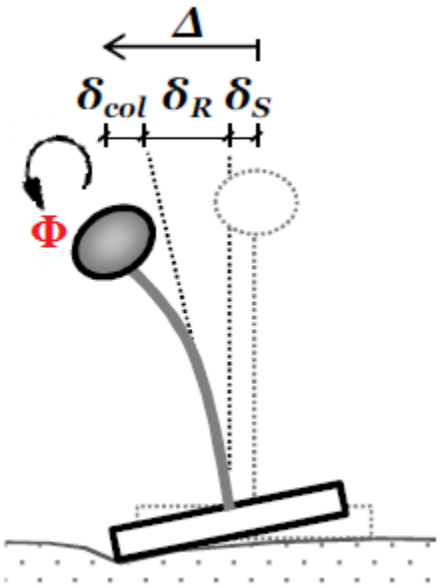

M.Sc Diploma Thesis

Yahya A. Zahran

Supervisor
Prof. G.Gazetas

Oct 2014

ΕΘΝΙΚΟ ΜΕΤΣΟΒΙΟ ΠΟΛΥΤΕΧΝΕΙΟ
Σχολή Πολιτικών Μηχανικών
Τομέας Γεωτεχνικής

National Technical University of Athens
School of Civil Engineering
Geotechnical Department

Rotational Inertia Effect on Seismic Performance of Highway Bridges Considering Soil–Structure Interaction

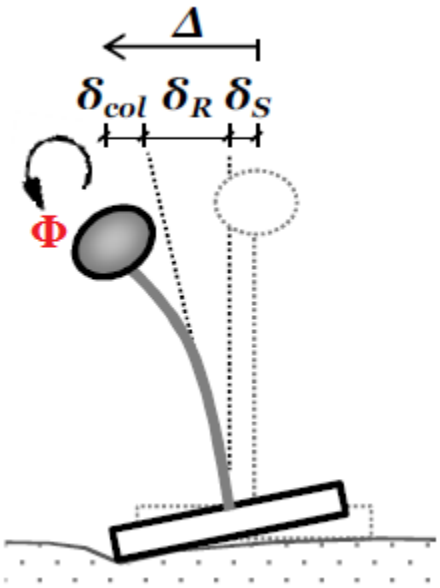

M.Sc Diploma Thesis

Yahya A. Zahran

Supervisor
Prof. G.Gazetas

Oct 2014

Acknowledgement

Upon completing this thesis diploma, I need to deeply thank the people who contributed towards achieving this goal.

Initially, I would like to thank Prof. G.Gazetas for the opportunity to work under his supervision it was most instructive and valuable to interact with him during this period.

Special thanks to M. Loli PhD. Her valuable guidance was crucial for the completion of this work.

Special thanks to Prof. M. Papadrakaikis, Dr. V. Plevris & Prof. S. Mehanny for the opportunity and support along the way.

Finally, A huge thanks for all the friends and family for their endless support.

Abstract

There has been a wide range of study, investigation and review of the seismic design suggested by the codes in recent years; one of these hot topics was the concept of "Rocking isolation design" [(1)].

The main goal of this new design approach is to investigate the possibility of allowing below ground supports systems to respond to strong seismic shaking by going beyond number of thresholds that would be conventionally imply failure and are today forbidden by design codes such as sliding at soil-foundation interface, separation and uplifting of shallow foundations, mobilization of bearing capacity failure mechanism for foundations, structural yielding of pile foundations & combination of some of the previous.

Of course some of the disadvantages are the residual angle of rotation and settlement may exceed the serviceability limits mentioned by the codes.

Here the question came in case of the seismic performance of highway bridges the new design concept proved to be safer in terms of protecting the structure from failure. But what if the superstructure in this case the deck of the bridge is huge thus it has influential rotational inertia that may affect the overall stability in that case and threatening the whole concept and takes away the advantage of preventing failure.

This study focuses mainly on the effect of the rotational inertia of the superstructure on the seismic performance of highway bridges. The effect generally was in fact ignored in most studies and experiments for simplicity in both numerical analysis and modeling. Whether this effect would diminish the advantages of the Rocking isolation design concept or it would confirm them and should it always be accounted for in analysis or modelling. This will be the scope of this study.

Table of Contents

INTRODUCTION

SCOPE OF THE THESIS

INTRODUCTION

Earthquakes damage civil engineering structures every year and bridges are no exception. Historically bridges have proven to be vulnerable to earthquakes. Sustaining damage to substructures and foundations and in some cases being totally destroyed as superstructures collapse from their supporting elements. Since typical highway bridges vibrate with frequencies in the range 0.5 to 20 Hz and typical earthquakes have the same frequency content. There is a very real possibility that the frequency matching will occur between a bridge and the ground during an earthquake. The United States, Chile & Japan have all experienced seismic damage to modern bridges in recent years. Of course the price of repairing and replace those bridges was massive.

The poor seismic behavior of bridge structures is surprising in view of the substantial advances made in design and construction for vertical loads. For more than a century bridge spans have been pushed further than before, alignment has become increasingly complex and aesthetic requirements have become more demanding. Nevertheless, these demands have been satisfied by using innovative materials and computer based analysis and design methods. However similar advances have not been made for the seismic performance of bridges.

The main reason for this paradox is that for the live load, the critical element in the bridge is the superstructure whereas for the seismic behavior, the critical elements are the substructures and foundations and their connections to the superstructure.

This focus mainly on the superstructure and little to no attention being given to the substructures and their performance to the high lateral loads fortunately has changes in the last years.

Structural engineering has long ago embraced the philosophy of "capacity design". The main idea is to design the various constituent members of a structure in such a way that the members crucial for its stability are stronger than the less critical members, for example in a column-beam connection the column would be the strong member and the weak member would be the beam.

The design criteria also imply that the plastification of members should result from exceedance of their moment capacity, not their shear capacity. Hence, the structure against the design motion flexural yielding is directed towards the weak members, the beams, dissipating energy without endangering the overall stability of the structure.

Although this design criteria is encouraged by modern seismic codes, it is conservatively limited to the superstructure. The foundation systems are treated differently. Current foundation design concept adopts overstrength factors to ensure that their ultimate capacity is larger than the calculated overturning bending moment capacity of the superstructure. The aim is insure that:

- No plastic hinges develops below the ground surface; i.e. piles, caps, footings remain structurally nearly elastic.
- No mobilization of bearing capacity failure mechanism takes place.

This approach is imposed on foundation design mainly because post-seismic inspection and repair below ground is hardly feasible unlike the above ground surface structural damage.

The levels of acceleration recorded in the last 30 years, with huge values of both peak ground acceleration (PGA) and spectral acceleration (SA) impose a very heavy load on the foundation ns. As examples of these records Kobe (1995) and Northridge (1994) had PGA values exceeding 0.8 g and maximum SA exceeding 2.0 g. Demanding a nearly elastic type of behavior of the soil-foundation system is not only an expensive demand, but also in some cases cannot be satisfied.

Although the "capacity design" criteria are generally successful the structures remain vulnerable to very strong shaking, as a number of modern structures suffered intense damage leading to partial or total collapse [e.g., 1, 2] which imposes the need to reevaluate the effectiveness of the design criteria. In response a number of studies have explored the possibility of a different design concept which allows the development of soil-foundation failure "plastic hinging" which can be either at the interface or in the soil to draw the damage away from the superstructure to avoid the overall instability of the structure.

In the case of shallow foundations for the sake of this study, Nonlinearity takes place as uplifting and/or soil yielding, a new design criteria is proposed where the foundation is intentionally under-designed under the dynamic load compared to the column to enforce rocking response and the occurrence of plastic deformation at the soil-foundation interface

These studies most important findings:

- The rocking response of the structure actually reduces the inertia load transmitted to the structure hence, the column sustains fewer load.
- Due to the nature of the seismic loading, rocking response doesn't necessarily imply overturning, when rocking is accompanied with yielding of the supporting soil and momentarily mobilization of bearing capacity failure a respectable amount of energy is dissipated which increases the safety margin against overturning.
- A number of studies recently investigated the scheme of rocking isolation with a focus on its effects on the structure, which consistently point to a beneficial role of the nonlinear behavior for the whole overall system performance.

These studies clearly illustrate the advantages and disadvantages of this new design philosophy "rocking isolation" [2-9]. This can be summarized:

- For moderate intensity earthquakes not exceeding the design limits: the performance would totally accepted the structure nearly sustains no big damage compared to what is expected from the capacity designed structure. But it would be in most cases subjected to slightly increased –but absolutely tolerable- drift and settlement.
- For large intensity earthquakes that clearly exceeds the design limits, the performance of the system according to the "rocking isolation" philosophy is quite better, while the conventionally designed structure may collapse or at least sustain severe structural damage, the new design would actually survive with the damage being in the form of increased settlement and drift.

1. Scope & objectives of the thesis

One main disadvantage is the residual structural drift, here the question rises since the new design philosophy will allow the structure (which for the sake of this study would be a bridge) to rock with respectable amount of sway, the effect then of having a structural deck wide enough in a sense that it would affect the overall stability as it may overturn the structural system or cause a bending failure at the deck-column connection.

This study will focus on the effect of the presence of the deck hence, the rotational inertia effect, since it has been always neglected in both numerical and analytical analysis for simplicity and for lack of effectiveness.

1.1 Main Structure of the thesis

This dissertation consists of six chapters. Apart from the first one which is the introduction to the scope and clarifying the objectives of this research.

Chapter 2 is an analytical examination of the problem and the effect of the rotational inertia on the dynamic properties of a SDOF bridge including soil-structure-interaction.

Chapter 3 examines the first bridge model taken from a recent study [11], while comparing the dynamic response of a full detailed model versus a lumped-mass model. While chapter 4 will deal with the same prototype, it compares the dynamic response while changing the deck geometry to double the rotational inertia.

Chapter 5,6 will examine a case study of two highway bridge prototype of Eleusis-Ymittos Ring road, also comparing the dynamic response in both full and lumped-mass models

Finally, Chapter 7 summarizes the main conclusions of this study

Introduction

Figures

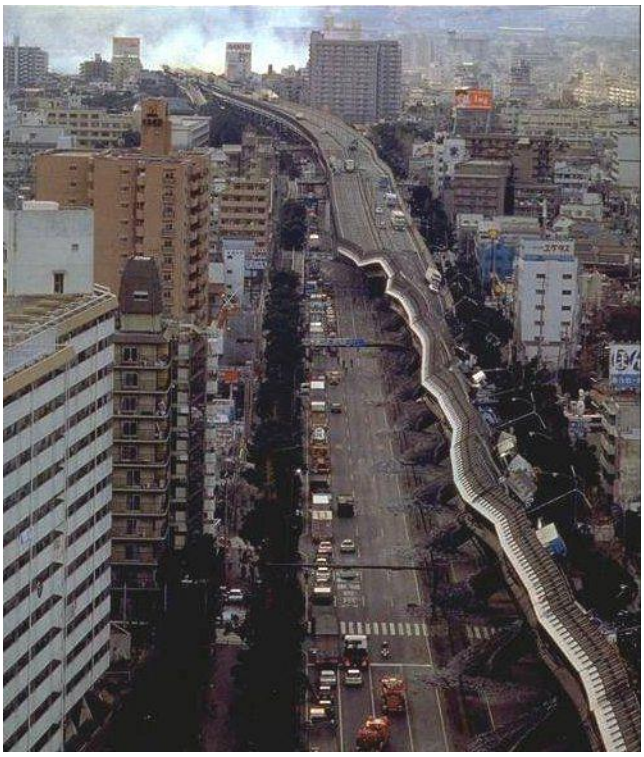

Fig (1, 2) – Kobe EQ (1995).

Chapter 2

Analytical Examination of the Rotational inertia effect.

2.1 Introduction

The effects of soil-structure interaction on the response of structures had not been seriously taken into account until the 1971 san Fernando earthquake and the beginning of the nuclear plant construction in California, since then a substantial amount of research focused on the soil-structure interaction (SSI) effects especially in the cases of strong motions where the soil-foundation interface moves or distorts differently from the corresponding soil surface of the freefield.

The limited number of bridge studies considering SSI can be primarily attributed to the complexity of the physical problem. Further, recent experimental and analytical studies have identified the significant role that SSI can play during the seismic excitation of bridges and have demonstrated the need to incorporate SSI in the design of bridge structures, as it has been found that SSI greatly affects the dynamic behavior of bridge piers leading to more flexible systems increased damping and larger total displacement.

2.2 Bridge-soil system and method of analysis

Consider the bridge-soil system shown in *Figure 1* that has a deck considerably stiffer than the piers and is excited by a seismic ground motion along the transverse direction. The bridge spans are equal and the piers are assumed identical in size and material properties. Further, the mass of the piers is considerably smaller than the mass of the bridge deck.

Under the previous assumptions, the transverse dynamic response of the bridge can be simulated with the aid of the four-degree-of-freedom model shown in *Figure 2*. The four degrees of freedom include the total lateral displacement of the bridge deck, U_t, the horizontal displacement of the foundation relative to the free-field motion, U_o, the rotation of the system at the foundation level, θ, and the rotation of the deck relative to the pier, Φ.

In the bridge model, the piers and the foundations are assumed to be massless. In order to simplify the analysis, all piers are identical in size and stiffness. Consequently the tributary mass for each pier is supposedly the whole deck mass divided by the number of piers.

The height and flexural stiffness of the pier are denoted as *h* and *k*, respectively. The overall damping in the pier is hysteretic and is characterized by a damping ratio, ζ. The soil supporting the pier through a massless foundation is modeled as spring dampers acting in the horizontal and rotational directions. Viscous damping is used to simulate the radiation damping in the soil, which is developed through the loss of energy emanating from the foundation in the semi-infinite soil medium. The material damping occurring in the soil is hysteretic and is characterized by a damping ratio ζ_g. This is represented in the simplified model sown in *Figure 2*.

2.3 Equations of motion

Using the virtual displacement concept to develop the equations of motion, which is done by introducing a small deformation corresponds to each degree of freedom then developing the equation of motion by setting the virtual work of the deformed system equals to zero.

2.3.1 Lateral displacement of the bridge deck

By applying horizontal equilibrium of forces at the base of the ground harmonic motion

$-\ddot{U}_g m e^{i\omega t} = \frac{12EI}{h^3}U + \frac{6EI}{h^2}\varphi + C\dot{U} + m\ddot{U}_t$ .. By eliminating the term $e^{i\omega t}$ for simplicity

$$-\ddot{U}_g m = \frac{12EI}{h^3 m}(1 + 2\zeta\iota)U + \frac{6EI}{h^2}\varphi + m\left(\ddot{U}_o + h\ddot{\vartheta} + \ddot{U}\right)$$

Assuming $\mathrm{K} = \frac{12EI}{h^3}$ and by differentiating

$$\left[\frac{K}{mw^2}(1 + 2\zeta\iota) - 1\right]U + \frac{K}{2mw^2}\varphi - U_o - h\vartheta = U_g \quad \ldots\ldots\ldots\ldots\ldots\ldots\ldots\ldots\ldots\ldots \quad (1)$$

2.3.2 Horizontal displacement of the foundation relative to the freefield

$-\ddot{U}_g m e^{i\omega t} = \frac{8GR}{(2-\upsilon)} U_o + C_h \dot{U}_o + C_g \dot{U}_o + m\ddot{U}_t$ .. By eliminating the term $e^{i\omega t}$ for simplicity

$-\ddot{U}_g m = \frac{8GR}{(2-\upsilon)}\left(1 + 2\zeta_h \iota + 2\zeta_g \iota\right) U_o + + m\left(\ddot{U}_o + h\ddot{\vartheta} + \ddot{U}\right)$ .. By differentiating

$$\left[\frac{K_h}{mw^2}\left(1 + 2\zeta_h \iota + 2\zeta_g \iota\right) - 1\right] U_o - h\vartheta - U = U_g \quad \ldots\ldots\ldots\ldots\ldots\ldots\ldots\ldots\ldots\ldots \quad (2)$$

Where $K_h = \frac{8GR}{(2-\upsilon)}$ [10]

2.3.3 Rotation of the system at foundation level

$$-\ddot{U}_g mhe^{i\omega t} = \frac{8GR^3}{3(1-\upsilon)}\vartheta + C_r\dot{\vartheta} + C_g\dot{\vartheta} + C\dot{\vartheta} + \frac{2EI}{h^2}\vartheta + m\ddot{U_t}h$$

By eliminating the term $e^{i\omega t}$ for simplicity

$-\ddot{U}_g mh = \frac{8GR^3}{3(1-\upsilon)}\left(1 + 2\zeta_r \iota + 2\zeta_g \iota\right)\vartheta + \frac{2EI}{h^2}(1 + 2\zeta\iota)\vartheta + m\ddot{U_t}h$ .. By differentiating

$$\left[\frac{K_r}{mw^2h^2}\left(1 + 2\zeta_r \iota + 2\zeta_g \iota\right) - 1 + \frac{K}{6mw^2}(1 + 2\zeta\iota)\right] h\vartheta - U_o - U = U_g \quad \ldots\ldots\ldots\ldots\ldots \quad (3)$$

Where $K_r = \frac{8GR^3}{3(1-\upsilon)}$ & $K = \frac{12EI}{h^3}$ [10]

2.3.4 Rotation of the deck prior to the pier

$-\ddot{U}_g mhe^{i\omega t} - J\ddot{\varphi} = \frac{4EI}{h}\varphi + \frac{6EI}{h^2}U + C\dot{\varphi}$ .. By eliminating the term $e^{i\omega t}$ for simplicity

$-\ddot{U}_g mh - J\ddot{\varphi} = \frac{4EI}{h}(1 + 2\zeta\iota)\varphi + \frac{6EI}{h^2}U$ .. By differentiating

$-\frac{J}{mh}\varphi + \frac{K}{3hw^2h^2}(1 + 2\zeta\iota)\varphi + \frac{K}{2mw^2}U = U_g$ ..... (4)

The previous four equations of motion can be summarized as follows

$$\begin{bmatrix} \left[\frac{K}{mw^2}(1 + 2\zeta\iota) - 1\right] & -1 & -1 & \frac{K}{2mw^2} \\ -1 & \left[\frac{K_h}{mw^2}\left(1 + 2\zeta_h\iota + 2\zeta_g\iota\right) - 1\right] & -1 & 0 \\ -1 & -1 & \left[\frac{K_r}{mw^2h^2}\left(1 + 2\zeta_r\iota + 2\zeta_g\iota\right) - 1 + \frac{K}{6mw^2}(1 + 2\zeta\iota)\right] & 0 \\ \frac{K}{2mw^2} & 0 & 0 & \frac{K}{3hw^2h^2}(1 + 2\zeta\iota) - \frac{J}{mh} \end{bmatrix}$$

$$* \begin{bmatrix} U \\ U_o \\ h\vartheta \\ \varphi \end{bmatrix} = \begin{bmatrix} 1 \\ 1 \\ 1 \\ 1 \end{bmatrix} U_g$$

While solving the equations of motion is rather a difficult task in the case of four degrees of freedom, it is easy to observe that the rotational inertial has a rule to play in the dynamic performance of the system and an influence especially in the lateral deformation of the column which is represented by the first degree of freedom U, trying to quantify this effect analytically is quite difficult and requires a very detailed example to substitute with all the required unknowns.

By comparing the stiffness matrices of this case under study and another case where the rotational deformation of the deck is ignored one can look more closely to the additional terms that come into play in this case.

$$\begin{bmatrix} \frac{12EI}{h^3} & 0 & 0 & \frac{6EI}{h^2} \\ 0 & \frac{8GR}{(2-\upsilon)} & 0 & 0 \\ 0 & 0 & \frac{8GR^3}{3(1-\upsilon)} + \frac{2EI}{h^2} & 0 \\ \frac{6EI}{h^2} & 0 & 0 & \frac{4EI}{h} \end{bmatrix} \quad \ldots\ldots\ldots (5)$$

$$\begin{bmatrix} \frac{12EI}{h^3} & 0 & 0 \\ 0 & \frac{8GR}{(2-\upsilon)} & 0 \\ 0 & 0 & \frac{8GR^3}{3(1-\upsilon)} + \frac{2EI}{h^2} \end{bmatrix} \quad \ldots\ldots\ldots\ldots\ldots (6)$$

The stiffness matrix (5) represents case 1, where the rotational deformation of the deck is taken in consideration. And the stiffness matrix (6) represents case 2, where the extra degree of freedom is ignored.

It is important to note that the assumption of a rigid deck brings the both cases close, as the column is viewed in both cases rotationally fixed from the top, thus using the lateral stiffness of the column equals $\frac{12EI}{h^3}$.

While only comparing the stiffness matrix gives the impression that the first case of four DOFs suggests a stiffer dynamic system, it is important also to remember that there is on the other hand an additional acting moment from the rotational inertia, while it is analytically difficult to assess which is the prevailing side of the two opposing actions.

It is important to note that this analytical examination while useful to observe the extra terms that comes into action in the dynamic response, lacks some important parameters influence such as the extra damping which comes from having extra elements of the deck and the influence of the rotational inertia on the period of the model under examination, not to mention the nonlinearity and the large displacement cases.

The next chapters will examine the problem by comparing different 3D & 2D models of typical bridge models to focus on the dynamic response against real seismic excitations.

Notation

a	radius of circular foundation
C_h	horizontal viscous damping coefficient for radiation soil damping
C_r	rocking viscous damping coefficient for radiation soil damping
E	Young's modulus for the pier
G	soil shear modulus
h	height of the pier
I	moment of inertia about the weak axis of the pier
ζ_h	damping ratio of viscous damping for lateral displacement
ζ	damping ratio of hysteretic soil damping
ζ_r	damping ratio of damping ratio of viscous soil damping for rocking motion
k	flexural stiffness of pier
k_h	horizontal stiffness of soil medium
k_r	rocking stiffness of soil medium
m	mass of bridge deck corresponding to one pier
U	relative lateral displacement of bridge deck
U_g	lateral ground displacement
U_o	relative lateral displacement of pier base
U_t	total lateral displacement
θ	rotation angle
φ	deck rotation relative to the pier
ω	frequency of the bridge pier

Chapter 2

Figures

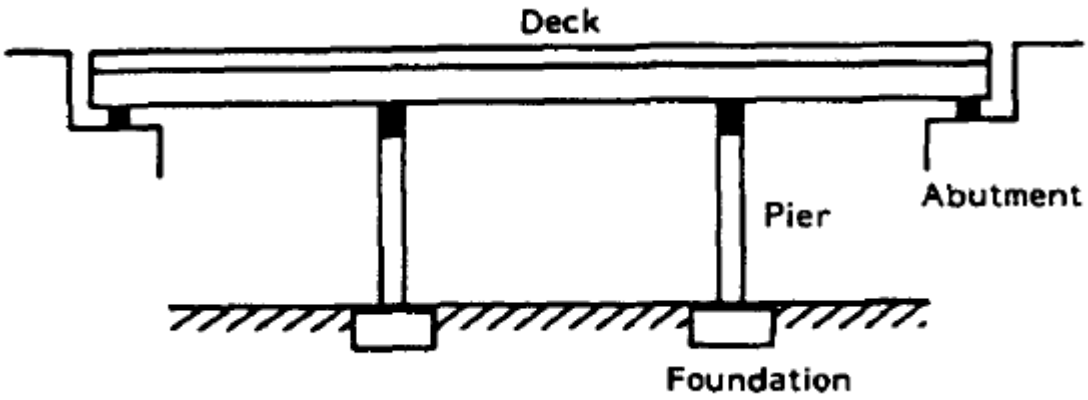

Figure 1. Typical elevation of a short span bridge.

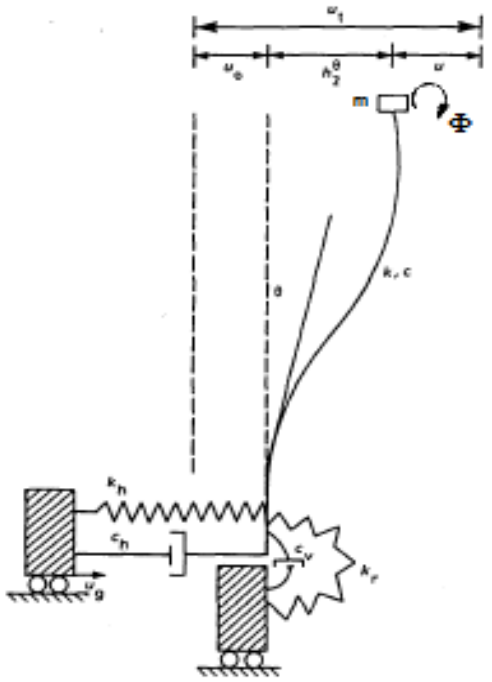

Figure 2. DOFs of pier-soil system subjected to horizontal excitation

CHAPTER 3

NUMERICAL ANALYSIS OF BRIDGE MODEL-A

3.1 Introduction

Based on the exploratory studies of the new “rocking design” philosophy, the study [7] seeks to provide experimental verification of the numerical findings of the mentioned studies suggesting that a conventionally designed RC pier on an adequately large shallow foundation would suffer structural failure of the RC column and would collapse in an earthquake sufficiently exceeding its design limits, rocking motion of an alternative under-designed foundation would allow the same pier to survive even extreme shaking scenarios.

A series of centrifuge tests were performed to investigate and compare the performance of the two RC model bridge piers, having the same structural section on each case, but each representing one of the two considered design approaches, namely, a conventional design and rocking isolation design.

This experimental study provided proof of the concept of the concept of deliberately designing the foundation nonlinearity to render RC structures under intense seismic excitation. where the rocking isolation design consistently exhibits a better performance compared with conventional capacity design, Nonlinear response of the soil footing interface efficiently acts as an effective energy dissipation fuse showing increased ductility capacity and resistance against cumulative damage. Counterintuitively the rocking isolated pier was found to be advantageous also in terms of drift demands suffering lower deck displacements.

Study [13] examined the use of ricker wavelets ground motions as an alternative to push-over testing, where a 3-D non-linear finite element modeling (FEM) was conducted to investigate the behavior of the bridge structure under different ground motions. In this study it has been demonstrated that a Ricker wavelet type ground motion can be used to validate the push-over response of shallow foundation systems. This finite element model will be borrowed to examine our problem being the effect of the rotational inertia of the deck.

3.2 FE Model set-up

A 3-D nonlinear finite element modeling is conducted using ABAQUS. The geometry of this prototype bridge, which represent a moderately tall (h=10.75 m) highway bridge pier carrying a deck with total dead load (q = 200 kN/m) supported by a square (B X B) shallow foundation. The 1.5 m x 1.5 m square section pier (cross sectional area A_c = 2.25 m^2) was simulated with 3-dimensional elastic beam elements assigned the geometric and stiffness properties of the aluminum section (E = 70 GPa, γ = 26 kN/m^3). Given the relatively high position of the lumped mass, second order (P – δ) effects are important and were therefore taken into account, Figure(1).

Taking in advantage the symmetry in the plane that crosses the foundation midpoint in the direction of the excitation allowed the simulation of only half of the full 3-D model, achieving greater computational efficiency.

The soil was modelled with nonlinear 8-noded hexahedral continuum elements C3D8. Representing the following properties (ρ = 1.8 Mg/m^3, S_u = 150 kPa, E = 270000 kPa, v = 0.3).The same element type (C3D8), but with the assumption of linear elastic behavior, was used for the footing. The soil – foundation interface was modelled using special contact elements, which allow sliding and uplifting to take pace being governed by a hard contact law and Coulomb's friction law in the normal and tangential direction respectively.

Four models were tested , the first two represent the conventional capacity design concept where the large foundation (B = 7.5 m) which follows the current code provisions ensuring minimum displacements of the soil-foundation interface under the design earthquake where the seismic actions on the foundation (Q_{Ed}, M_{Ed}) are substantially magnified (by as much as 40% in this case) in comparison to the actual loads at the column base to avoid nonlinear response and accumulation of plastic deformations ant the column base, The factor of safety (FS_v) is greater than one under the expected seismic action. The only difference between these first two models is the modeling of the upper deck geometry in the first model it is modeled as a lumped mass with no physical dimensions, While the other model the deck is modelled as a (4 x 3.5 x 2) m box which will represent the case where the rotational inertia comes into action. *Figure 2.*

The next two models will represent the alternative design philosophy of rocking isolation. Where the footing dimensions is smaller (B = 4 m) which represents a factor of safety (FS_v) < 1 under the design seismic conditions. *Figure 3.*

Table 1 summarizes the design of the two foundation alternatives listing the actual loads and the design actions, the bearing capacity in pure vertical loading and in combined seismic loading, and the corresponding factors of safety for static vertical loads (FS_v) and seismic lateral loading (FS_E).

Foundation capacity was firstly calculated using well established relationships from literature, [12] for combined N-M-Q loading respectively. Numerical simulations with finite elements were then used to verify these theoretical predications. *Figure 4.*

Property	***Unit***	***Conventional***	***Rocking***
Breadth	B : m	7.5	4
Total Vertical Load	N : MN	6.07	5
Seismic Shear Load	Q_E : MN	0.9	0.9
Seismic Moment Load	M_E : MN	13.7	13.7
Design Shear Load	Q_{Ed} : MN	0.9	0.9
Design Moment Load	M_{Ed} : MN	13.7	13.7

Property	*Unit*	*Conventional*	*Rocking*
Ultimate Shear Load	Q_u : MN	1.71	0.55
Ultimate Moment Load	M_u : MN	18.3	5.9
Safety Factor in Vertical Loading	Q_E : MN	8.2	3.09
Safety Factor in Seismic Loading	M_E : MN	1.34	0.44

Table 1.Foundation Design: Summary of loads and safety factors

3.3 Dynamic Analysis

A series of dynamic analysis was conducted; the model base was excited by a variety of Ricker pulses with different magnitude and frequency along with real excitation from Greece and japan to further examine the model comparisons.

3.3.1 Ricker Pulses

Ricker pulses has shown to validate the pushover behavior of the bridge structure [13], while having the advantage of the wavelet in a form of continuous acceleration , In the study five different frequency ricker wavelet will be used each with three different peak ground acceleration (0.2g, 0.4g, 0.6g). *Figure 5a* shows the different ricker pulses used in the analysis with 0.6g PGA.

3.3.1.1 Ricker Pulse 1Hz

a) Peak Ground Acceleration (PGA) = 0.2g.

Dynamic results shown in *Figure 6*, represents the response of the first two conventional models. The comparison is showing the lumped mass model to have a slightly higher peak deck acceleration, where the difference increases with the excitation period where the "Full Model" is showing higher damping, this can be explained due to the existence of the extra elements forming the deck which have damping characteristics and the re-centering of the deck which acts as an energy dissipation fuse.

The response is also showing a higher foundation rotation in the case of the lumped-mass model, along with higher deck displacement.

Figure 7 shows the dynamic response of the second two models representing the rocking isolation case; the comparison is showing the lumped mass to have quite the same peak deck acceleration and higher damping properties for the "full model" along with higher rotation and deck displacement in the case of the "lumped-mass model".

b) Peak Ground Acceleration (PGA) = 0.4g.

Figure 8 shows the dynamic response and comparison of the conventional models, where the peak deck acceleration is arguably equal but the degradation is quite different as the "full model" is showing higher damping, also the comparison is showing a significant difference in the response period where the full model is showing a smaller period.

The foundation rotation of the "full model" is higher comparing with el "lumped-mass" model especially after the excitation duration, where the full model shows higher damping and self-centering characteristic.

Figure 9 shows the dynamic response and comparison of the Rocking models. Where the peak deck acceleration is arguably equal and the degradation is quite faster in the case of the "full model". The foundation rotation and deck acceleration is shown to be quite less compared to the "lumped-mass model".

c) Peak Ground Acceleration (PGA) = 0.6g.

Figure 10 shows the dynamic response of the conventional models, the results is consistent with the previous as the two models shows the same peak deck acceleration along with a significant difference in period and damping where the "Full Model" shows higher damping and lower period, also the same consistency with the higher rotation in the case of the "lumped-mass model" along with deck displacement.

Figure 11 shows the response and comparison of the rocking models, where the difference on the deck acceleration is not as significant as the conventional models especially the absence of the periodical variation between the two models, the foundation rotation is shown to be more is the case of the lumped-mass model where the full model has a higher damping.

3.3.1.2 Ricker Pulse 0.5Hz

a) Peak Ground Acceleration (PGA) = 0.2g.

Figure 12 shows the dynamic results for the conventional models. This particular case shown a different response entirely as the "full model" results a higher peak deck acceleration but still consistent in terms of showing a higher damping compared to the lumped-mass model. Also the full model shows higher deck rotation significantly compared to the lumped-mass one.

Figure 13 shows the response of the rocking models, where the peak deck acceleration is arguably the same and the full model is showing a higher damping and foundation rotation compared to the lumped-mass model.

b) Peak Ground Acceleration (PGA) = 0.4g.

Figure 14 shows the dynamic response of the conventional models, the results are consistent where the full model shows higher damping and significant shift in period compared with the lumped mass model which also results in a higher foundation rotation and deck displacements.

Figure 15 shows the response of the rocking models, where the peak deck acceleration is arguably the same and the full model is showing a higher damping, while the lumped-mass model shows higher deck displacements, foundation rotation and settlement.

c) Peak Ground Acceleration (PGA) = 0.6g.

Figure 16 shows the dynamic response of the conventional models, the results are consistent where the full model shows higher damping and significant shift in period compared with the lumped mass model which also results in a higher foundation rotation and deck displacements.

Figure 17 shows the response of the rocking models, where the peak deck acceleration is arguably the same and the full model is showing a higher damping, while the lumped-mass model shows higher deck displacements, foundation rotation and settlement. It is noticed that that the difference in the response in this PGA is lower compared to the lower PGA in previous cases.

3.3.1.3 Ricker Pulse 0.25Hz

a) Peak Ground Acceleration (PGA) = 0.2g.

Under this very low frequency excitation the behavior resembles a very slow push of the system, *Figure 18* shows the response of the conventional models, where under the duration of this pulse the comparison doesn't show much difference early but shows significant difference later on in terms of deck acceleration where the full model is showing a higher damping, while the lumped mass model responds with higher foundation rotation and deck displacement.

The response of the rocking models shown in *Figure 19* is showing a small difference in deck acceleration with some shift in the period and the lumped-mass model showing higher foundation rotation, deck displacement and settlement.

b) Peak Ground Acceleration (PGA) = 0.4g.

Under this PGA the difference in deck acceleration in the case of conventional models shown in *Figure 20* doesn't have a significant difference compared with the previous case, but consistent when it comes to the lumped-mass model showing higher foundation rotation, deck displacement.

The case of rocking models was not useful as the models fails as shown in *Figure 21*.

c) Peak Ground Acceleration (PGA) = 0.6g.

Figure 22 shows the response of the conventional models, the results are consistent where the full model shows higher damping and significant shift in period compared with the lumped mass model which also results in a higher foundation rotation and deck displacements.

The case of rocking models was not useful as the models fails as shown in *Figure 23*.

3.3.1.4 Ricker Pulse 2Hz

a) Peak Ground Acceleration (PGA) = 0.2g.

The comparison between the conventional models doesn't show mush difference in terms of deck acceleration as shown in *Figure 24*, where it is consistent that the full model shows higher damping. On the contrary in this case the full model also shows higher foundation rotation and deck displacement.

Figure 25 shows the response of the rocking models, where the peak deck acceleration is arguably the same and the full model is showing a higher damping, while the lumped-mass model shows higher deck displacements, foundation rotation and settlement.

b) Peak Ground Acceleration (PGA) = 0.4g.

Figure 26 shows the response of the conventional models, where under the duration of this pulse the comparison doesn't show much difference early but shows significant difference later on in terms of deck acceleration where the full model is showing a higher damping, while the lumped mass model responds with higher foundation rotation and deck displacement.

Figure 27 shows the response of the rocking models, where the peak deck acceleration is arguably the same and the full model is showing a higher damping, while the lumped-mass model shows higher deck displacements, foundation rotation and settlement.

c) Peak Ground Acceleration (PGA) = 0.6g.

Figure 28 shows the response of the conventional models, the results are consistent where the full model shows higher damping and significant shift in period compared with the lumped mass model which also results in a higher foundation rotation and in this particular case a residual rotation which is absent in the full model case.

Figure 29 shows the response of the rocking models, where the peak deck acceleration is arguably the same and the full model is showing a higher damping, while the lumped-mass model shows higher deck displacements, foundation rotation and settlement.

3.3.1.5 Ricker Pulse 3Hz

Under this particular high frequency excitation the results was somewhat useful in comparing the "Full Model" vs the "Lumped-mass Model".

3.3.2 Real EQ Records

In this section the dynamic response will be examined under 6 real earthquake records with various intensity and period shown in *Figure 5b.*

3.3.2.1 Kalamata EQ Greece (1986).

Examining the first two conventional models, the response shown in *Figure30* comparing the two models where it shows the "Full Model" with higher damping effect while the peak deck acceleration is arguably the same. Also the "Lumped-mass Model" shows much higher foundation rotation, settlement and deck displacement.

Figure 31 shows the response of the rocking models, where the difference in behavior is not as evident as the previous case but it can be noticed that the "Lumped-mass Model" shows also higher rotation, settlement and deck displacement.

3.3.2.1 Aegion EQ Greece (1995).

By further examining the rotational inertia effect this time under Aegion EQ which is a shorter excitation but has higher amplitude compared with the previous excitation.

Figure 32 shows the response of the conventional models, the same difference is consistent as there is not much difference in the peak deck acceleration, the "Full Model " showing higher damping, while the "Lumped-mass Model" results in higher foundation rotation, settlement and deck displacement.

Figure 33 shows the response of the rocking models, where the "Full Model" shows higher damping property, while the "Lumped-mass Model" results in higher foundation rotation, settlement and deck displacement. It can be noticed also that the "Full Model" results in a higher residual rotation and deck displacement.

3.3.2.1 Lefkada EQ Greece (2003).

Figure 34 shows the results for the conventional models, where the deck acceleration have a slight difference in behavior, the "Lumped-mass Model" showing much higher foundation rotation, settlement and deck displacement.

Figure 35 shows the results for the Rocking models, where the deck acceleration doesn't show much difference except for the "Full Model" to have higher damping, while the "Lumped-mass Model" results in higher foundation rotation, settlement and deck displacement especially later towards the end of the excitation.

It should be noted that these higher foundation rotation towards the end of the excitation results in a higher plastic deformation around the edge of the foundation.

3.3.2.1 LAquila EQ Italy (2009).

Results shown in *Figure 36* represent the comparison of the conventional models, where the "lumped-mass model" shows higher deck acceleration along with higher foundation rotation and deck displacement.

Figure 37 shows the results for the Rocking models, where the deck acceleration doesn't show much difference except for the "Full Model" to have higher damping, while the "Lumped-mass Model" results in slightly higher foundation rotation, settlement and deck displacement

3.3.2.1 Takatori EQ Kobe, Japan (1995).

Figure 38 shows the results for the conventional models, where the deck acceleration have a slight difference in behavior later in the excitation with a slight shift in the case of the "lumped-mass Model" which also results in higher foundation rotation and deck displacement.

Figure 39 shows the results for the Rocking models, where the deck acceleration doesn't show much difference except in the last couple cycles, while the "Lumped-mass Model" results in a much higher foundation rotation, settlement and deck displacement especially later towards the end of the excitation.

3.3.2.1 Northridge Rinaldi (1994).

Examining the first two conventional models, the response shown in *Figure40* comparing the two models where it shows the "Full Model" with higher damping effect while the peak deck acceleration is arguably the same. Also the "Lumped-mass Model" shows much higher foundation rotation and deck displacement.

Figure 41 shows the results for the Rocking models, where the deck acceleration doesn't show much difference, while the "Lumped-mass Model" results in a higher foundation rotation, settlement and deck displacement especially later towards the end of the excitation.

3.4 Conclusions

From all the previous analysis, it can be noted that the presence of the bridge deck geometry in the FE model has some effect on the overall response of the dynamic system, even so the results seems somewhat random in effectiveness among the cases previously studied, however it can be concluded that :

- The “Full Model” results in higher property for the dynamic system especially towards the end of the excitation.
- The “Lumped-Mass Model” results in higher Foundation rotation where this difference is varying from one case to another, this difference also leads to different values of plastic deformation along the edges of the foundation.
- Also the “Lumped-Mass Model” results in most cases in higher settlement and deck displacement.
- The presence of the deck geometry in the FE model doesn’t diminish the advantages of the “Rocking Isolation” design philosophy since the nature of the excitation is repetitive with varying direction the rotational inertia doesn’t have the time to really affect the response in the extent of leading the system to failure.

Chapter 3

Figures

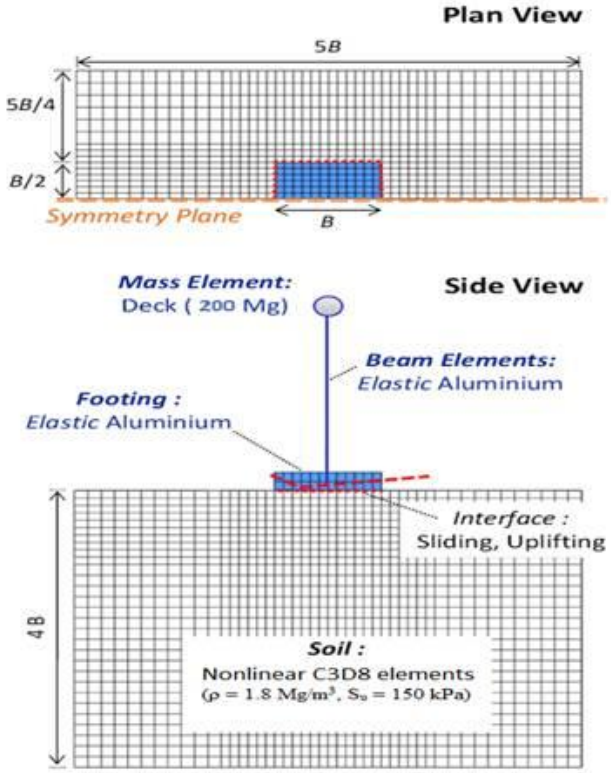

Figure 3.1 Details of 3-D Finite Element model

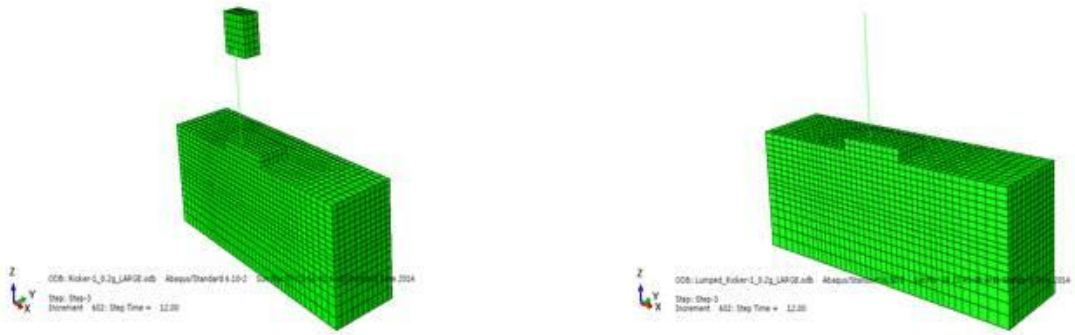

Figure 3.2 First Two Compared FE models representing the conventionally designed Brodge

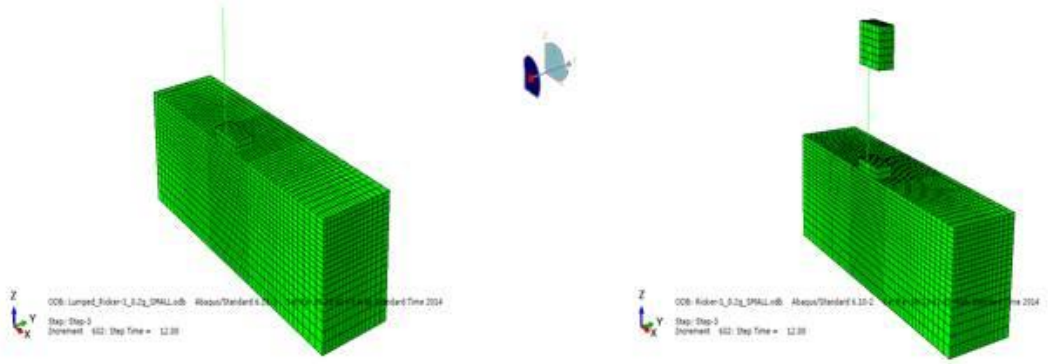

Figure 3.3 Second Two Compared FE models representing the conventionally designed Bridge

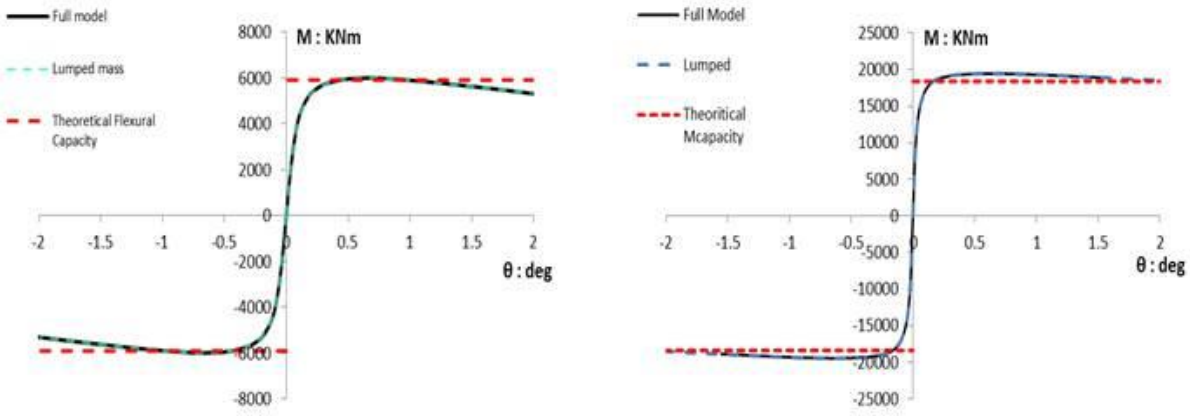

a) Rocking Isolation Models.

b) Conventional Models.

Figure 3.4a Push-over Result: Moment rotation and comparison with theoretical flexural capacity.

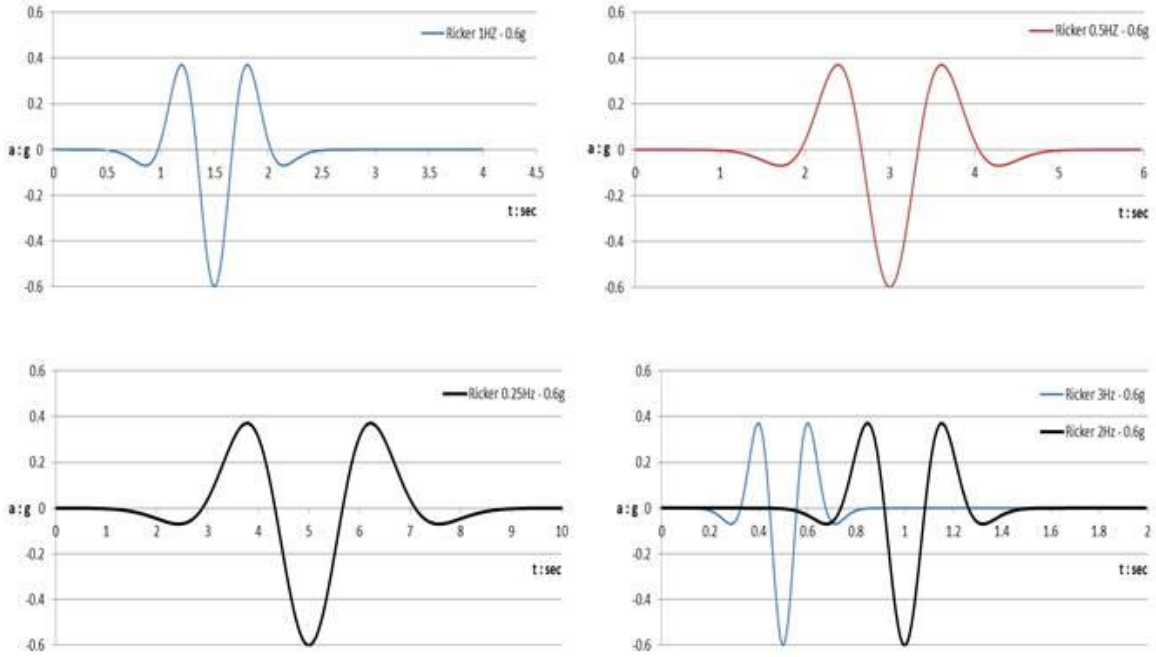

Figure 3.5 a) Ricker pulses used in the dynamic analysis with 0.6 PGA.

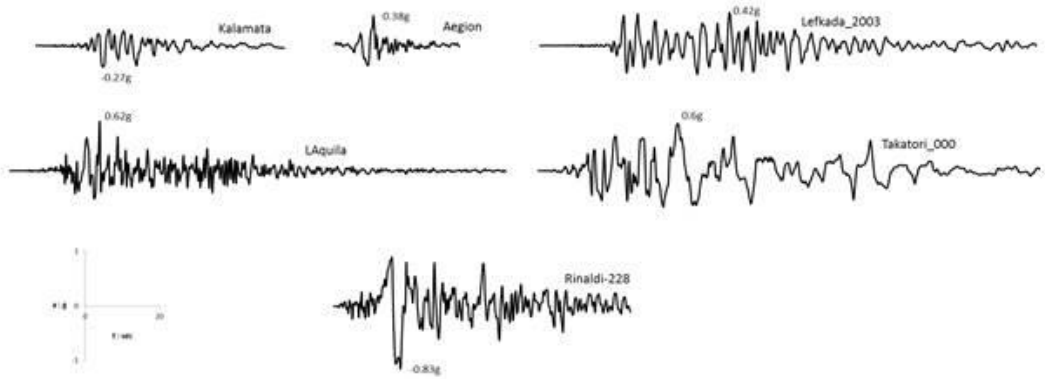

Figure 3.5 b) Real Earthquake Records used in the analysis.

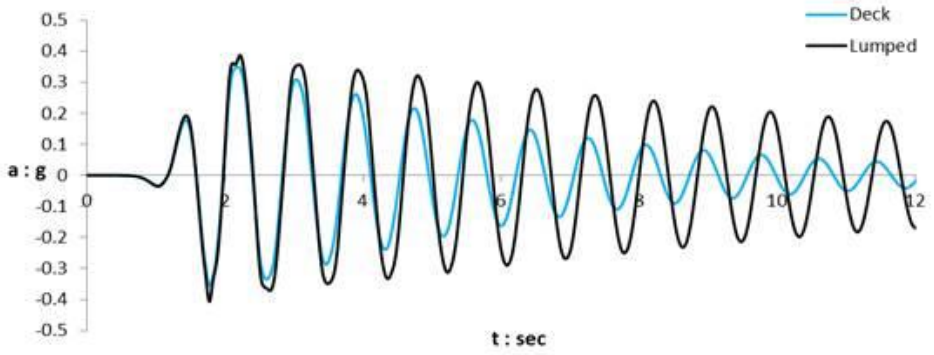

a) Deck Acceleration

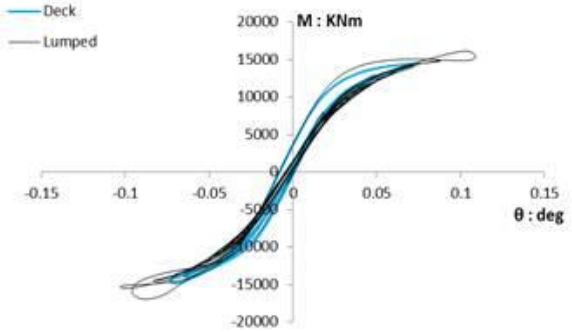

b) Foundation Moment - Rotation

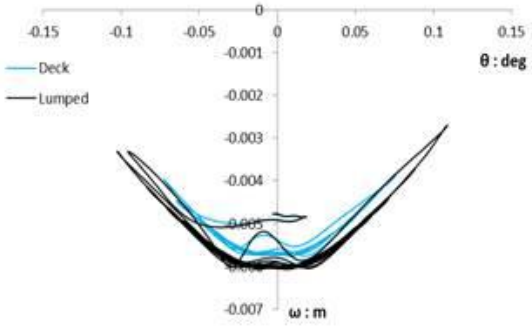

c) Settlement - Foundation Rotation

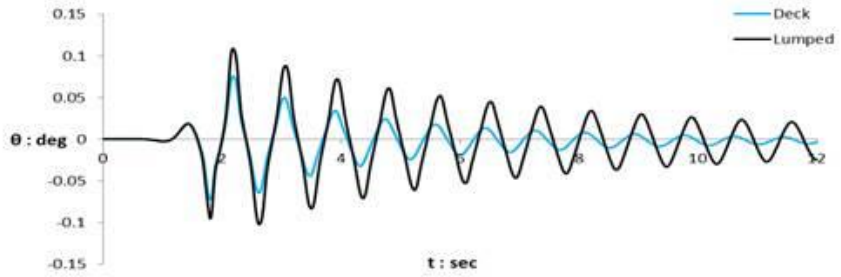

d) Foundation Rotation - time

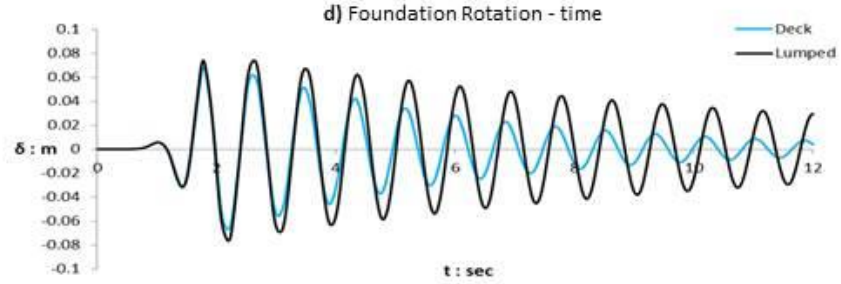

Figure 3.6 Dynamic Results of the conventional Models under Ricker 1Hz – 0.2g base excitation.

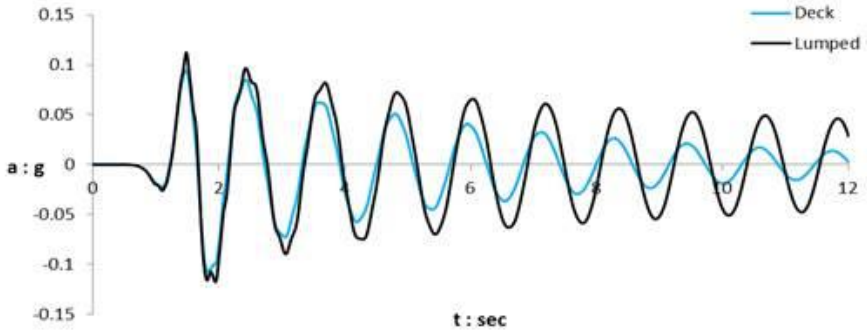

a) Deck Acceleration

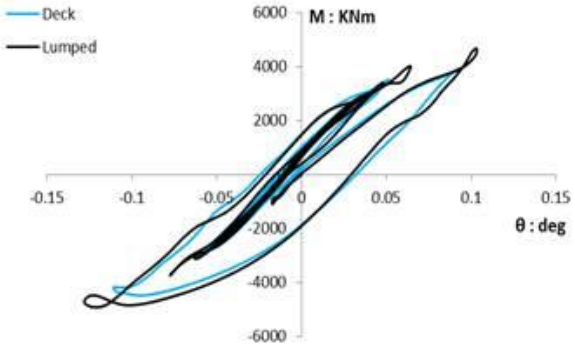

b) Foundation Moment - Rotation

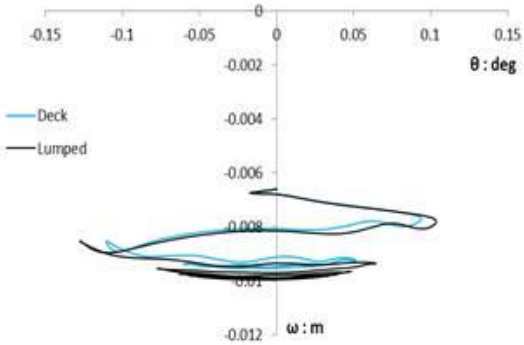

c) Settlement - Foundation Rotation

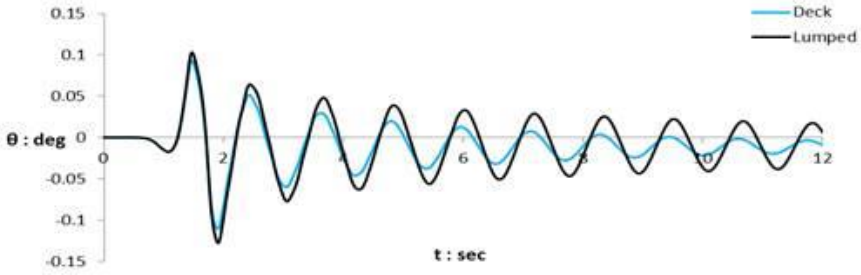

d) Foundation Rotation - time

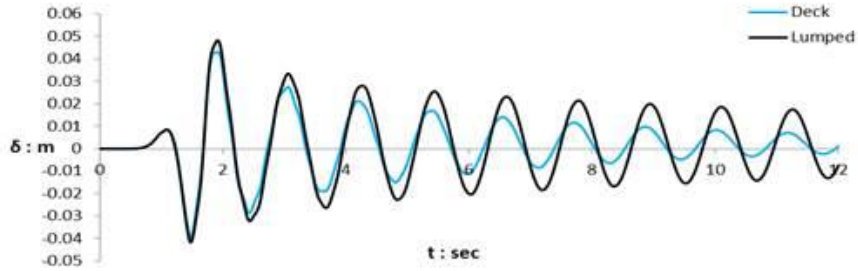

e) Deck Displacement - time

Figure 3.7 Dynamic Results of the Rocking Models under Ricker 1Hz – 0.2g base excitation.

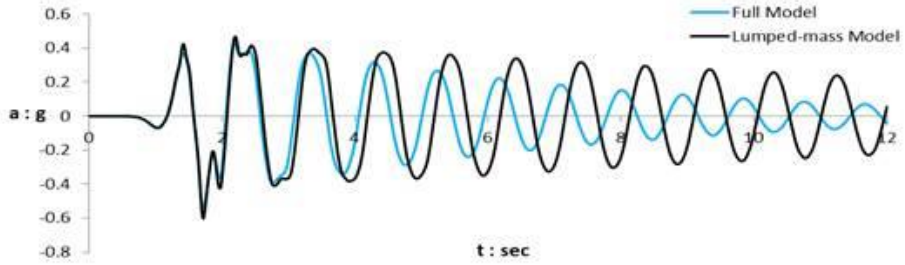

a) Deck Acceleration

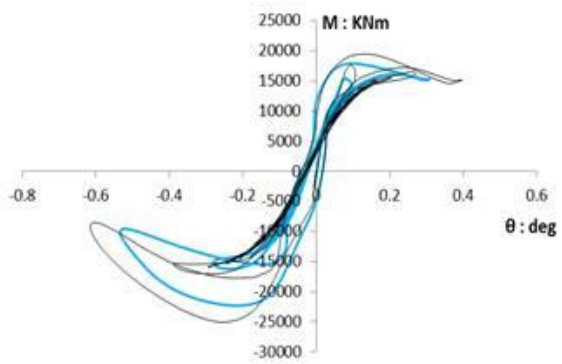

b) Foundation Moment - Rotation

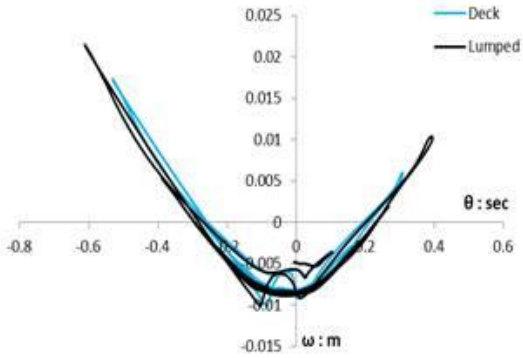

c) Settlement - Foundation Rotation

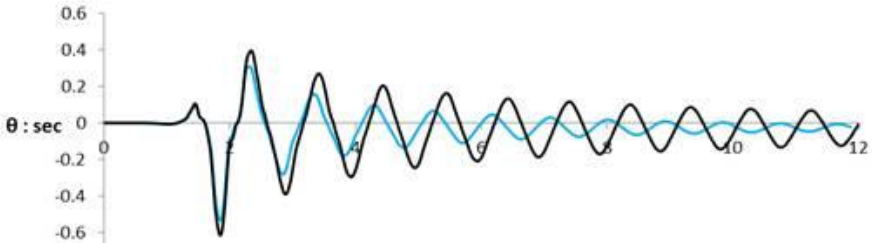

d) Foundation Rotation - time

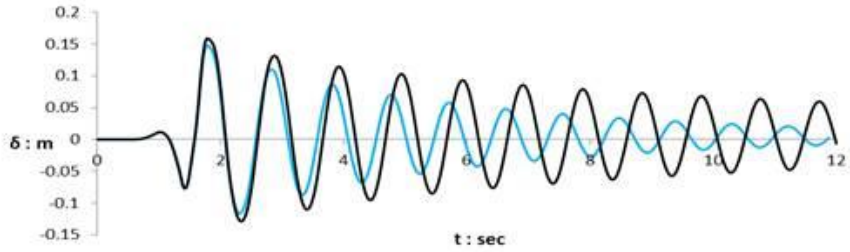

e) Deck Displacement - time

Figure 3.8 Dynamic Results of the Conventional Models under Ricker 1Hz – 0.4g base excitation.

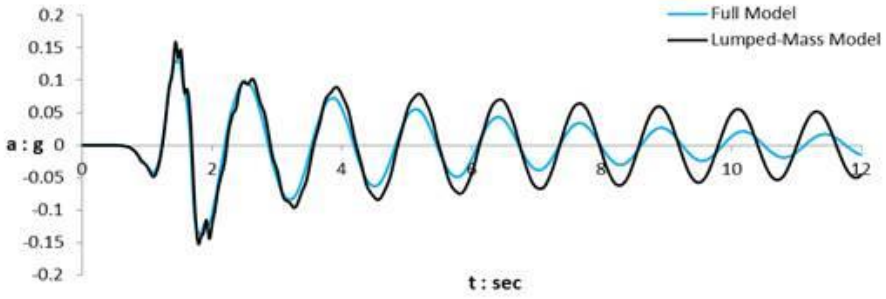

a) Deck Acceleration

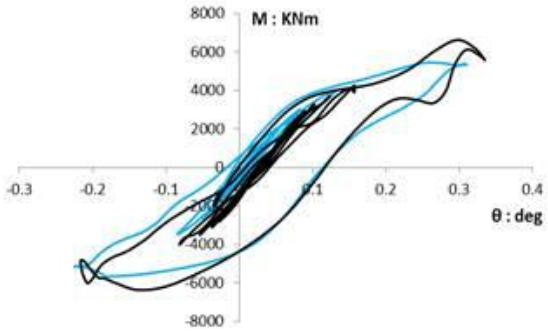

b) Foundation Moment - Rotation

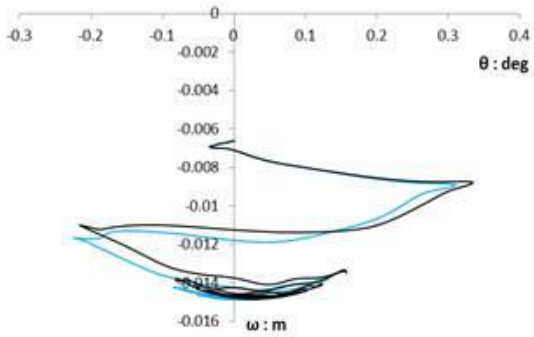

c) Settlement - Foundation Rotation

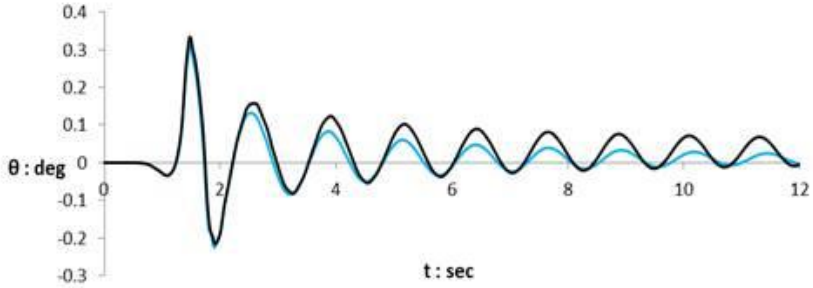

d) Foundation Rotation - time

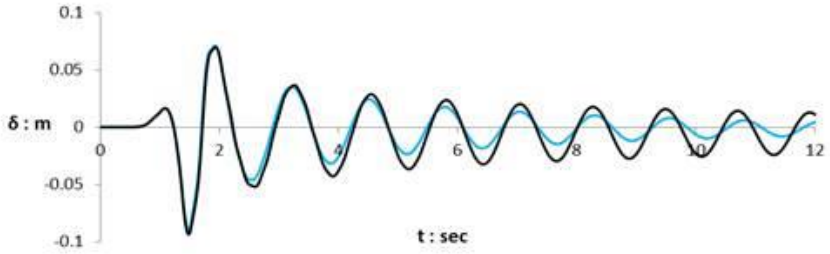

e) Deck Displacement - time

Figure 3.9 Dynamic Results of the Rocking Models under Ricker 1Hz – 0.4g base excitation.

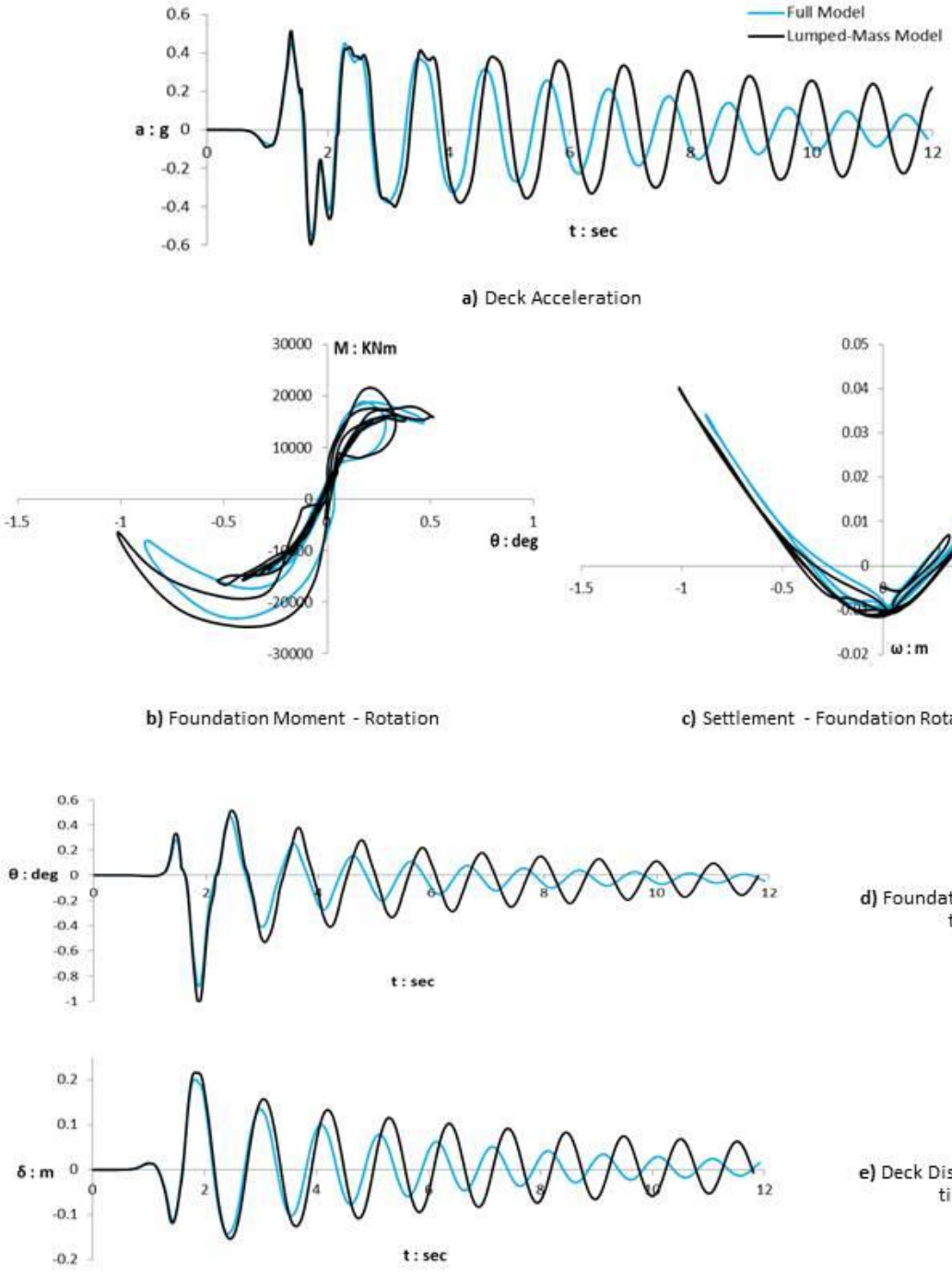

Figure 3.10 Dynamic Results of the Conventional Models under Ricker 1Hz – 0.6g base excitation.

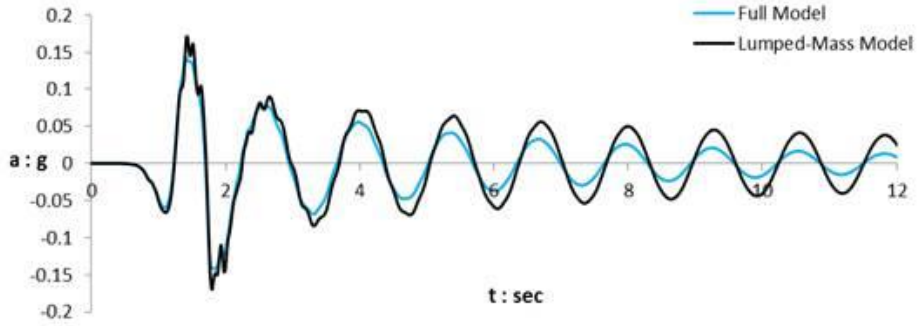

a) Deck Acceleration

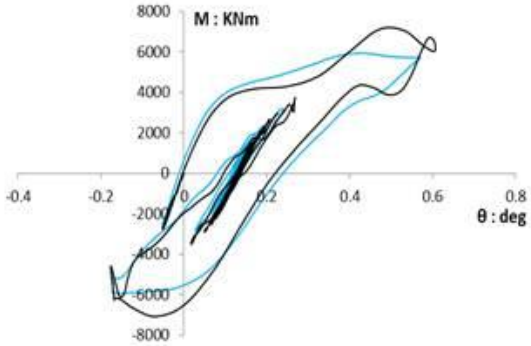

b) Foundation Moment - Rotation

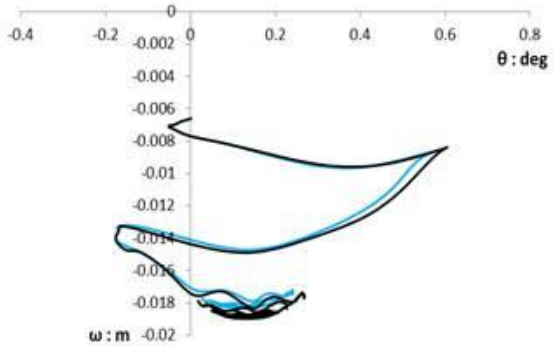

c) Settlement - Foundation Rotation

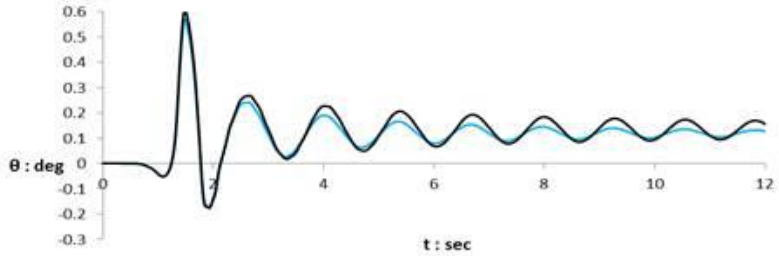

d) Foundation Rotation - time

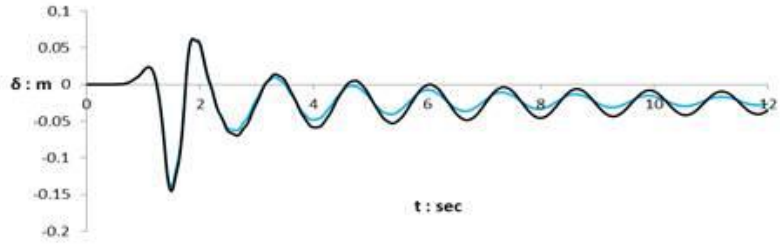

e) Deck Displacement - time

Figure 3.11 Dynamic Results of the Rocking Models under Ricker 1Hz – 0.6g base excitation.

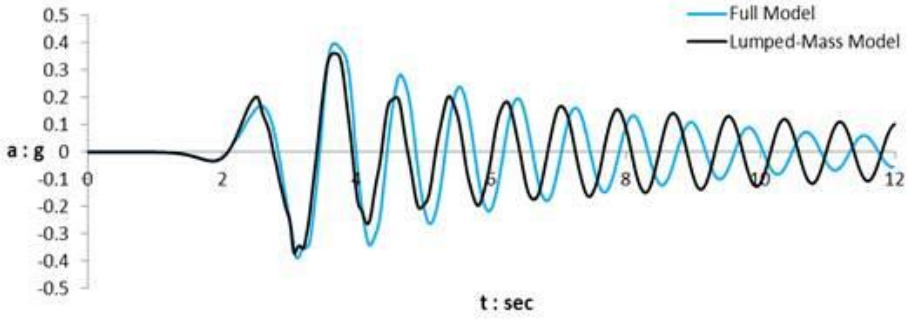

a) Deck Acceleration

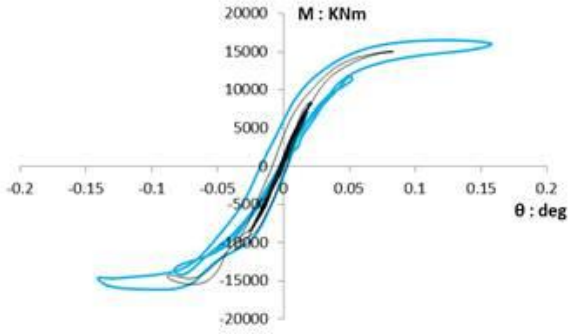

b) Foundation Moment - Rotation

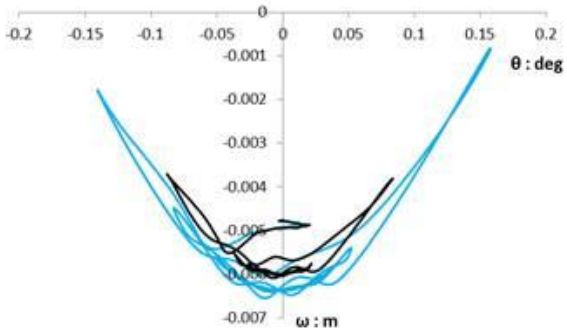

c) Settlement - Foundation Rotation

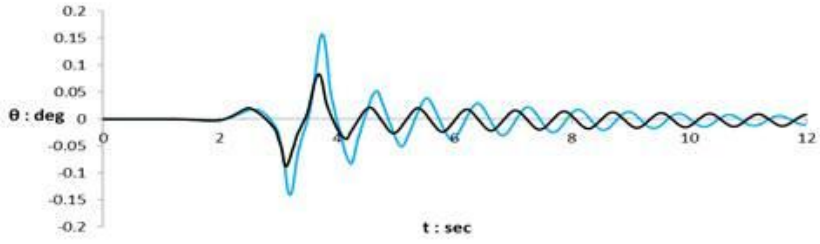

d) Foundation Rotation - time

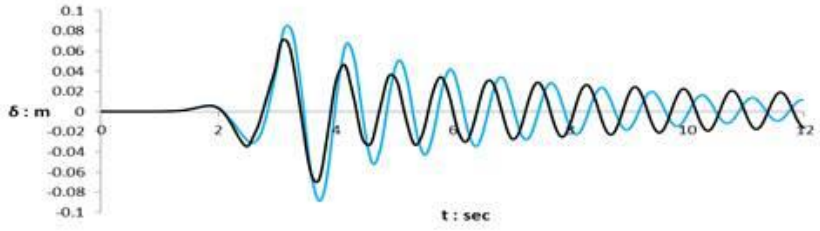

e) Deck Displacement - time

Figure 3.12 Dynamic Results of the Conventional Models under Ricker 0.5Hz – 0.2g base excitation.

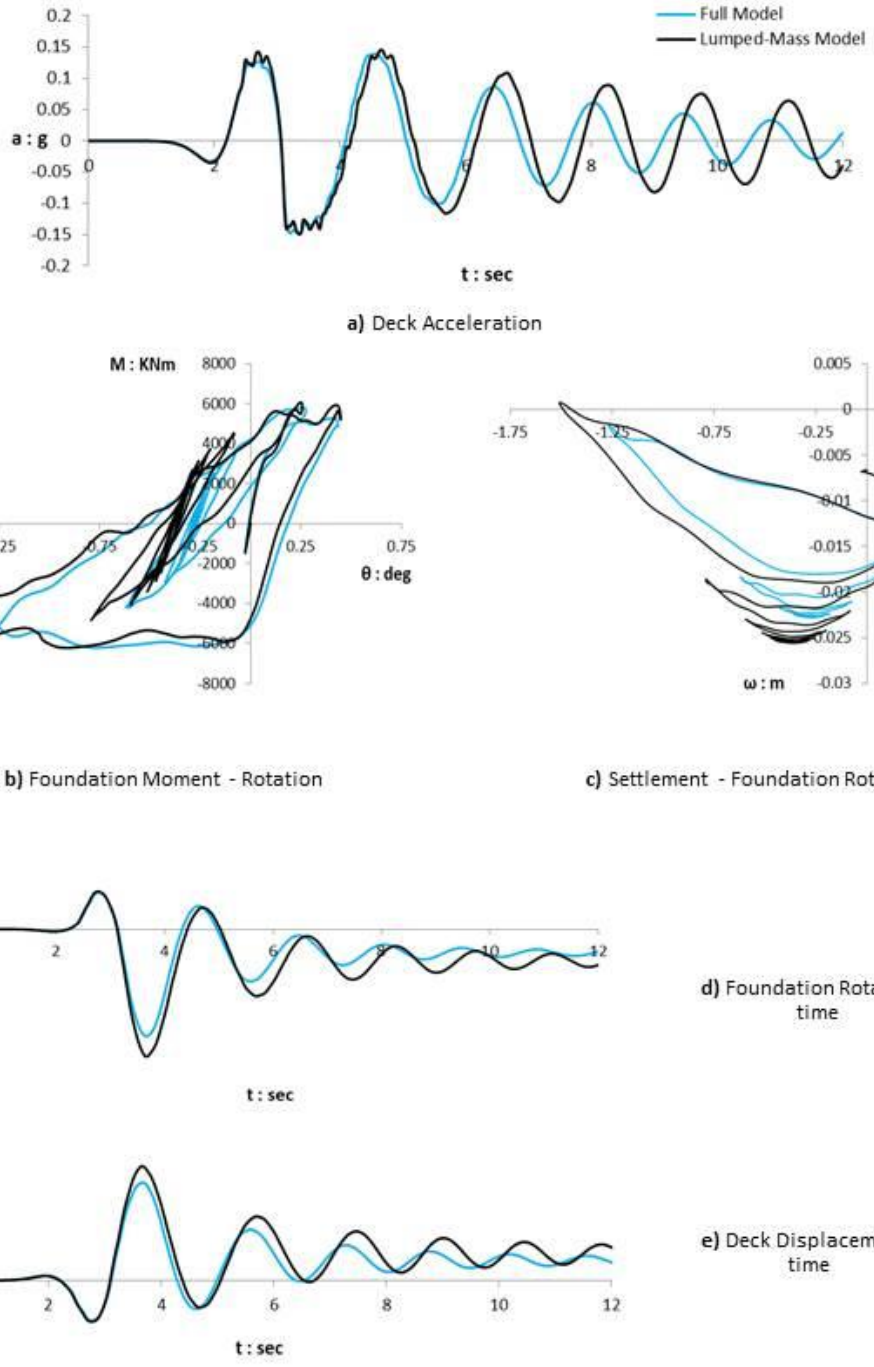

Figure 3.13 Dynamic Results of the Rocking Models under Ricker 0.5Hz – 0.2g base excitation.

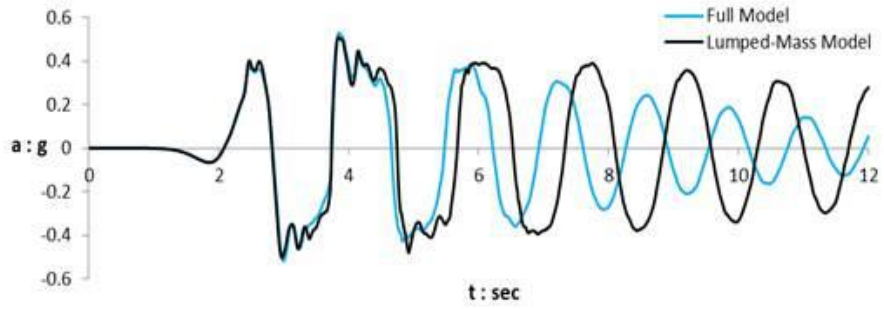

a) Deck Acceleration

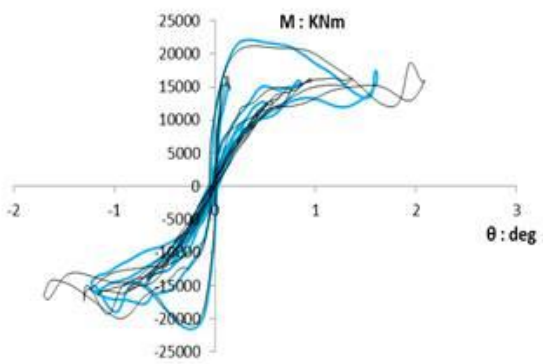

b) Foundation Moment - Rotation

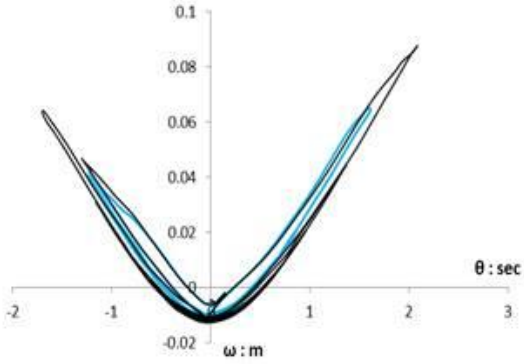

c) Settlement - Foundation Rotation

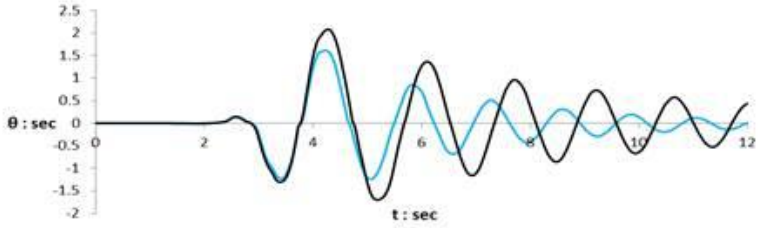

d) Foundation Rotation - time

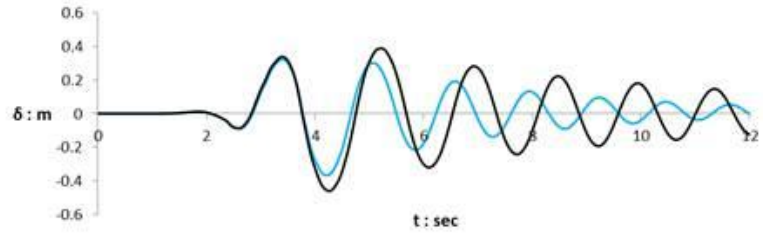

e) Deck Displacement - time

Figure 3.14 Dynamic Results of the Conventional Models under Ricker 0.5Hz – 0.4g base excitation.

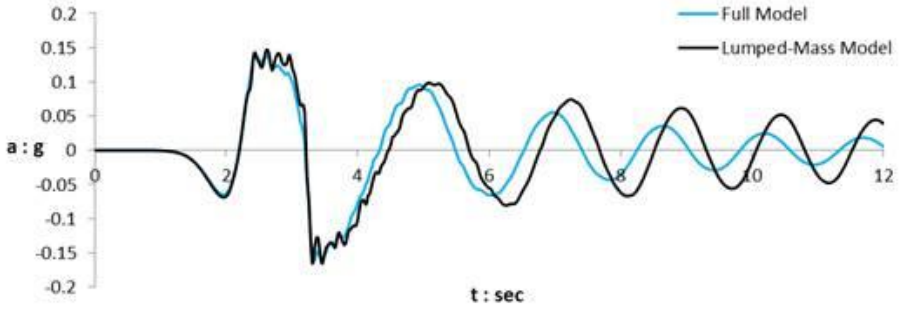

a) Deck Acceleration

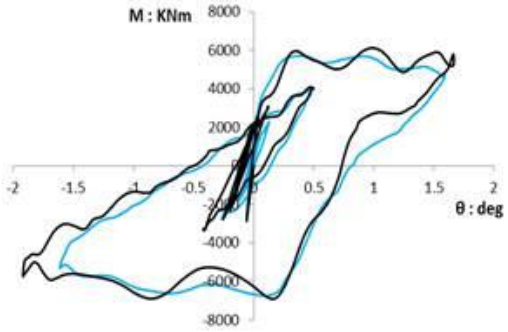

b) Foundation Moment - Rotation

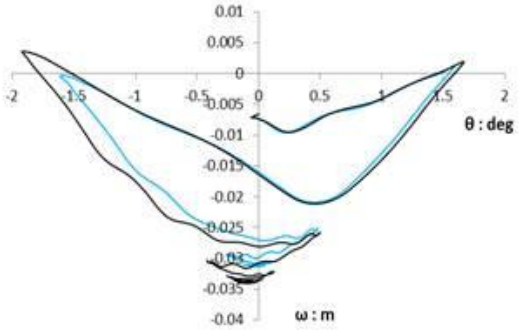

c) Settlement - Foundation Rotation

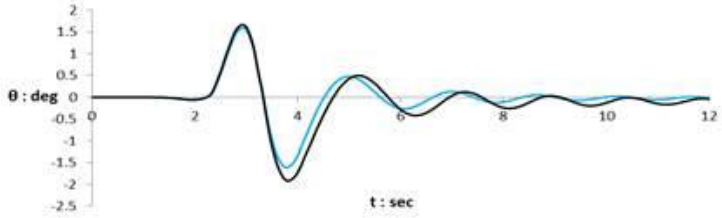

d) Foundation Rotation - time

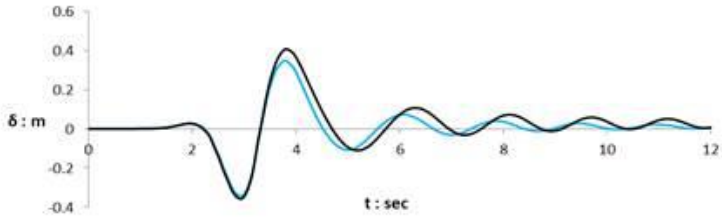

e) Deck Displacement - time

Figure 3.15 Dynamic Results of the Rocking Models under Ricker 0.5Hz – 0.4g base excitation.

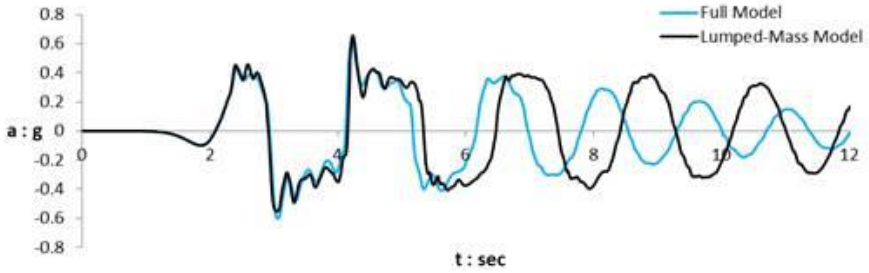

a) Deck Acceleration

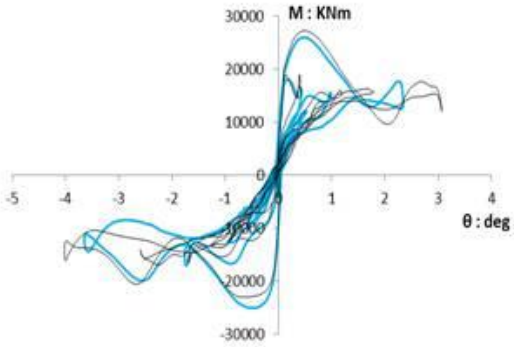

b) Foundation Moment - Rotation

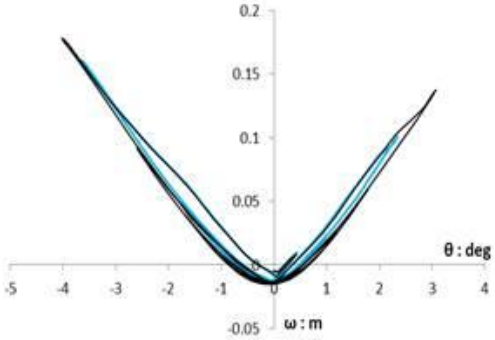

c) Settlement - Foundation Rotation

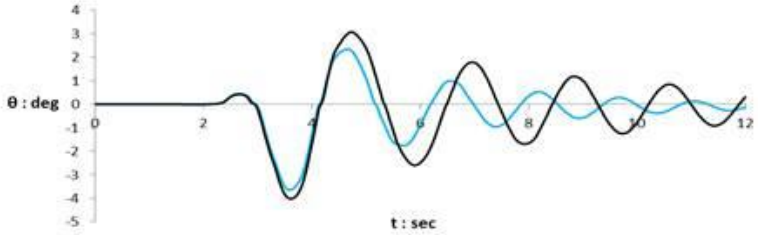

d) Foundation Rotation - time

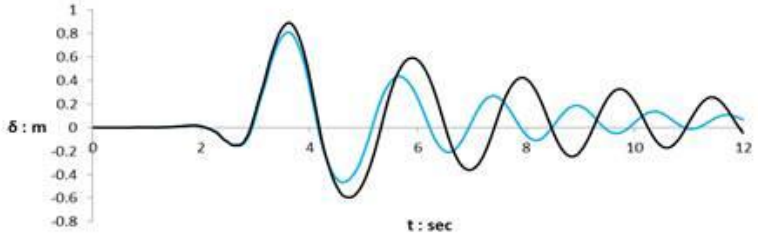

e) Deck Displacement - time

Figure 3.16 Dynamic Results of the Conventional Models under Ricker 0.5Hz – 0.6g base excitation.

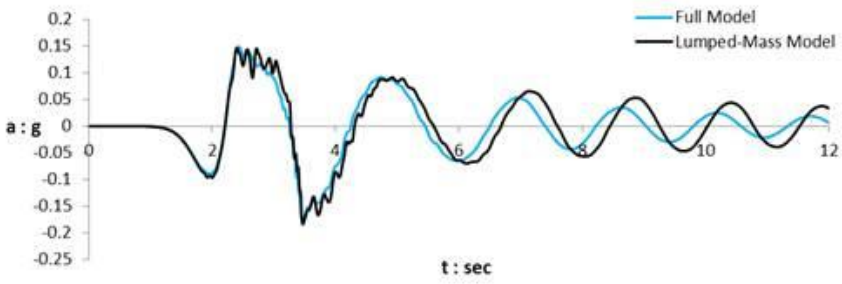

a) Deck Acceleration

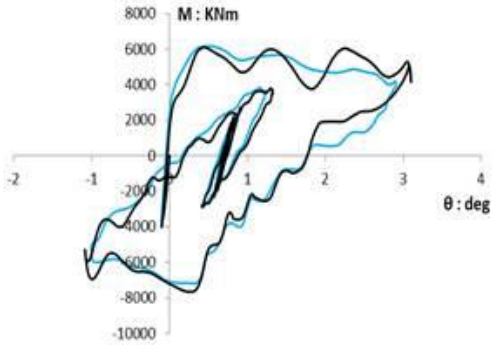

b) Foundation Moment - Rotation

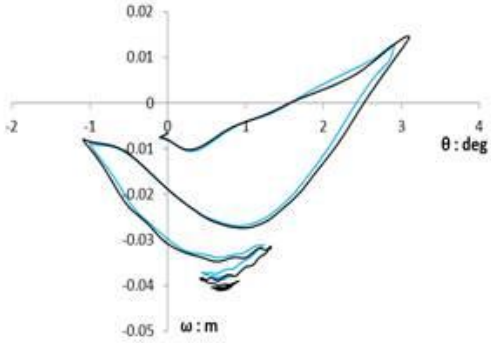

c) Settlement - Foundation Rotation

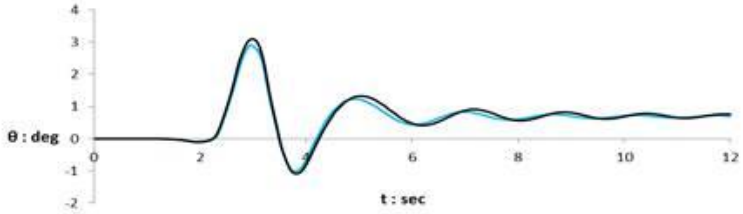

d) Foundation Rotation - time

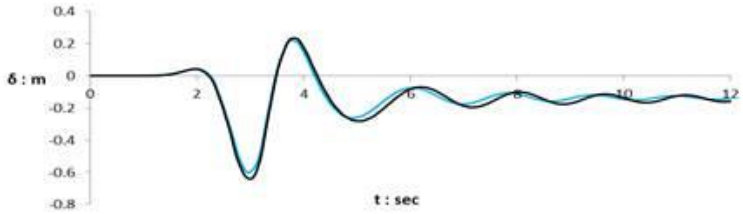

e) Deck Displacement - time

Figure 3.17 Dynamic Results of the Rocking Models under Ricker 0.5Hz – 0.6g base excitation.

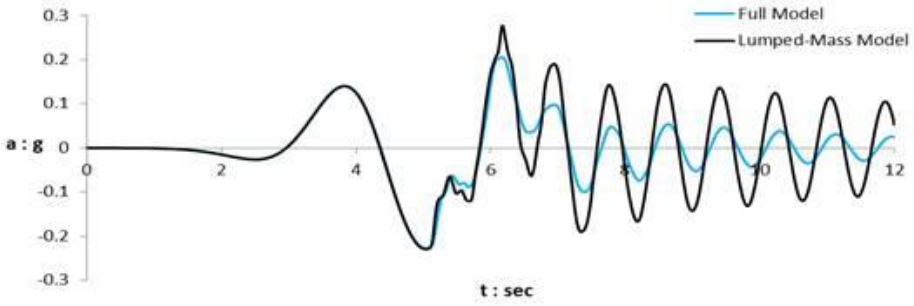

a) Deck Acceleration

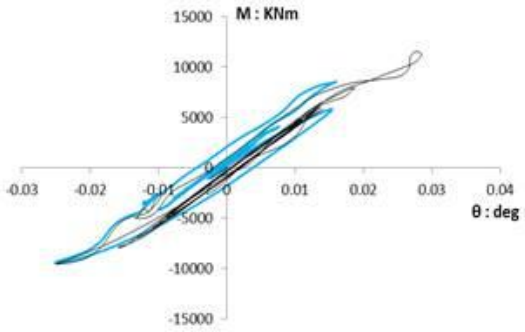

b) Foundation Moment - Rotation

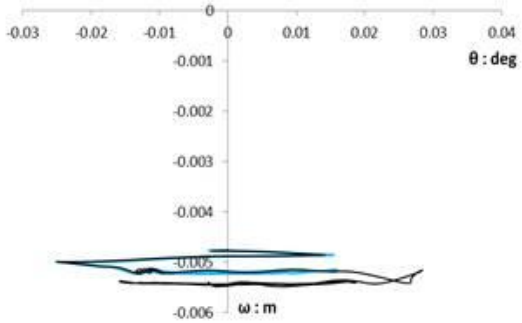

c) Settlement - Foundation Rotation

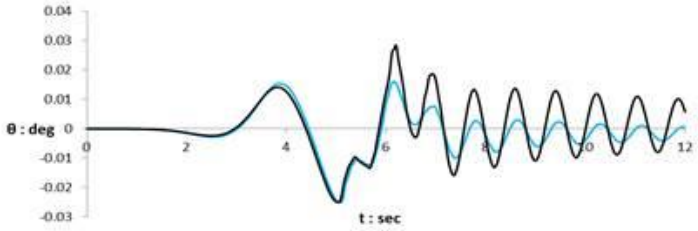

d) Foundation Rotation - time

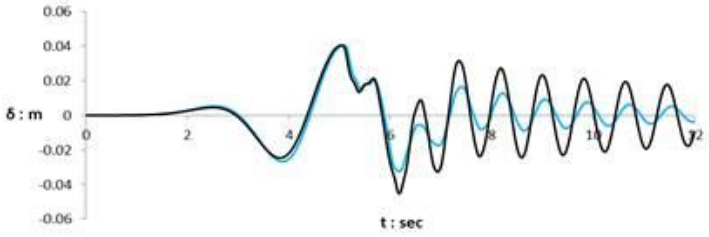

e) Deck Displacement - time

Figure 3.18 Dynamic Results of the Conventional Models under Ricker 0.25Hz – 0.2g base excitation.

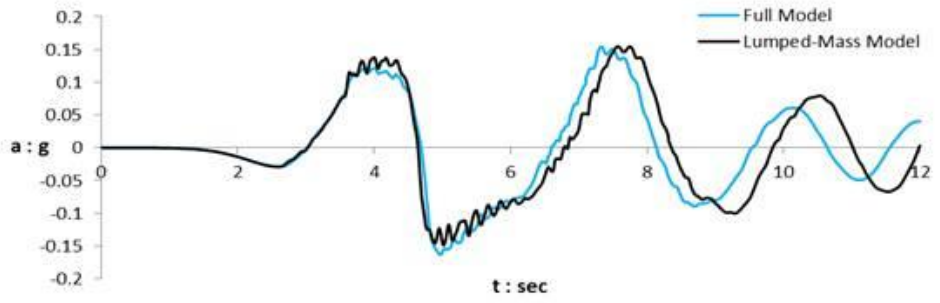

a) Deck Acceleration

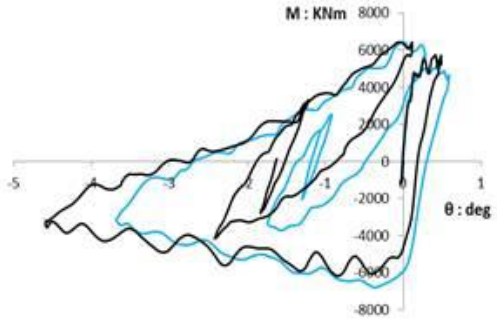

b) Foundation Moment - Rotation

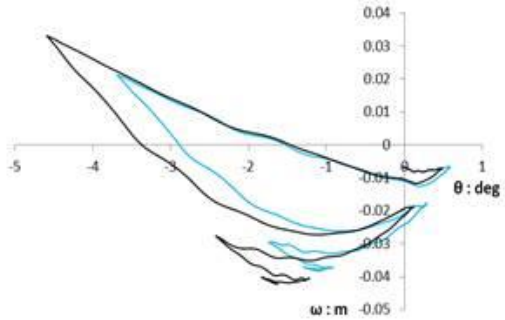

c) Settlement - Foundation Rotation

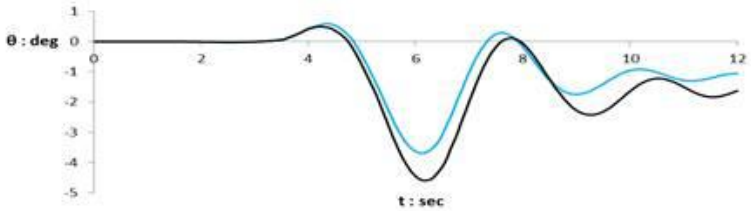

d) Foundation Rotation - time

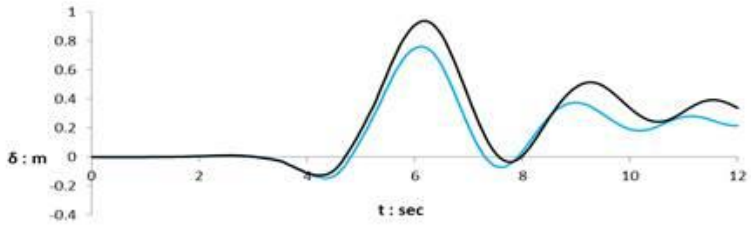

e) Deck Displacement - time

Figure 3.19 Dynamic Results of the Rocking Models under Ricker 0.25Hz – 0.2g base excitation.

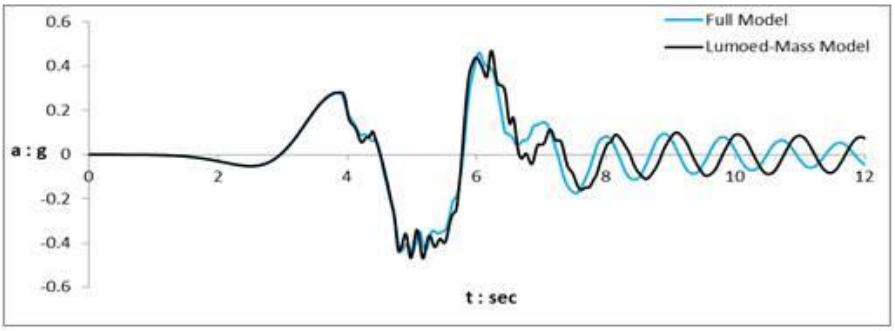

a) Deck Acceleration

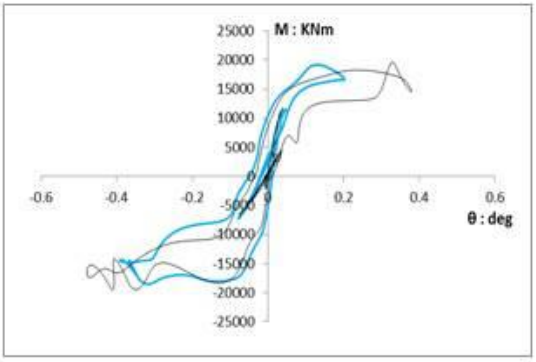

b) Foundation Moment - Rotation

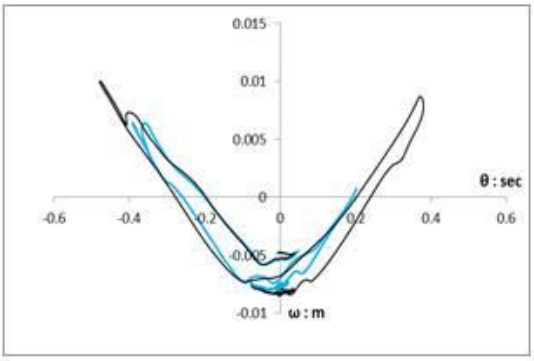

c) Settlement - Foundation Rotation

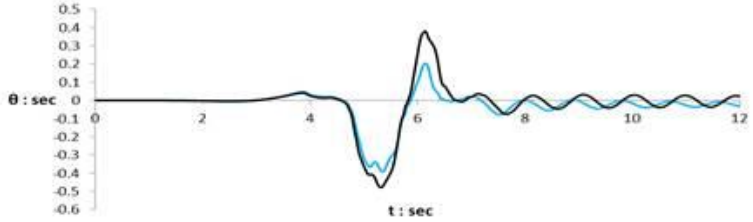

d) Foundation Rotation - time

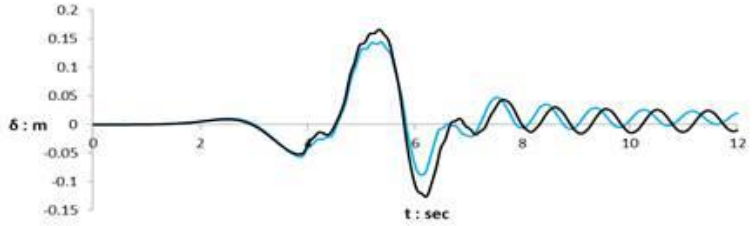

e) Deck Displacement - time

Figure 3.20 Dynamic Results of the Conventional Models under Ricker 0.25Hz – 0.4g base excitation.

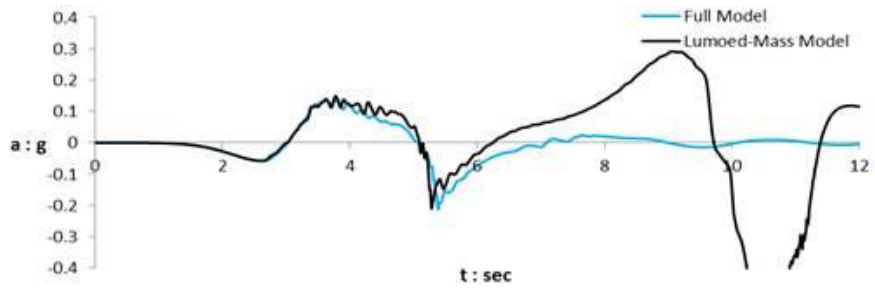

a) Deck Acceleration

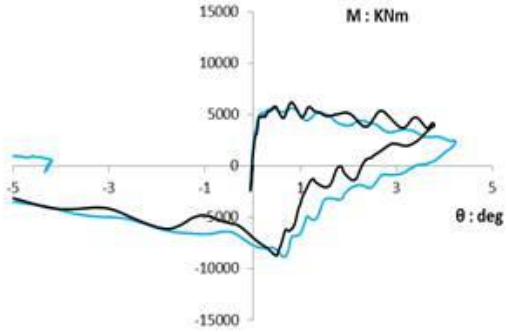

b) Foundation Moment - Rotation

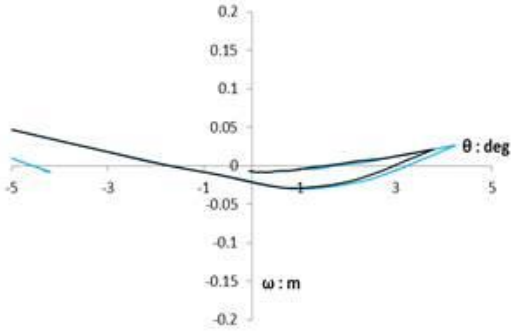

c) Settlement - Foundation Rotation

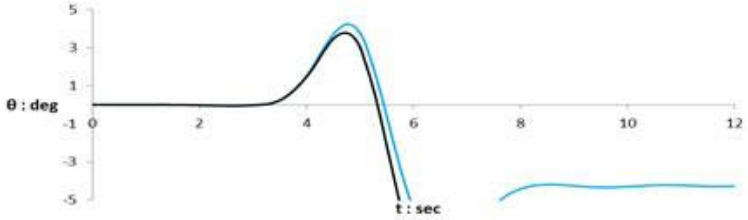

d) Foundation Rotation - time

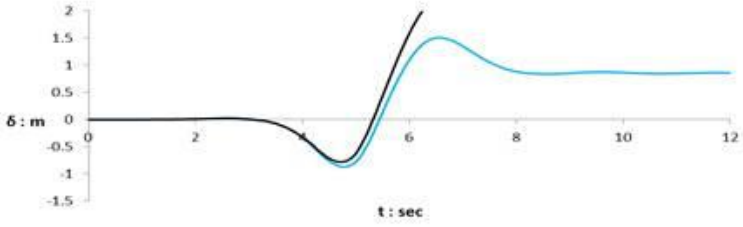

e) Deck Displacement - time

Figure 3.21 Dynamic Results of the Rocking Models under Ricker 0.25Hz – 0.4g base excitation.

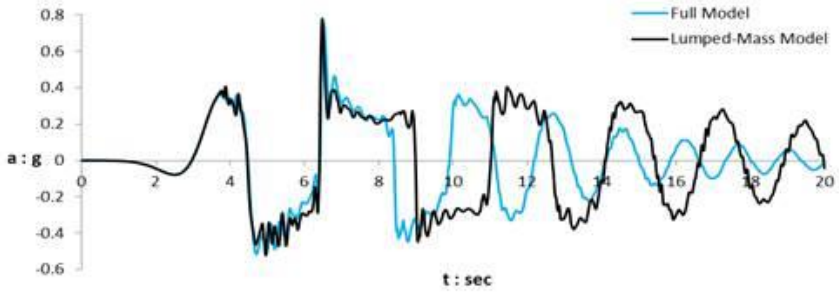

a) Deck Acceleration

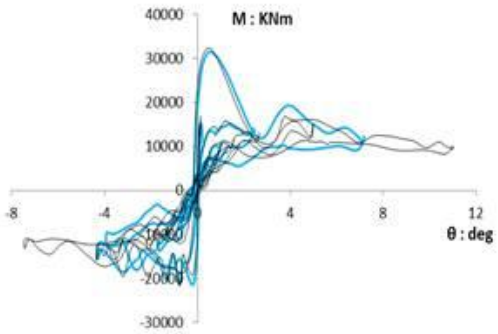

b) Foundation Moment - Rotation

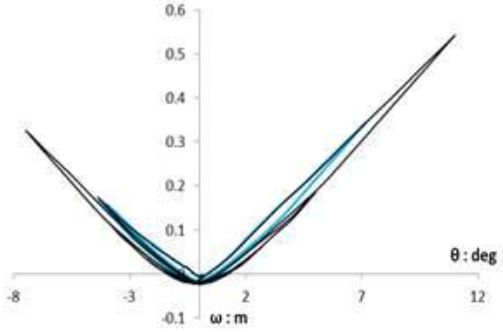

c) Settlement - Foundation Rotation

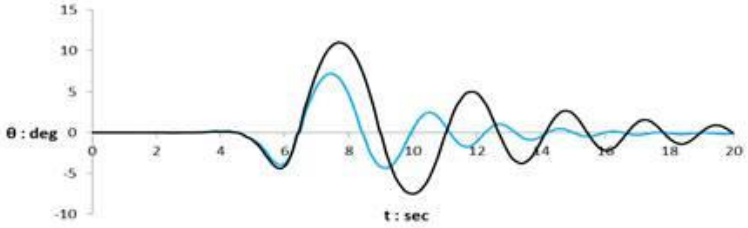

d) Foundation Rotation - time

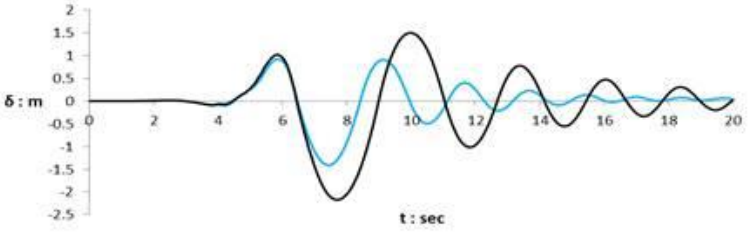

e) Deck Displacement - time

Figure 3.22 Dynamic Results of the Conventional Models under Ricker 0.25Hz – 0.6g base excitation.

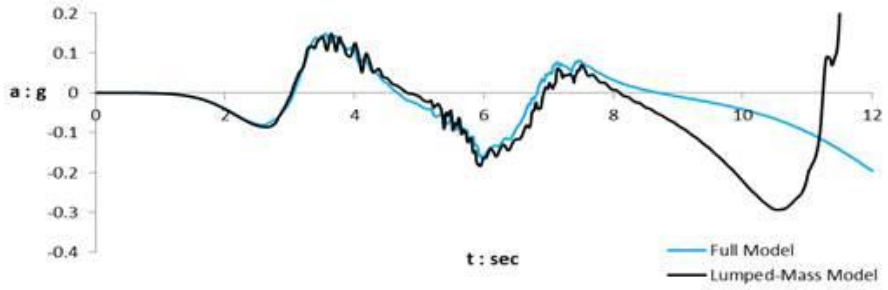

a) Deck Acceleration

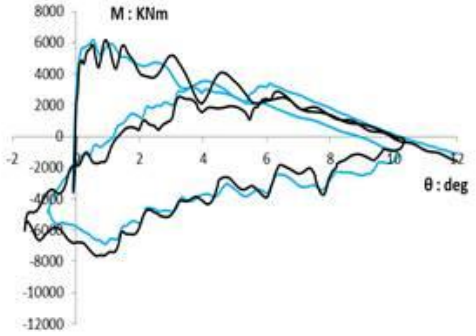

b) Foundation Moment - Rotation

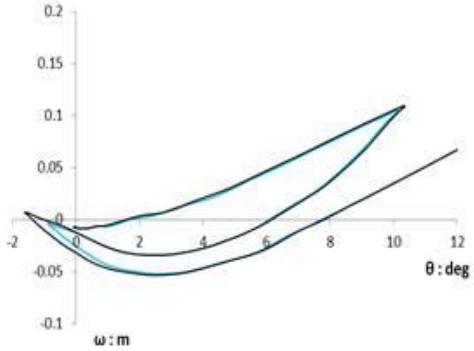

c) Settlement - Foundation Rotation

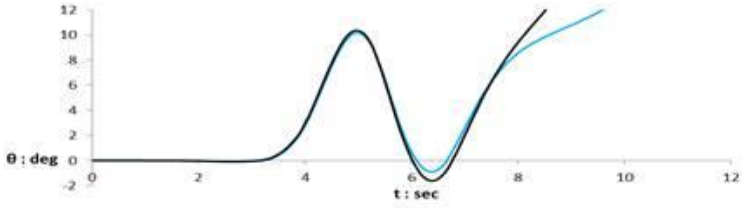

d) Foundation Rotation - time

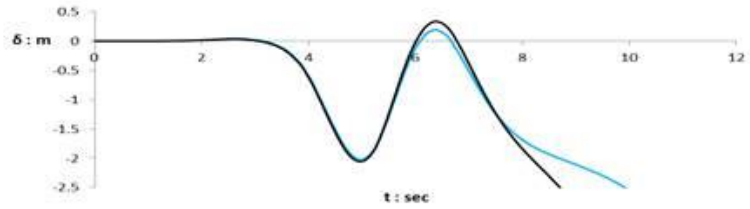

e) Deck Displacement - time

Figure 3.23 Dynamic Results of the Rocking Models under Ricker 0.25Hz – 0.6g base excitation.

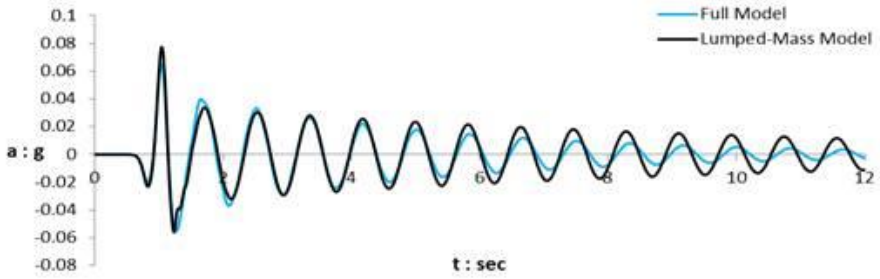

a) Deck Acceleration

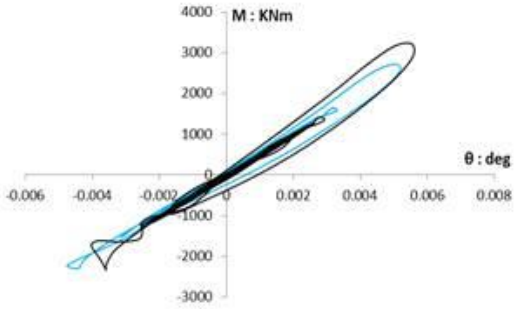

b) Foundation Moment - Rotation

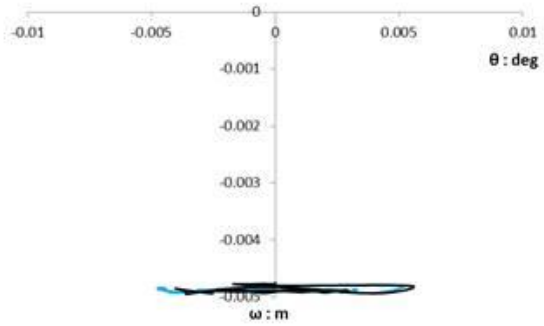

c) Settlement - Foundation Rotation

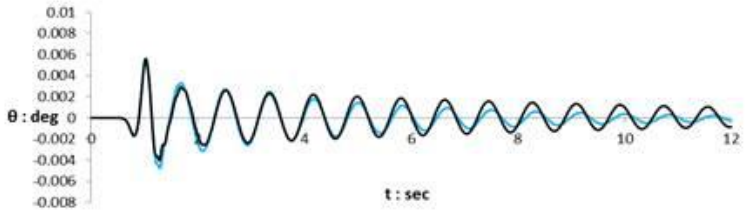

d) Foundation Rotation - time

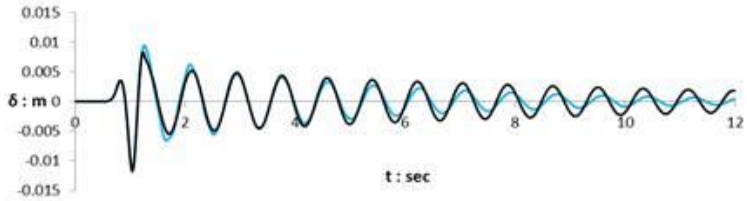

e) Deck Displacement - time

Figure 3.24 Dynamic Results of the Conventional Models under Ricker 2Hz – 0.2g base excitation.

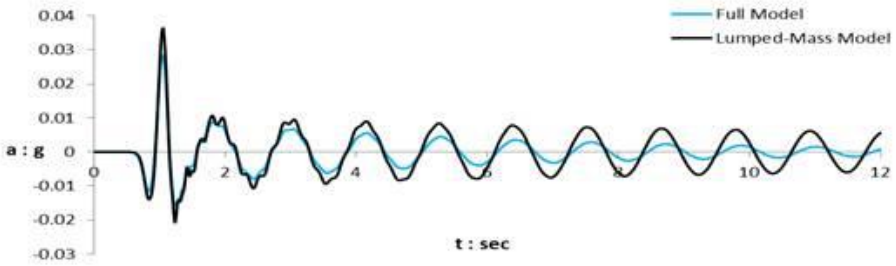

a) Deck Acceleration

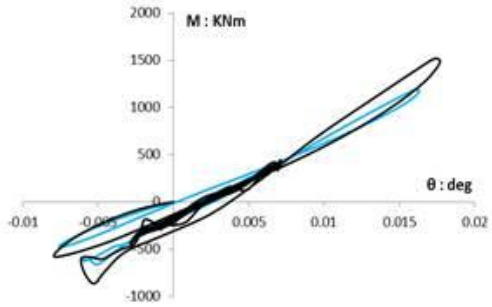

b) Foundation Moment - Rotation

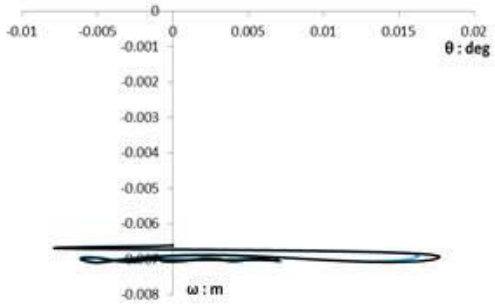

c) Settlement - Foundation Rotation

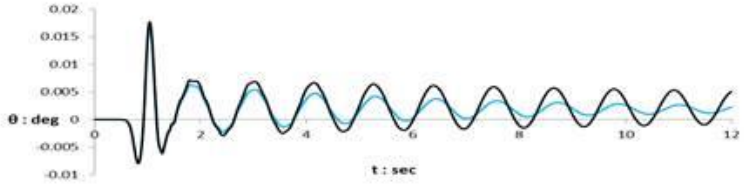

d) Foundation Rotation - time

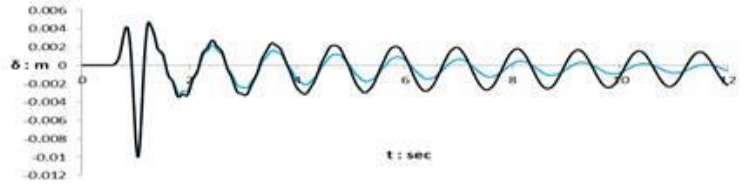

e) Deck Displacement - time

Figure 3.25 Dynamic Results of the Rocking Models under Ricker 2Hz – 0.2g base excitation.

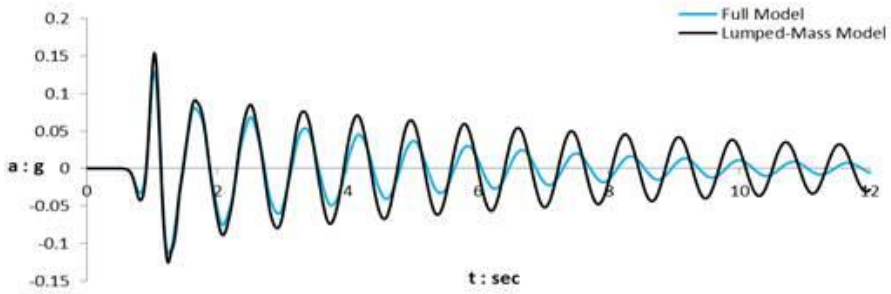

a) Deck Acceleration

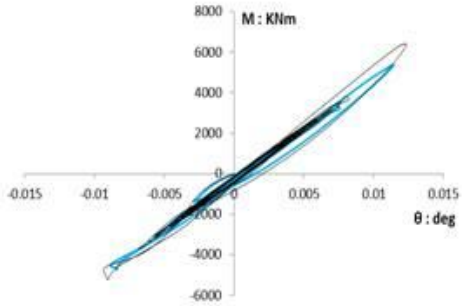

b) Foundation Moment - Rotation

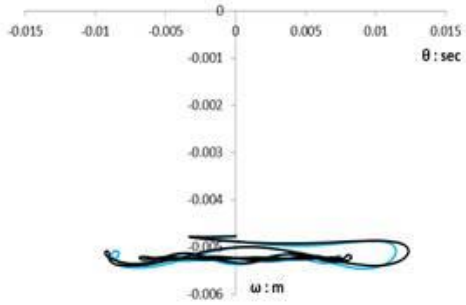

c) Settlement - Foundation Rotation

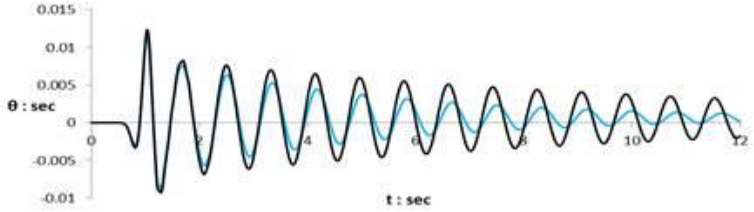

d) Foundation Rotation - time

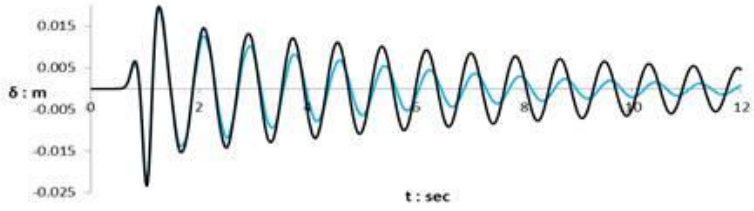

e) Deck Displacement - time

Figure 3.26 Dynamic Results of the Conventional Models under Ricker 2Hz – 0.4g base excitation.

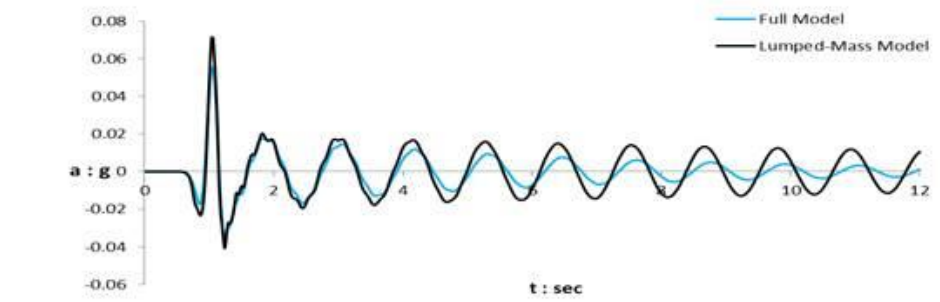

a) Deck Acceleration

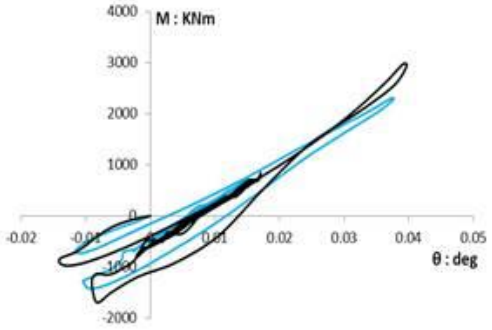

b) Foundation Moment - Rotation

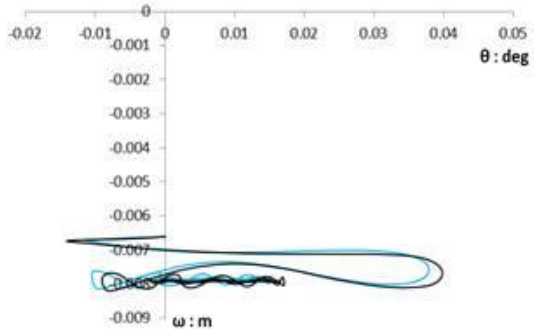

c) Settlement - Foundation Rotation

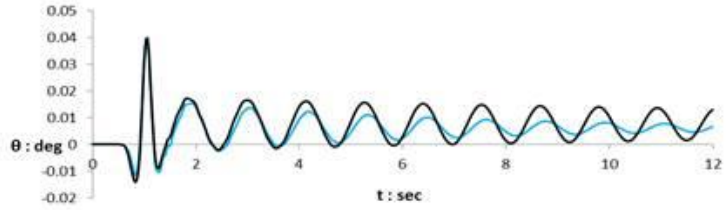

d) Foundation Rotation - time

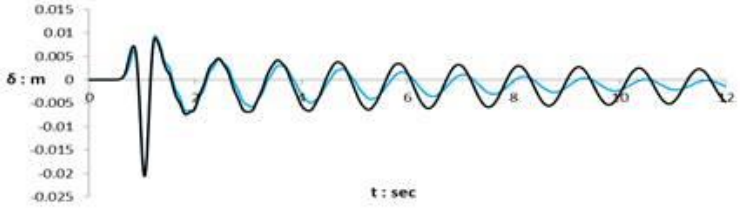

e) Deck Displacement - time

Figure 3.27 Dynamic Results of the Rocking Models under Ricker 2Hz – 0.4g base excitation.

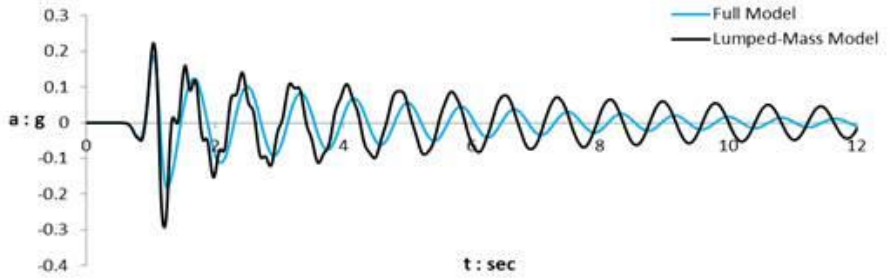

a) Deck Acceleration

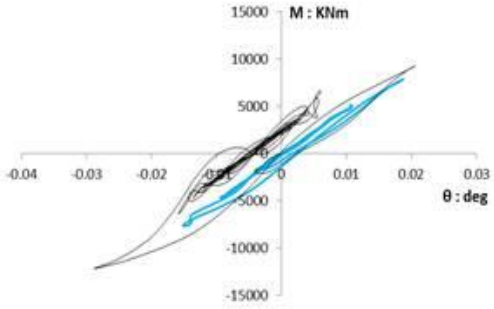

b) Foundation Moment - Rotation

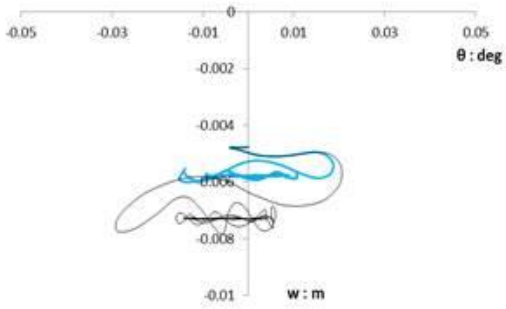

c) Settlement - Foundation Rotation

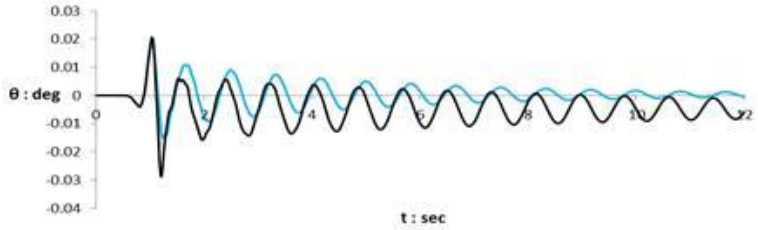

d) Foundation Rotation - time

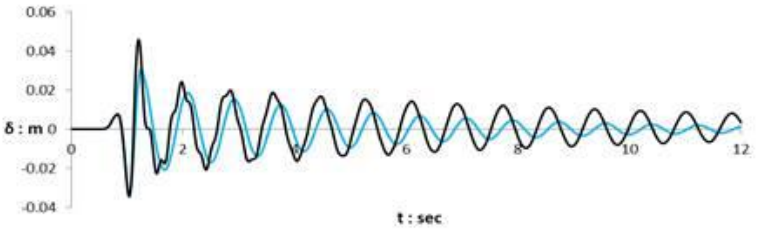

e) Deck Displacement - time

Figure 3.28 Dynamic Results of the Conventional Models under Ricker 2Hz – 0.6g base excitation.

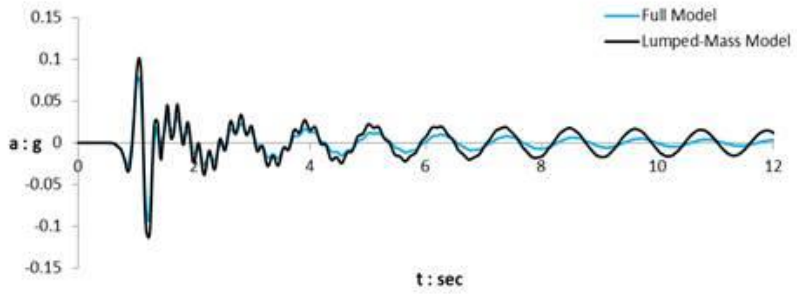

a) Deck Acceleration

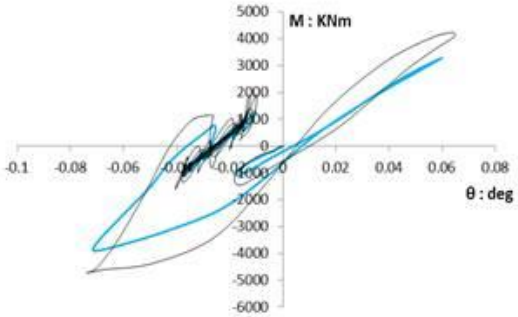

b) Foundation Moment - Rotation

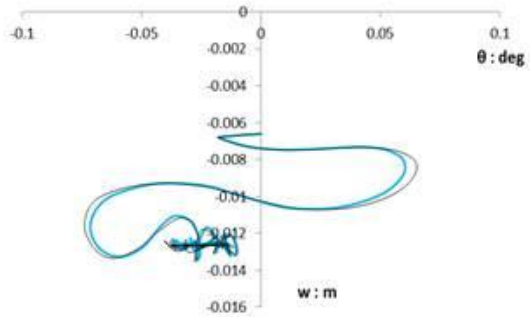

c) Settlement - Foundation Rotation

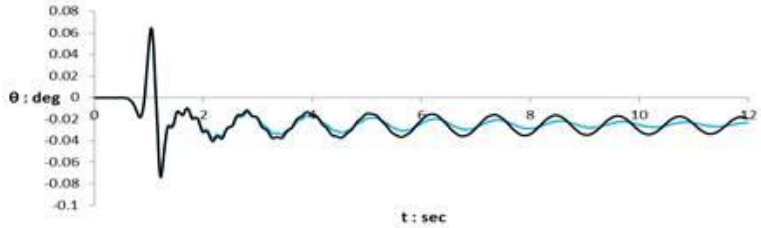

d) Foundation Rotation - time

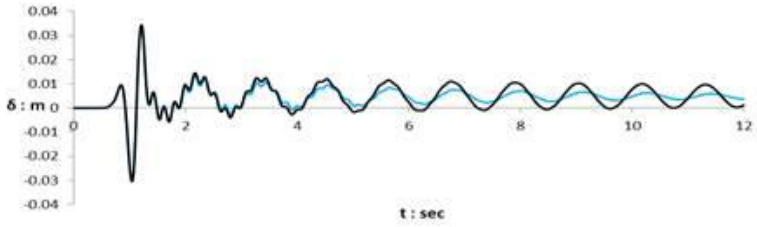

e) Deck Displacement - time

Figure 3.29 Dynamic Results of the Rocking Models under Ricker 2Hz – 0.6g base excitation.

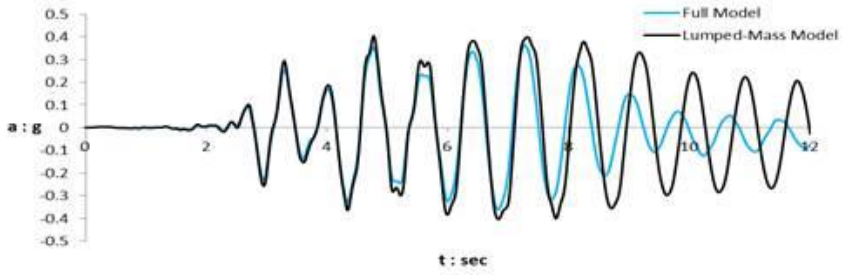

a) Deck Acceleration

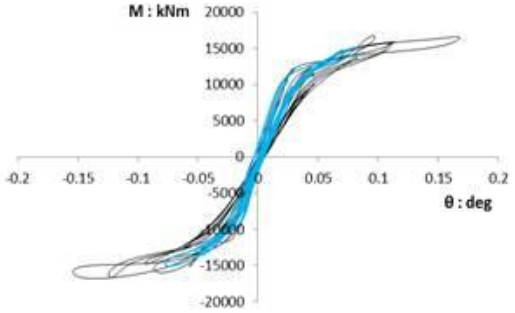

b) Foundation Moment - Rotation

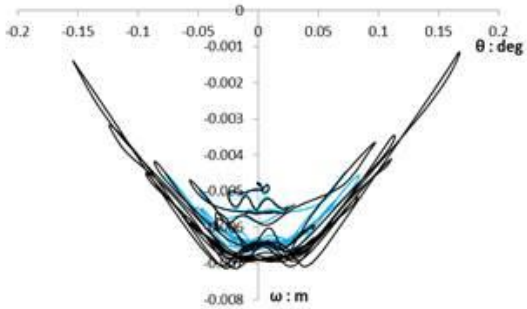

c) Settlement - Foundation Rotation

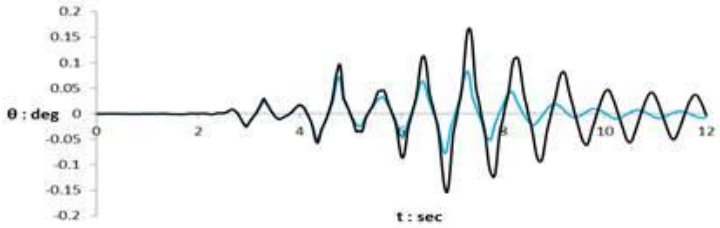

d) Foundation Rotation - time

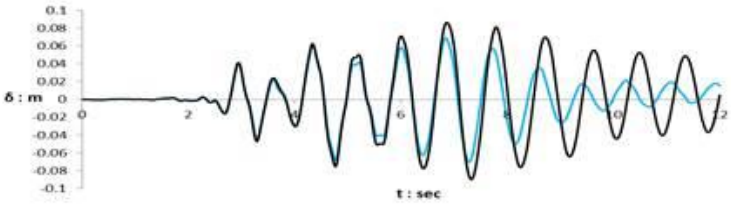

e) Deck Displacement - time

Figure 3.30 Dynamic Results of the Conventional Models under Kalamata EQ base excitation.

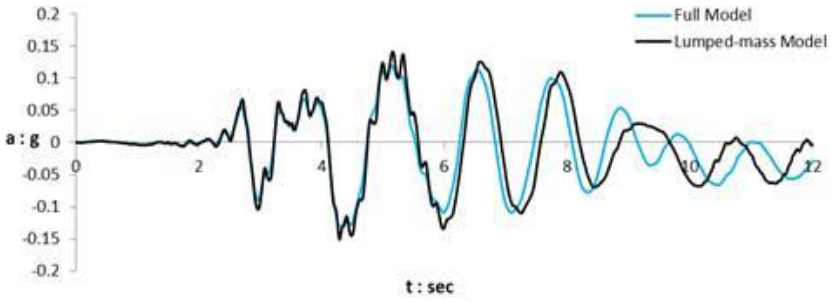

a) Deck Acceleration

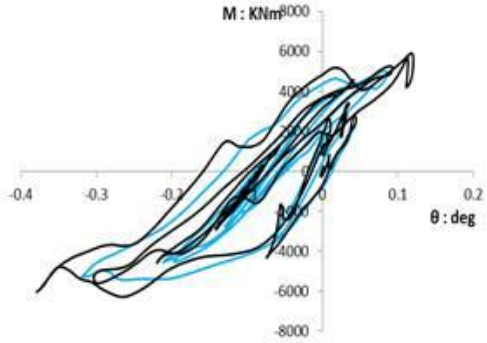

b) Foundation Moment - Rotation

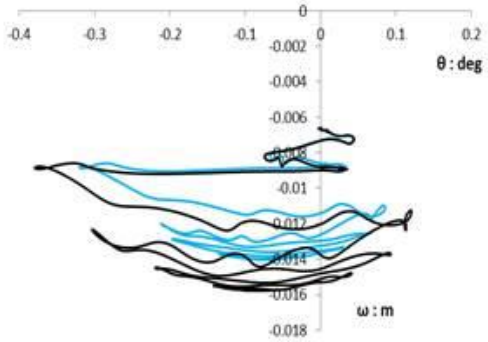

c) Settlement - Foundation Rotation

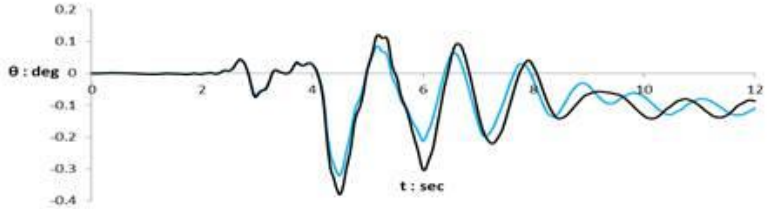

d) Foundation Rotation - time

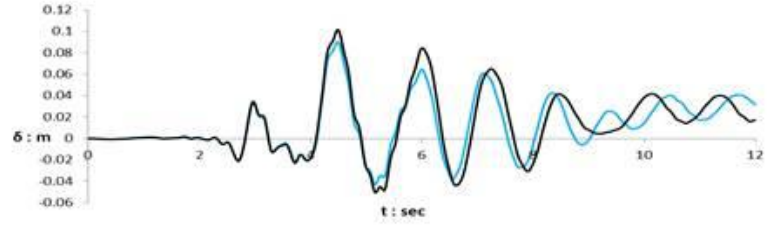

e) Deck Displacement - time

Figure 3.31 Dynamic Results of the Rocking Models under Kalamata EQ base excitation.

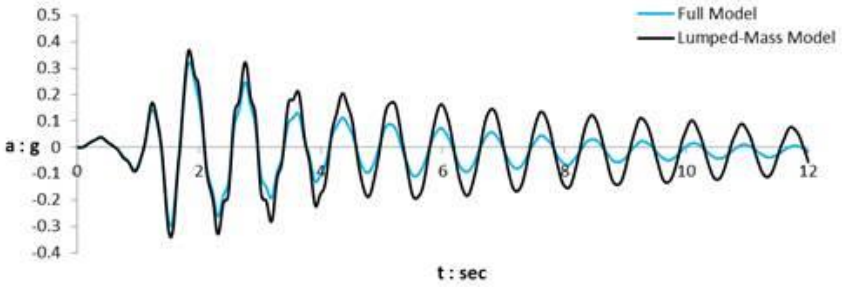

a) Deck Acceleration

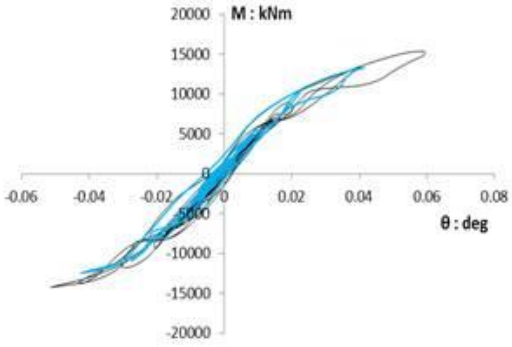

b) Foundation Moment - Rotation

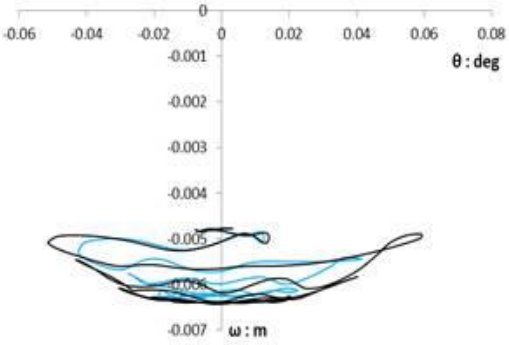

c) Settlement - Foundation Rotation

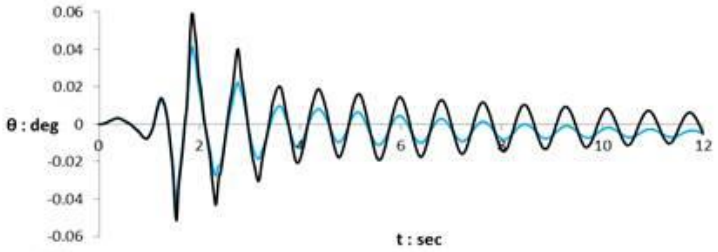

d) Foundation Rotation - time

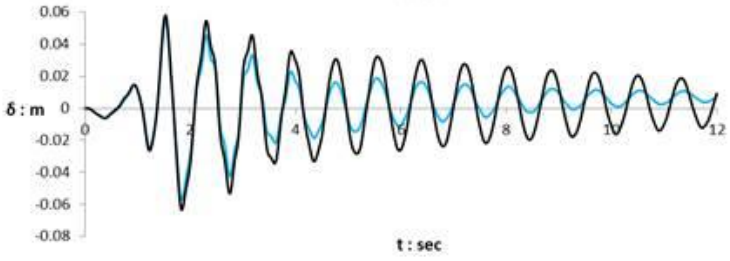

e) Deck Displacement - time

Figure 3.32 Dynamic Results of the Conventional Models under Aegion EQ base excitation.

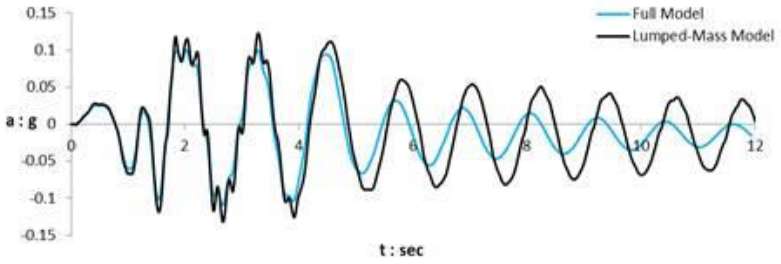

a) Deck Acceleration

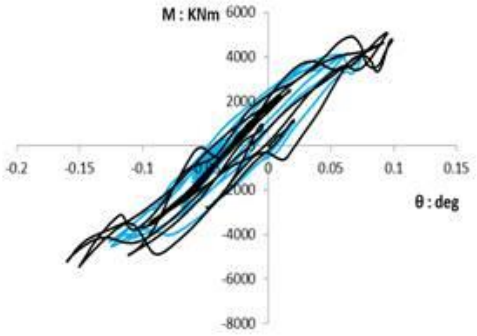

b) Foundation Moment - Rotation

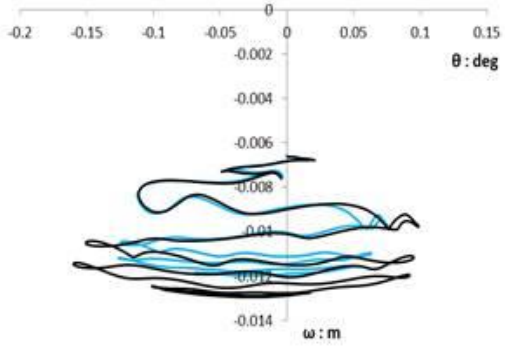

c) Settlement - Foundation Rotation

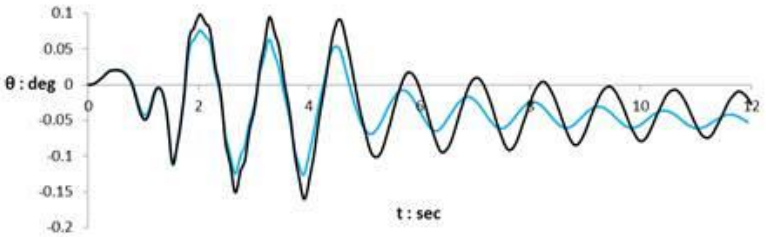

d) Foundation Rotation - time

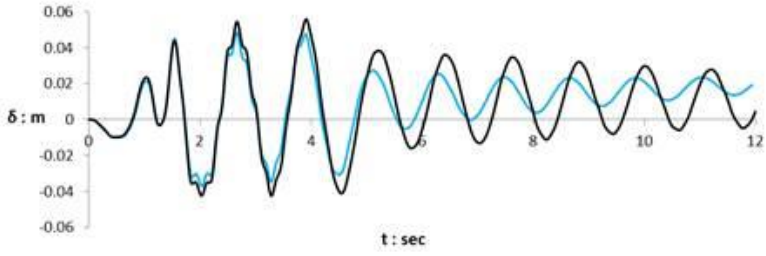

e) Deck Displacement - time

Figure 3.33 Dynamic Results of the Rocking Models under Aegion EQ base excitation.

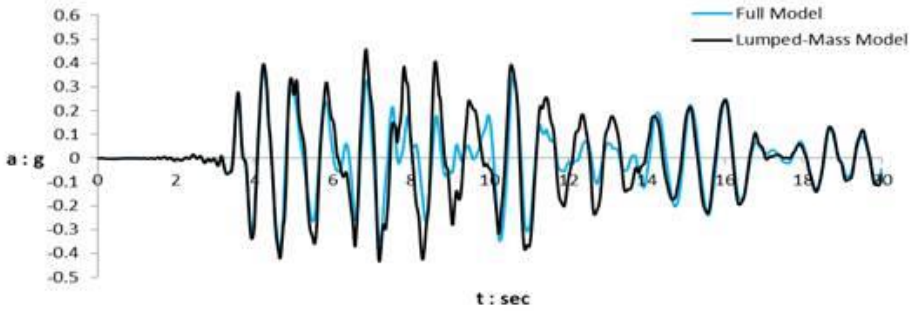

a) Deck Acceleration

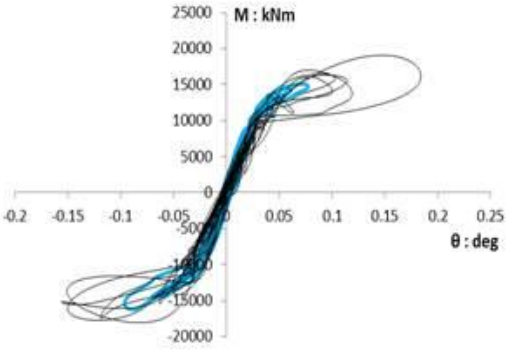

b) Foundation Moment - Rotation

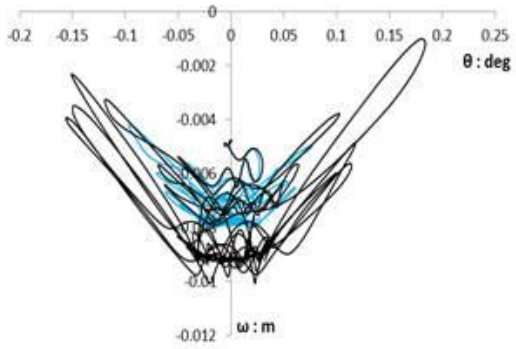

c) Settlement - Foundation Rotation

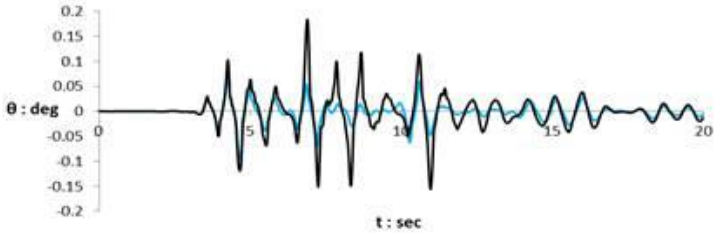

d) Foundation Rotation - time

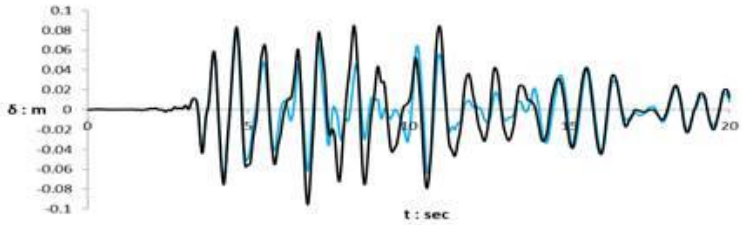

e) Deck Displacement - time

Figure 3.34 Dynamic Results of the Conventional Models under Lefkada EQ base excitation.

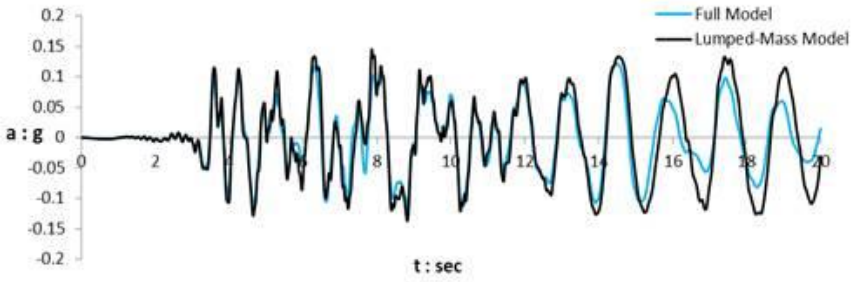

a) Deck Acceleration

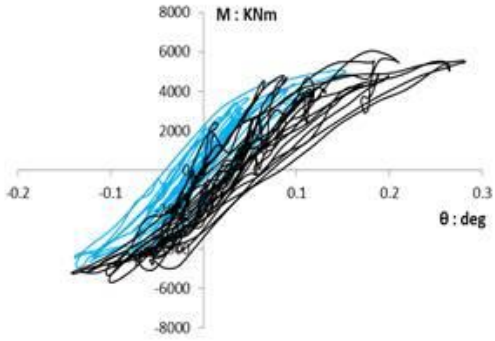

b) Foundation Moment - Rotation

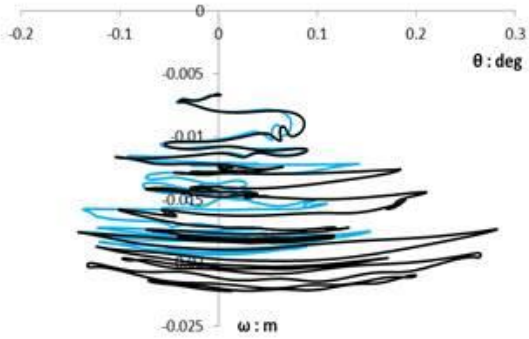

c) Settlement - Foundation Rotation

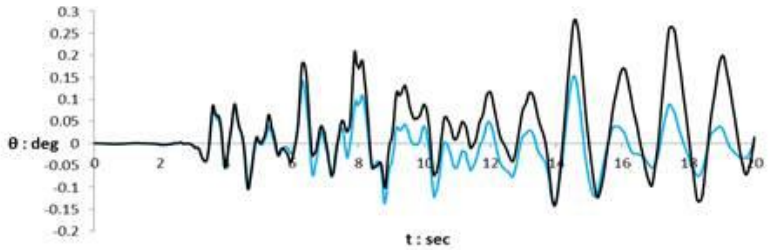

d) Foundation Rotation - time

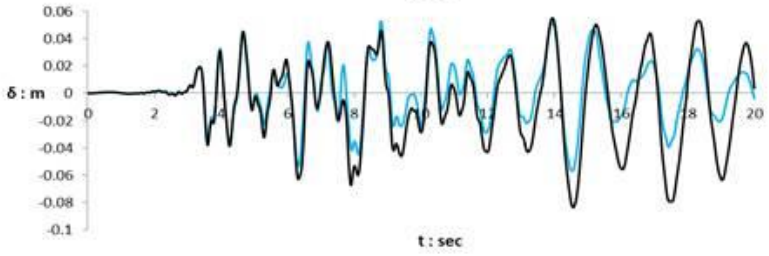

e) Deck Displacement - time

Figure 3.35 Dynamic Results of the Rocking Models under Lefkada EQ base excitation.

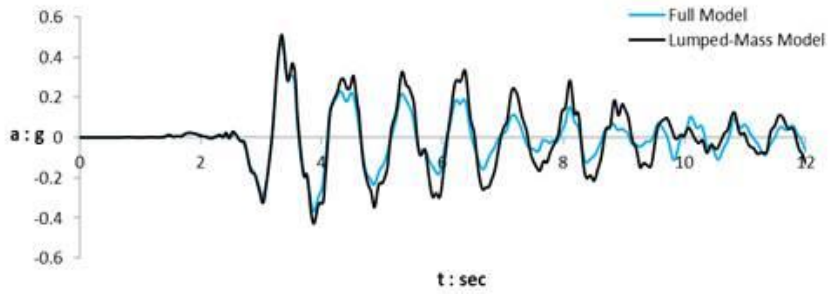

a) Deck Acceleration

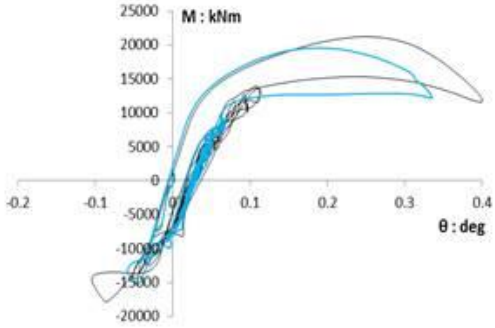

b) Foundation Moment - Rotation

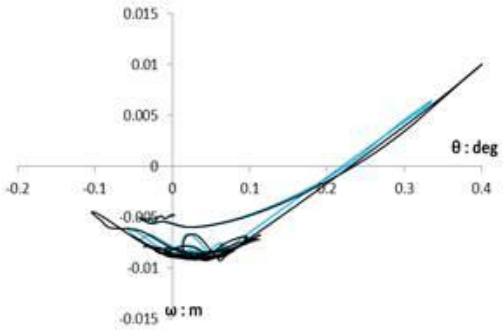

c) Settlement - Foundation Rotation

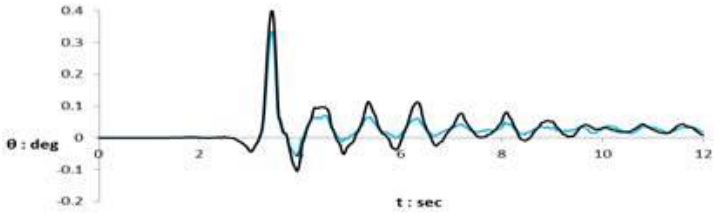

d) Foundation Rotation - time

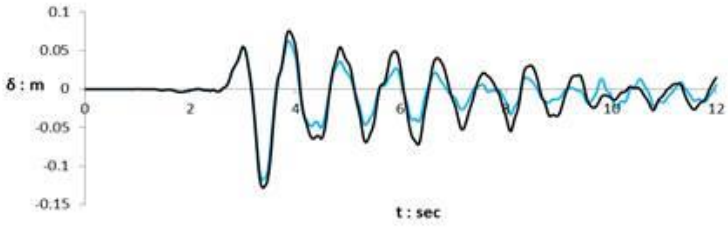

e) Deck Displacement - time

Figure 3.36 Dynamic Results of the Conventional Models under LAquila EQ base excitation.

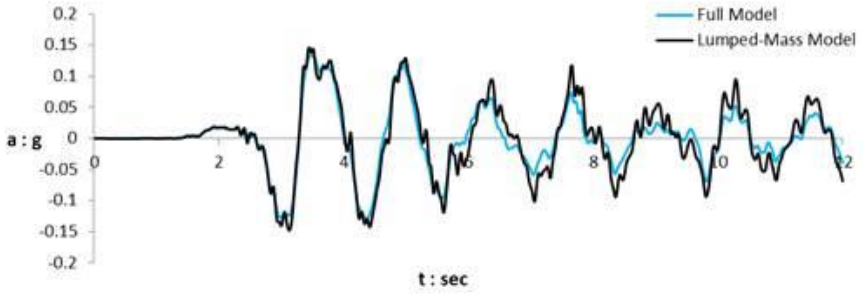

a) Deck Acceleration

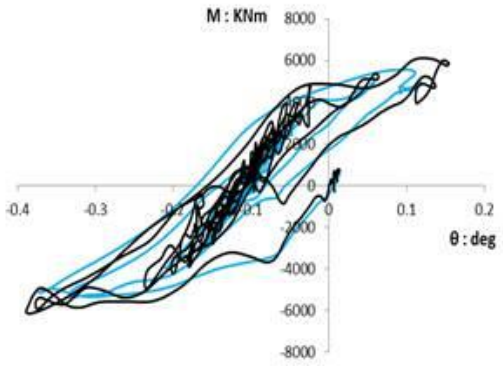

b) Foundation Moment - Rotation

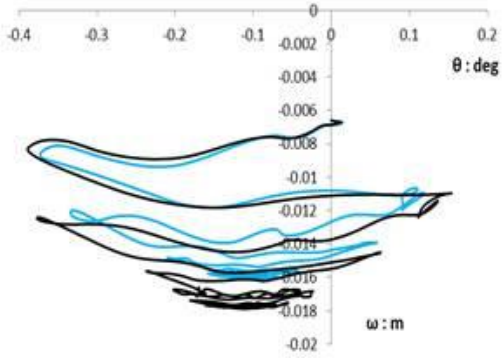

c) Settlement - Foundation Rotation

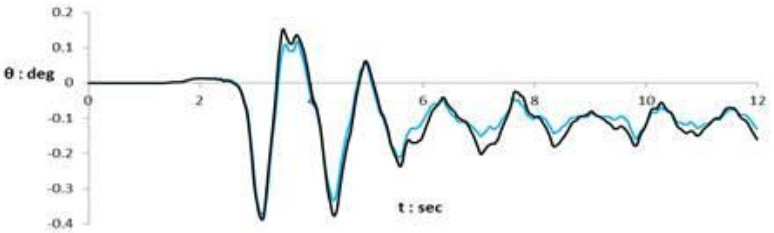

d) Foundation Rotation - time

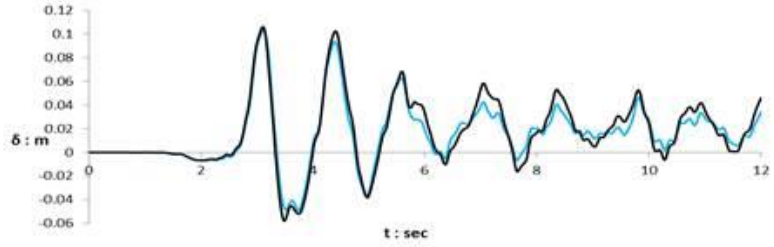

e) Deck Displacement - time

Figure 3.37 Dynamic Results of the Rocking Models under LAquila EQ base excitation.

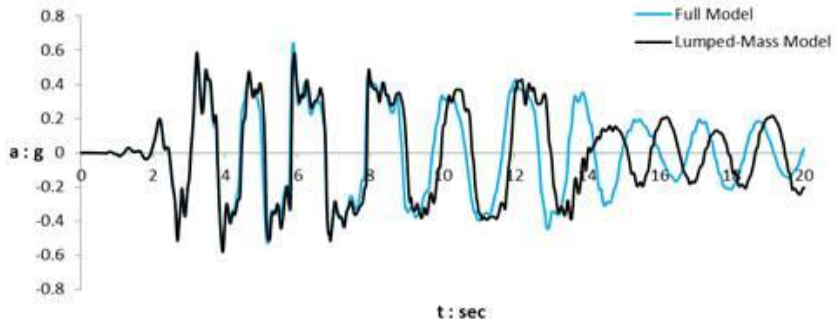

a) Deck Acceleration

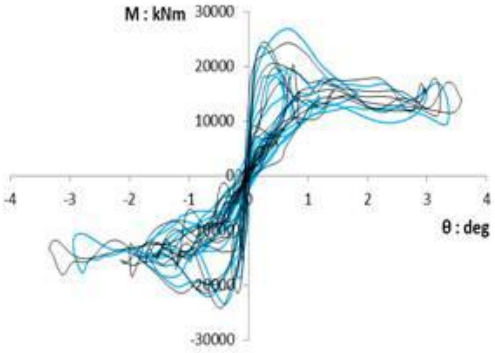

b) Foundation Moment - Rotation

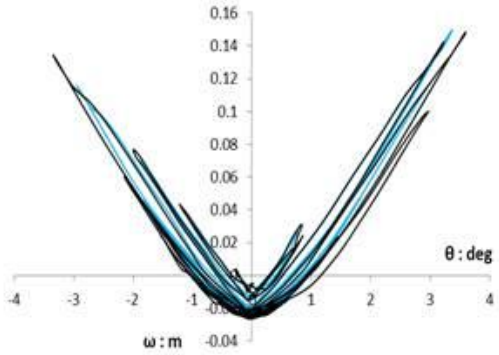

c) Settlement - Foundation Rotation

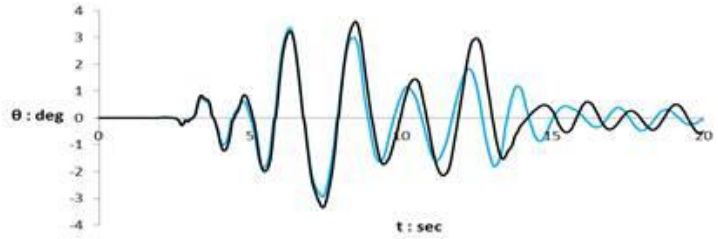

d) Foundation Rotation - time

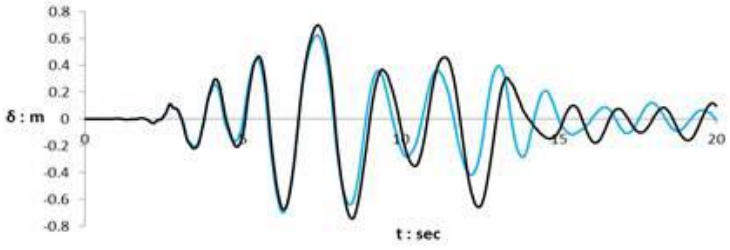

e) Deck Displacement - time

Figure 3.38 Dynamic Results of the Conventional Models under Takatori EQ base excitation.

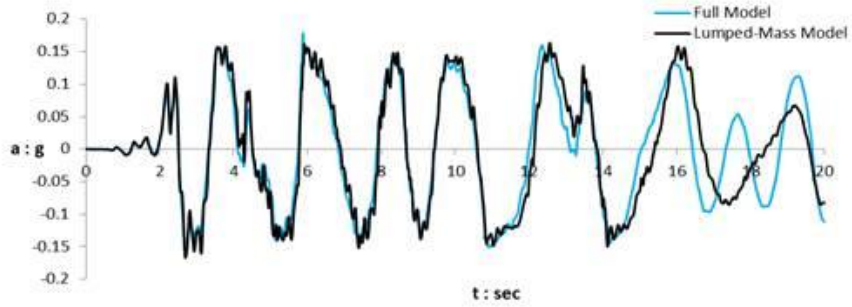

a) Deck Acceleration

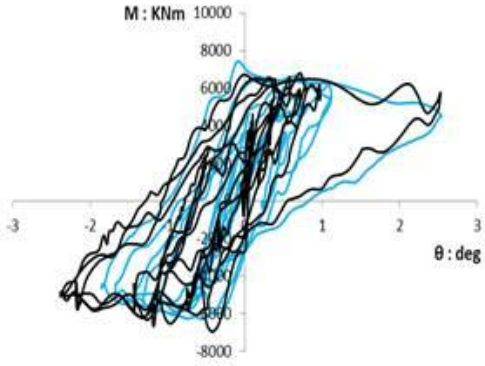

b) Foundation Moment - Rotation

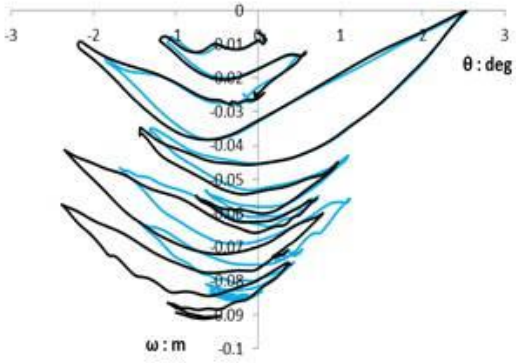

c) Settlement - Foundation Rotation

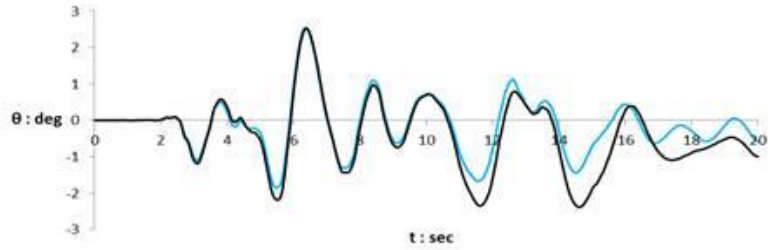

d) Foundation Rotation - time

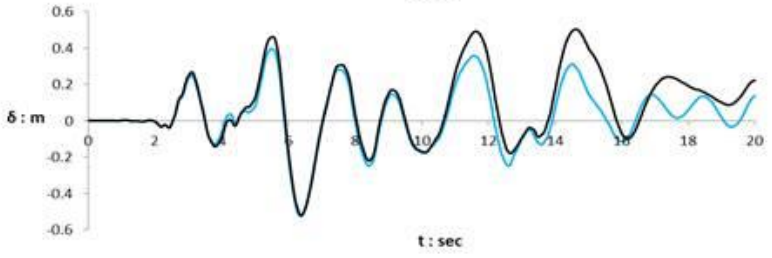

e) Deck Displacement - time

Figure 3.39 Dynamic Results of the Rocking Models under Takatori EQ base excitation.

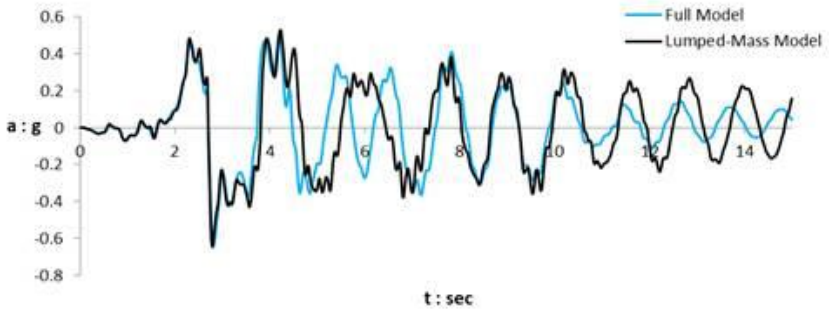

a) Deck Acceleration

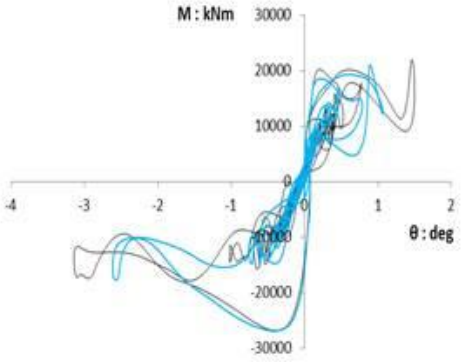

b) Foundation Moment - Rotation

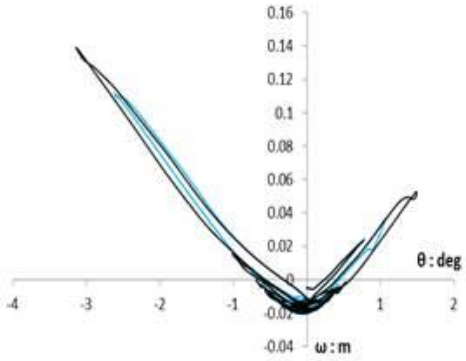

c) Settlement - Foundation Rotation

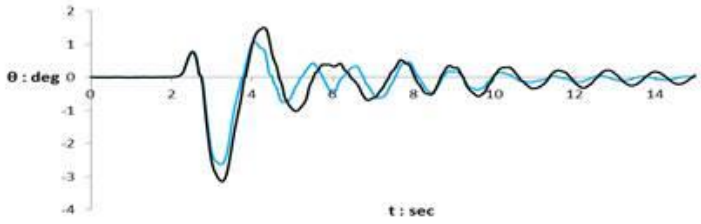

d) Foundation Rotation - time

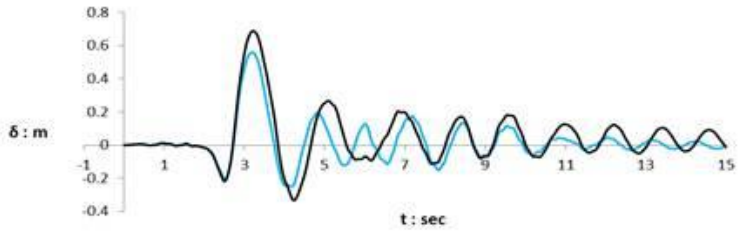

e) Deck Displacement - time

Figure 3.40 Dynamic Results of the Conventional Models under Northridge Rinaldi EQ base excitation.

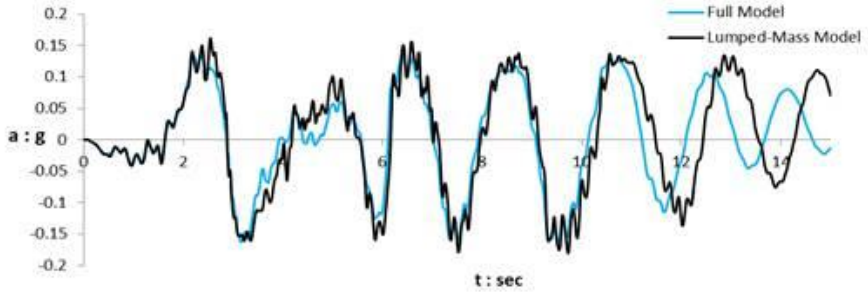

a) Deck Acceleration

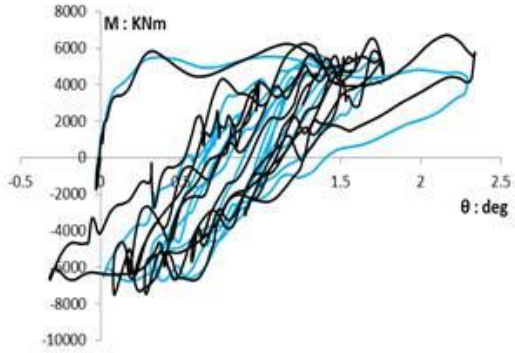

b) Foundation Moment - Rotation

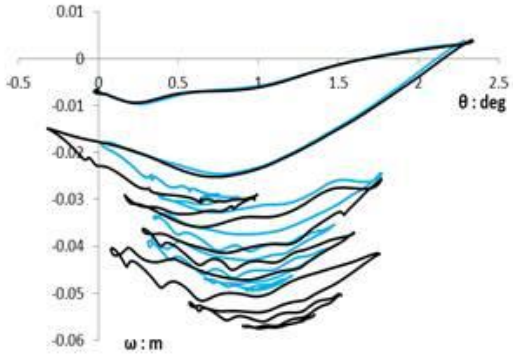

c) Settlement - Foundation Rotation

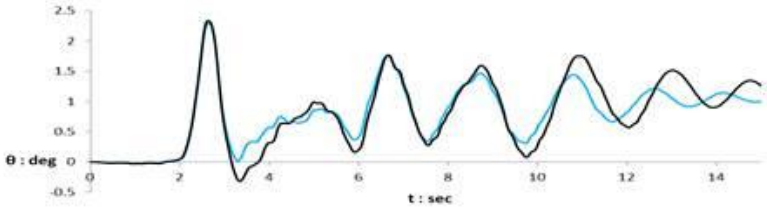

d) Foundation Rotation - time

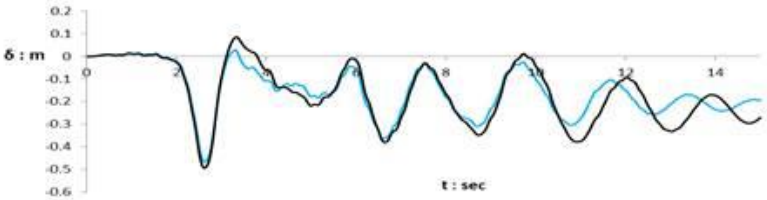

e) Deck Displacement - time

Figure 3.41 Dynamic Results of the Rocking Models under Northridge Rinaldi EQ base excitation.

CHAPTER 4

SEISMIC PERFORMANCE OF BRIDGE MODEL-A: EFFECTIVNESS OF DOUBLING THE ROTATIONAL INERTIA

4.1 Introduction

In the previous chapter, a bridge simple model was examined in both conventional seismic design and the new philosophy of rocking isolation design, in an effort to examine the effect of the rotational inertia of the deck and comparing the cases of the lumped and geometrical deck.

To further more examine the problem under study and to assess the effects concluded in the previous chapter. In this chapter the previous FE model will be compared with another similar FE models, only different in the geometry of the deck (different rotational inertia).

4.2 FE Model Setup

In this chapter, three different Finite element models are compared in each of the cases of conventional design and rocking isolation design. The first model is the exact same used in the previous chapter which resembles the initial deck geometry and rotational inertia, the other two models, the deck geometry will be changed to increase the rotational inertia to the double compared to the preceding model while maintaining the deck mass by changing the density of the elements forming the deck geometry. *Figure 4.1*.

Model	***Deck Geometry***	***Rotational Inertia***
Model-A	(4 x 2 x 3.5) m	475.54 m^4
Model-B	(8 x 2 x 2) m	1144.67 m^4
Model-C	(12 x 2 x 2) m	2491.33 m^4

Table 4.1 Different Models used in the analysis and the corresponding rotational inertia

4.3 Dynamic Analysis

The previous models will be subjected to two base excitations different in intensity to examine the comparison in different cases.

4.3.1 Kalamata EQ Greece (1986).

Figure 4.2 shows the dynamic results for the three conventional models. By comparing the response Model-B is showing lower deck acceleration compared to Model-A, also Model-B shows lower foundation rotation, settlement and deck displacement.

Figure 4.3 shows the dynamic results for the three Rocking models. By comparing the response, the deck acceleration in both cases doesn't show much difference, while Model-B shows slightly higher settlement and lower foundation rotation.

Model-B also shows higher induced moment compared to Model-A.

Model-C shows that increasing the rotational inertia by changing the deck geometry to this extent is not very illustrative and comparable to the previous models in both the conventional design and rocking design cases.

4.3.1 Northridge Rinaldi EQ (1994).

Figure 4.4 shows the dynamic results of the three conventional models. By comparing the response, the deck acceleration and foundation rotation doesn't have a significant difference, Only Model-B results in a slightly higher settlement.

Figure 4.5 shows the dynamic results of the three Rocking models. By comparing the response the deck acceleration doesn't show much difference in peak values while Model-B shows higher vibrations, Model-B shows slightly lower foundation rotation and higher resulting moment.

Model-C shows that increasing the rotational inertia by changing the deck geometry to this extent is not very illustrative and comparable to the previous models in both the conventional design and rocking design cases.

4.4 Conclusions

From observing the above analysis, while the results didn't appear to have some obvious trend it can be concluded that changing the deck geometry in order to have more rotational inertia had some effects, more obvious in the case of the less strong motion (Kalamata) compared to the stronger motion (Rinaldi). This can be summarized as:

- Model-B shows lower foundation rotation compared to the original model especially significant in the case of Kalamata EQ
- Model –B also shows higher induced moment on the foundation, which would result to higher soil plastic deformation.
- The Full model in both cases shows higher damping characteristics and compared to the Lumped-mass model it shows less deck acceleration and foundation rotation.
- In the case of Model-C, increasing the rotational inertia to that extent proved to be not practical and incomparable with the previous two models.

Chapter 4

Figures

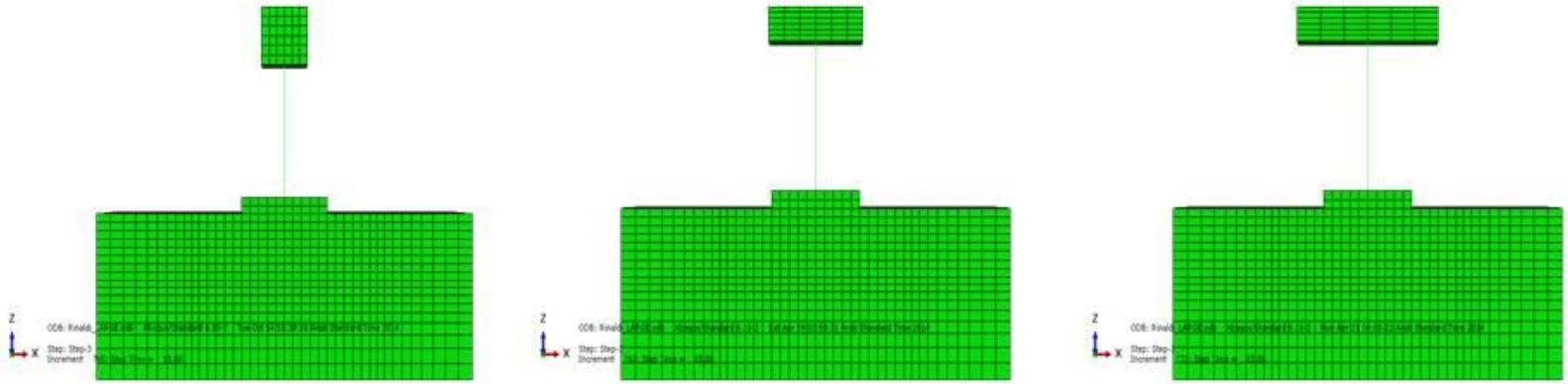

a) Conventional Models with the three different deck geometries

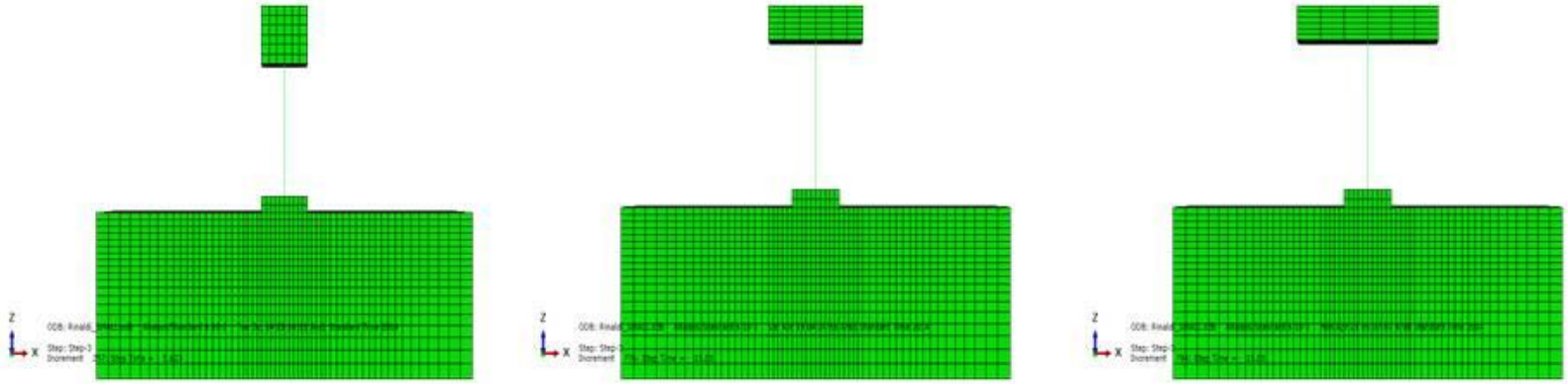

a) Rocking Models with the three different deck geometries

Figure 4.1 Different FE models used in the comparison.

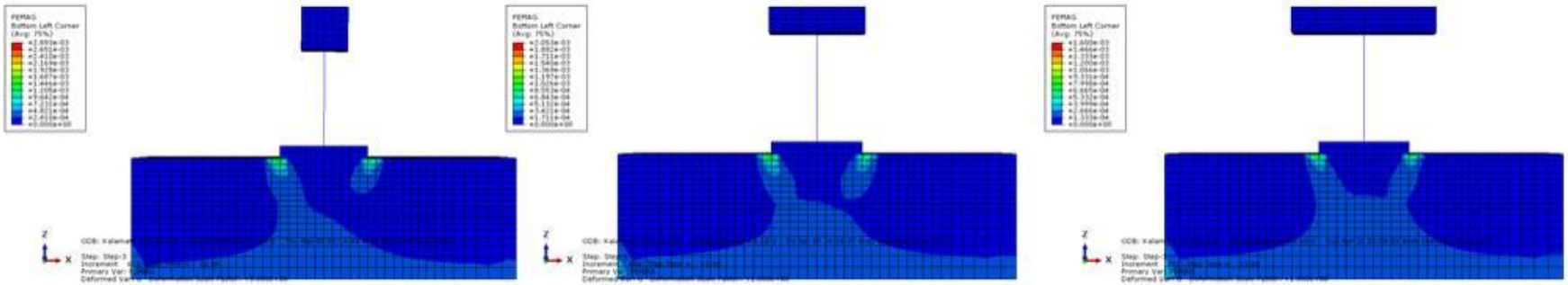

a) Models Used in the analysis, from left to right A, B & C.

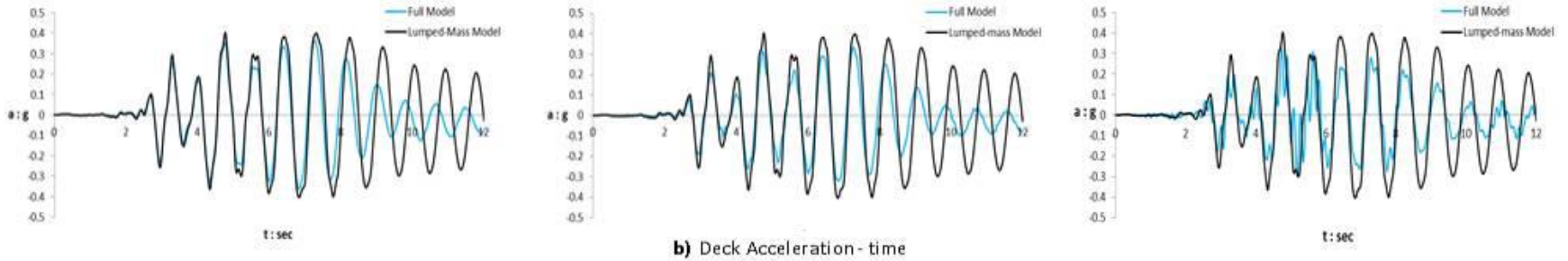

b) Deck Acceleration - time

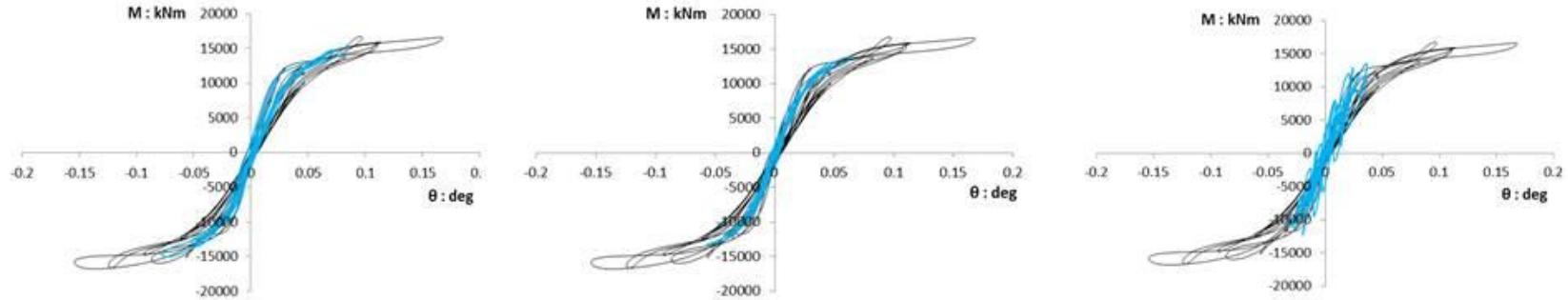

c) Moment – Foundation Rotation

Figure 4.2 Dynamic Results of The Conventional Models A,B&C Subjected to Kalamata EQ Excitation.

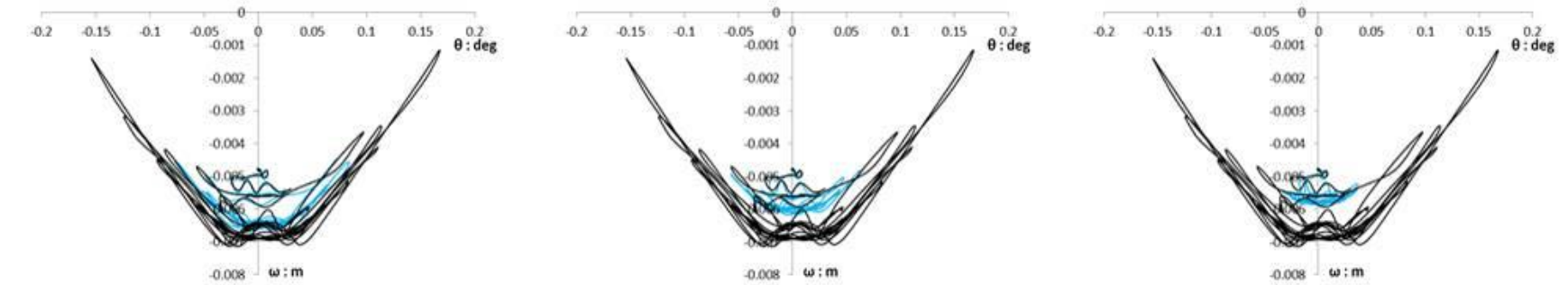

a) Settlement – Foundation Rotation.

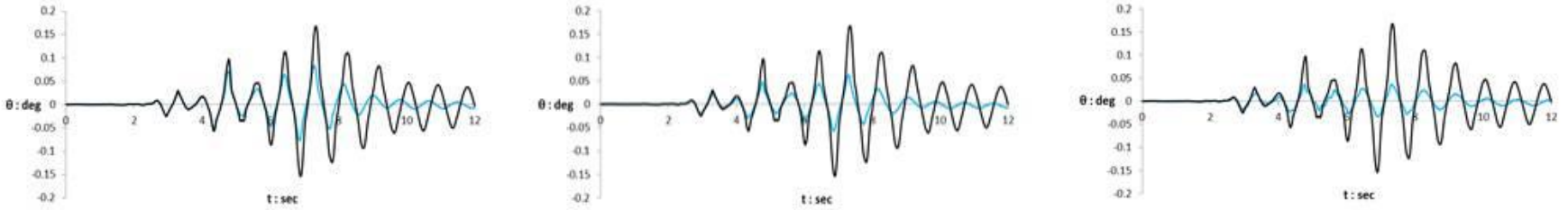

b) Foundation Rotation – time.

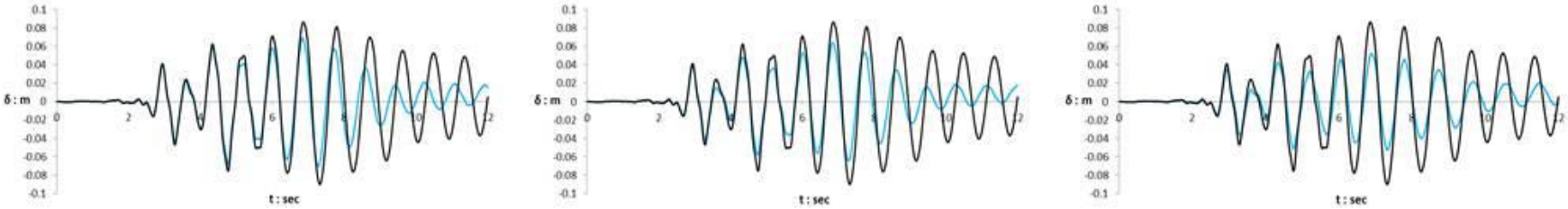

c) Deck Displacement – Time.

Figure 4.2 Dynamic Results of The Conventional Models A,B&C Subjected to Kalamata EQ Excitation.

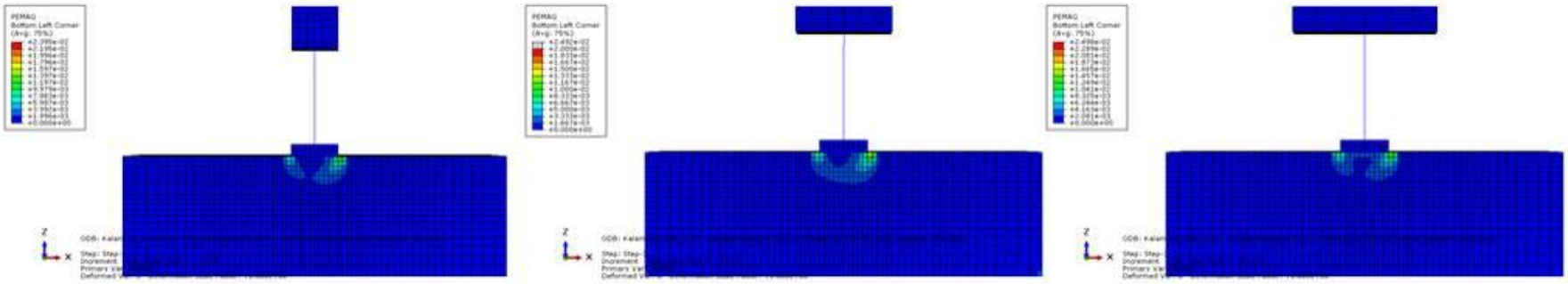

a) Models Used in the analysis, from left to right A, B & C.

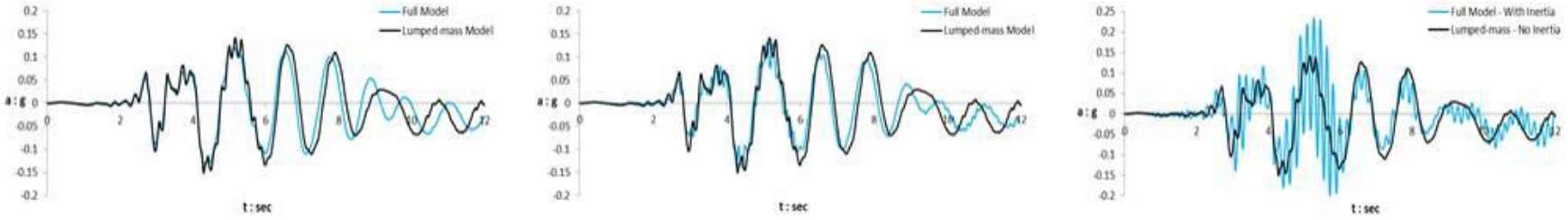

b) Deck Acceleration - time

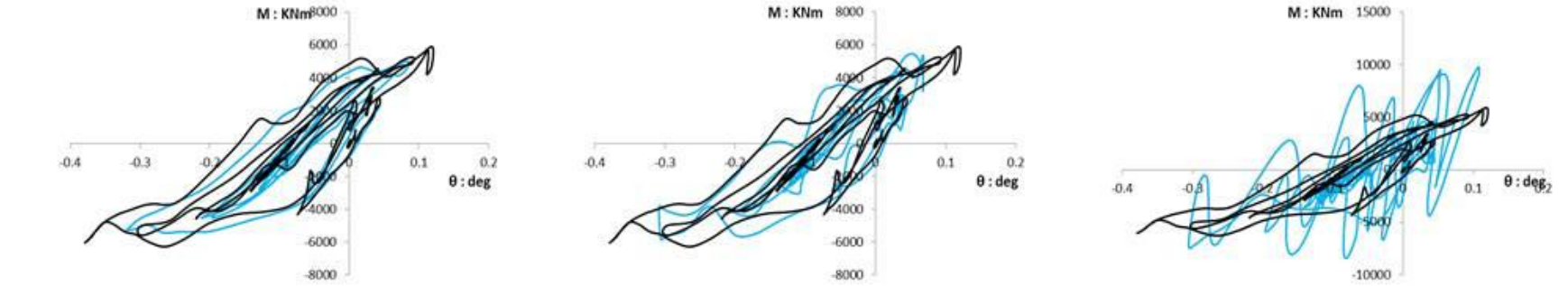

c) Moment – Foundation Rotation

Figure 4.3 Dynamic Results of The Rocking Models Subjected to Kalamata EQ Excitation.

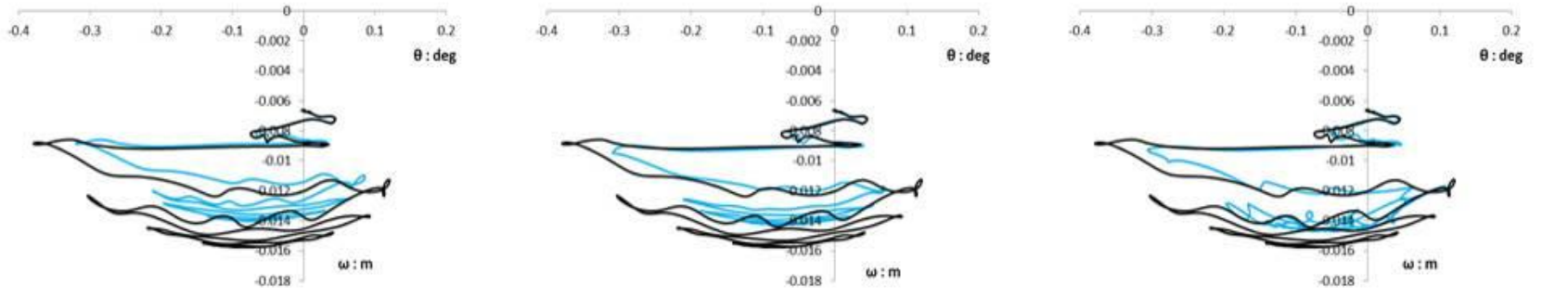

a) Settlement – Foundation Rotation.

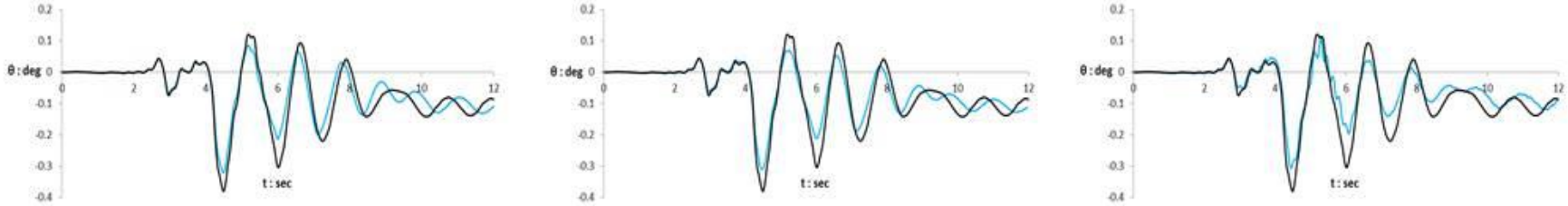

b) Foundation Rotation – time.

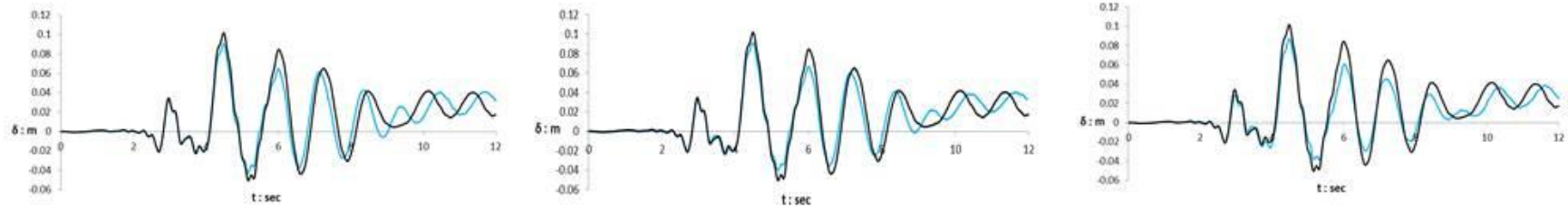

c) Deck Displacement – Time.

Figure 4.3 Dynamic Results of The Rocking Models Subjected to Kalamata EQ Excitation.

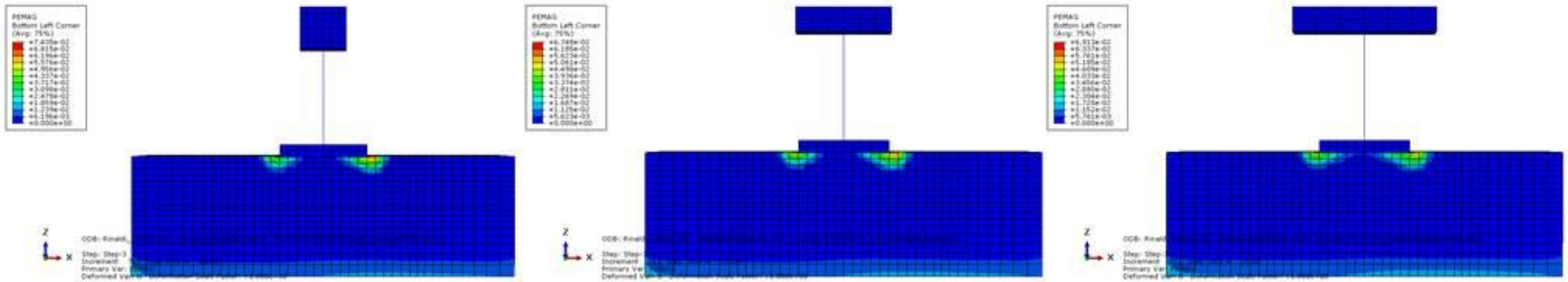

a) Models Used in the analysis, from left to right A, B & C.

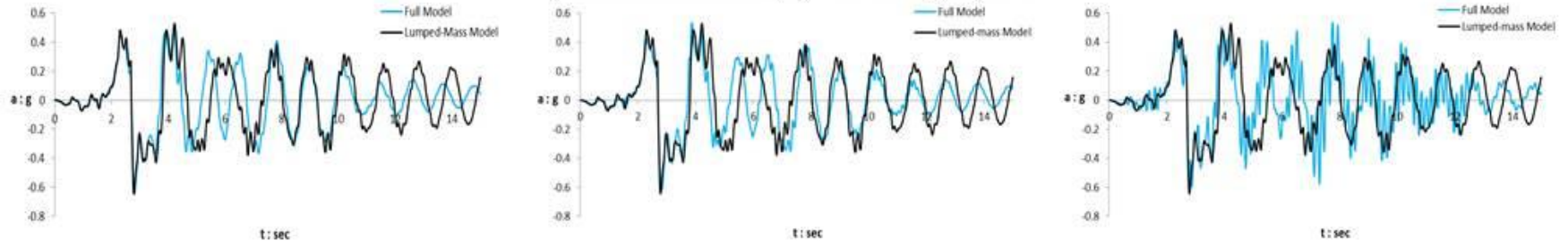

b) Deck Acceleration - time

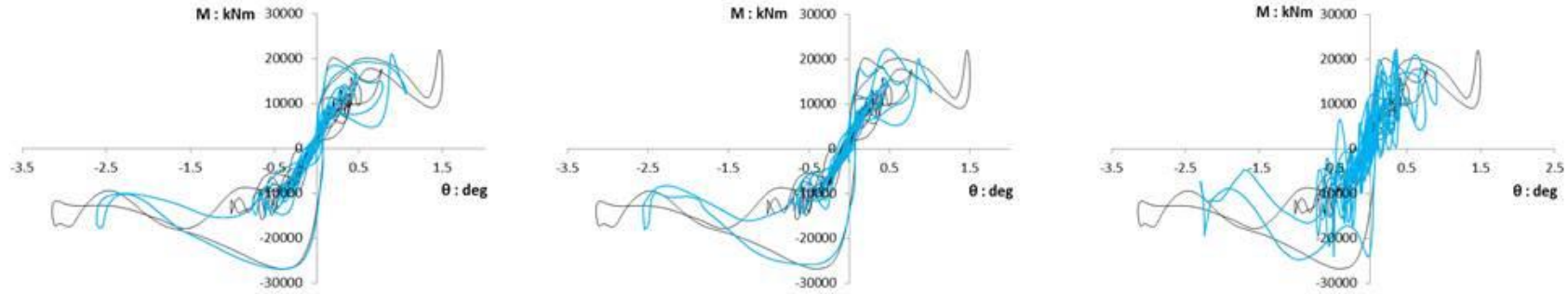

c) Moment – Foundation Rotation

Figure 4.4 Dynamic Results of The Conventional Models Subjected to Northridge Rinaldi EQ Excitation.

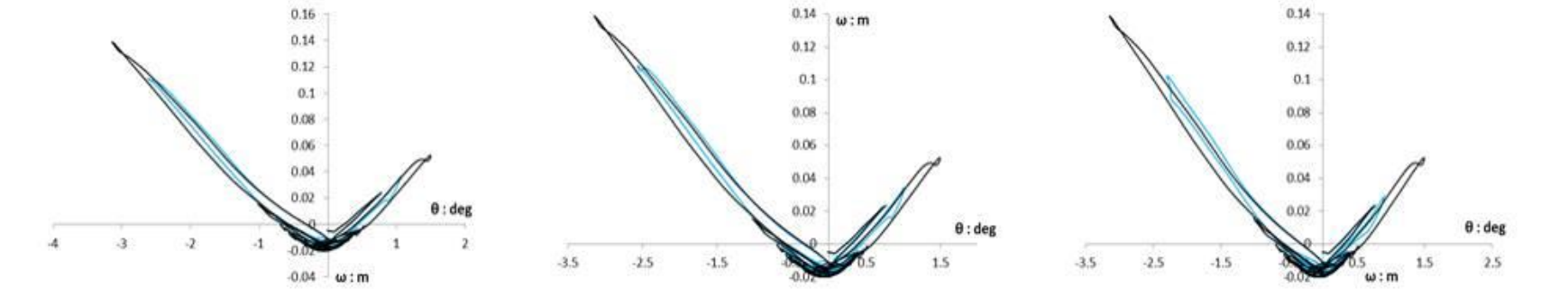

a) Settlement – Foundation Rotation.

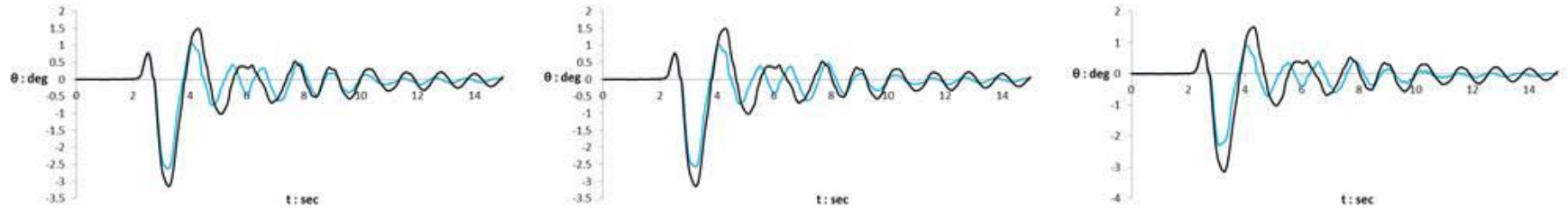

b) Foundation Rotation – time.

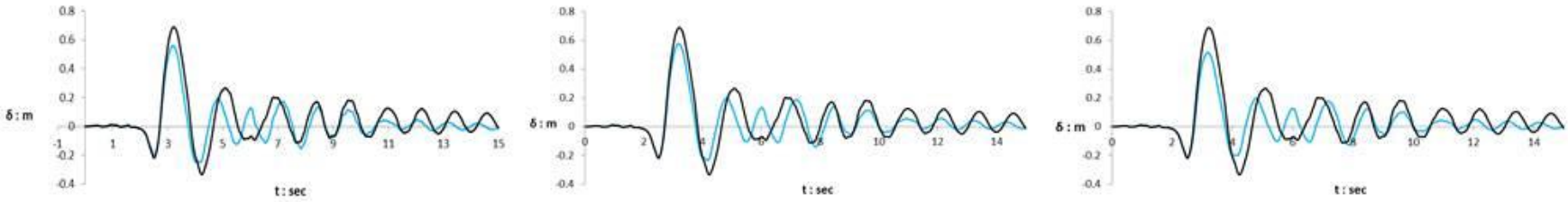

c) Deck Displacement – Time.

Figure 4.4 Dynamic Results of The Conventional Models Subjected to Northridge Rinaldi EQ Excitation.

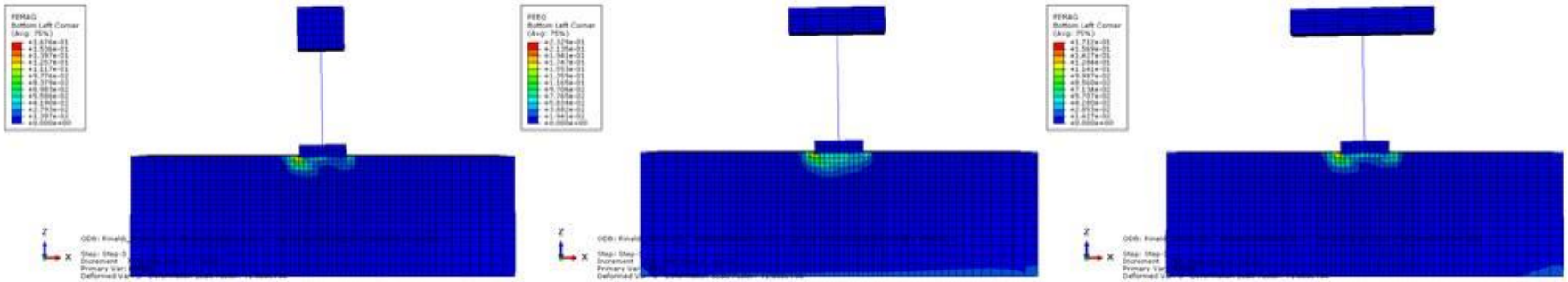

a) Models Used in the analysis, from left to right A, B & C.

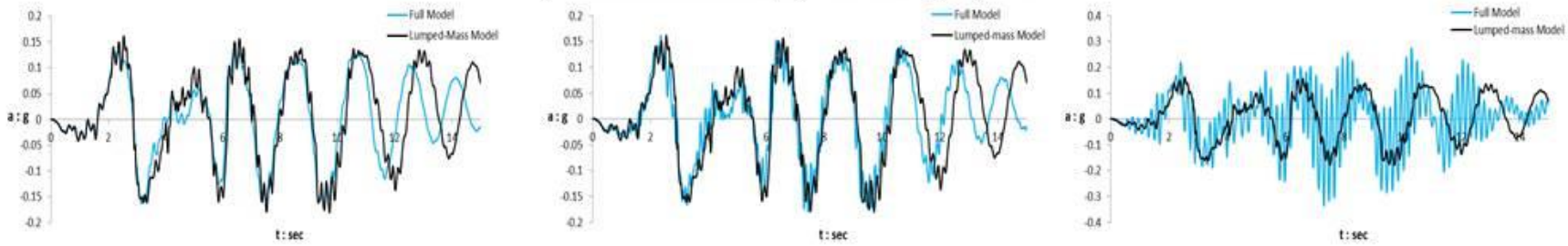

b) Deck Acceleration - time

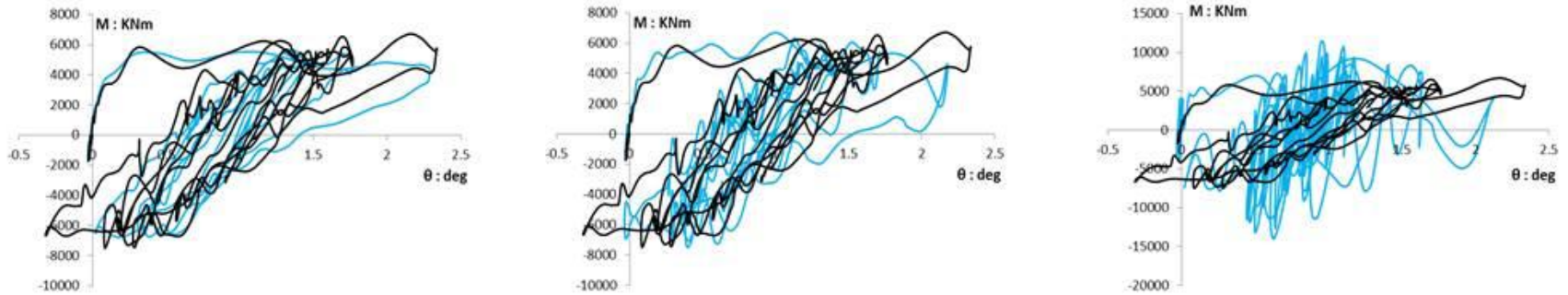

c) Moment – Foundation Rotation

Figure 4.5 Dynamic Results of The Rocking Models Subjected to Northridge Rinaldi EQ Excitation.

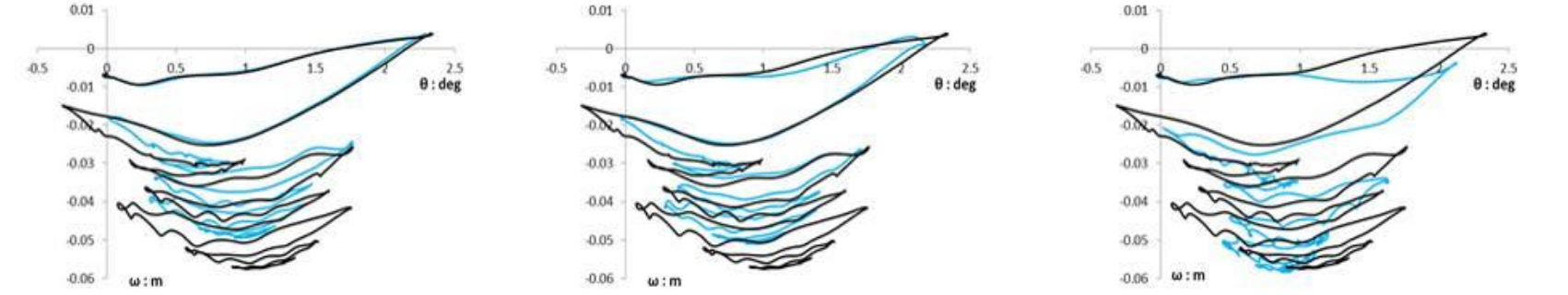

a) Settlement – Foundation Rotation.

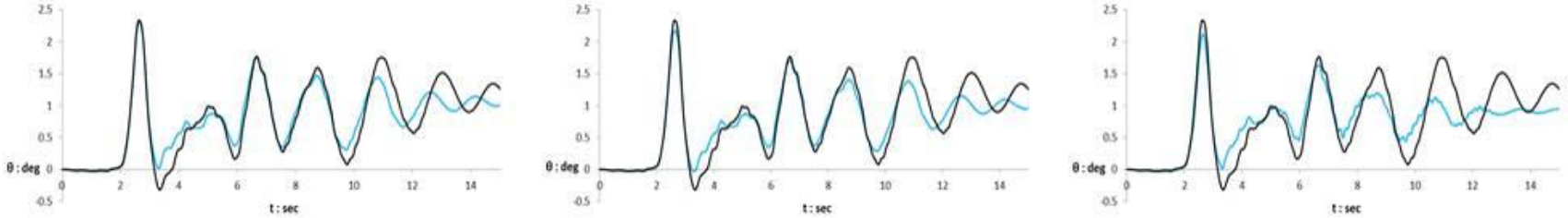

b) Foundation Rotation – time.

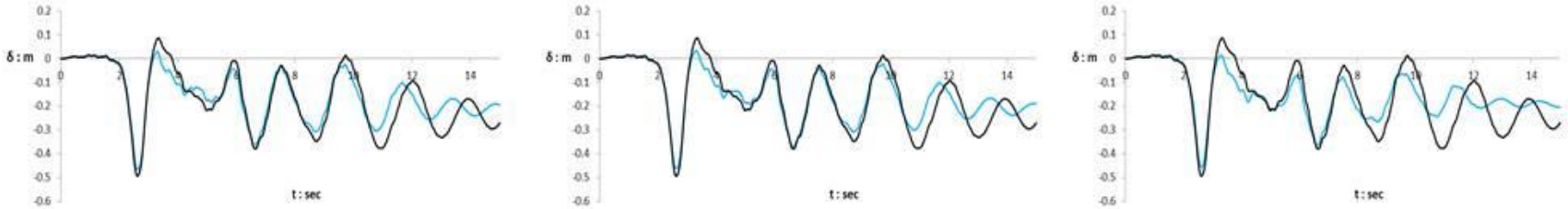

c) Deck Displacement – Time.

Figure 4.5 Dynamic Results of The Rocking Models Subjected to Northridge Rinaldi EQ Excitation.

CHAPTER 5

CASE STUDY OF FREEWAY CROSSING "ELEFSINAS - WEST REGIONAL Ave. YMITTOU" BRIDGE MODEL TE-23.

5.1 Introduction

Based on the study in the previous chapters, since the presence of the deck geometry is influential on the dynamic performance of the previous model. This effect need to be studied further more on more realistic deck geometry to further examine the effects.

In this chapter, a bridge model will be examined typical to a Bridge Crossing "ELEFSINAS - WEST REGIONAL Ave. YMITTOU", which is a five span 115.6 m crossing bridge with a varying span length and pier height. The section under study is the mid pier which centers the longest spans and the larger in height.

The Bridge dimensions and layout are shown in *Figure 1*. The deck is box type girder supported by a single column Pier, The Bridge Pier is supported by a shallow rectangular foundation.

5.2 FE Model Setup

A 2-D nonlinear finite element modeling is conducted using ABAQUS. The geometry of this bridge, which represent a tall (h=13.5 m) highway bridge pier carrying a deck with total dead load (Q = 650 Mgm) supported by a square (B X B) shallow foundation. The 1.8 m circular section pier (cross sectional area A_c = 2.54 m^2) was simulated with 2-dimensional inelastic beam elements assigned the geometric and stiffness properties of the concrete section (E = 70 GPa, γ = 25 kN/m^3 , Transverse shear stiffness = 27019375 kN/m^2) and inelastic behavior as shown in *Figure 2*. Given the relatively high position of the lumped mass, second order (P – δ) effects are important and were therefore taken into account.

The soil was modelled with 4-node bilinear continuum elements CPE4. Representing the following properties (ρ = 1.6 Mg/m^3, S_u = 150 kPa, E = 270000 kPa, v = 0.3).The same element type (CPE4), but with the assumption of linear elastic behavior, was used for the footing. The soil – foundation interface was modelled using special contact elements, which allow sliding and uplifting to take pace being governed by a hard contact law and Coulomb's friction law in the normal and tangential direction respectively.

Four models were tested , the first two represent the conventional capacity design concept where the large foundation (B = 8 m) which follows the current code provisions ensuring minimum displacements of the soil-foundation interface under the design earthquake where the seismic actions on the foundation (Q_{Ed}, M_{Ed}) are substantially magnified (by as much as 40% in this case) in comparison to the actual loads at the column base to avoid nonlinear response and accumulation of plastic deformations ant the column base, The factor of safety (FS_v) is greater than one under the expected seismic action. The only difference between these first two models is the modeling of the upper deck geometry in the first model it is modeled as a lumped mass with no physical dimensions, While the other model the deck geometry is modelled as a box girder which will represent the case where the rotational inertia comes into action. *Figure 3a.*

The next two models will represent the alternative design philosophy of rocking isolation. Where the footing dimensions is smaller (B = 5.5 m) which represents a factor of safety (FS_v) < 1 under the design seismic conditions. *Figure 3b.*

Table 1 summarizes the design of the two foundation alternatives listing the actual loads and the design actions, the bearing capacity in pure vertical loading and in combined seismic loading, and the corresponding factors of safety for static vertical loads (FS_v) and seismic lateral loading (FS_E).

Foundation capacity was firstly calculated using well established relationships from literature, [12] for combined N-M-Q loading respectively. Numerical simulations with finite elements were then used to verify these theoretical predications. *Figure 4.*

It is important to note that in this chapter, the damping effect of the deck elements in the FE models was taken out to further focus on the rotational inertia effect and since that the damping effect of the presence of the deck elements was consistent in the previous analysis.

Property	*Unit*	*Conventional*	*Rocking*
Breadth	B : m	8	5.5
Total Vertical Load	N : MN	10.3	8.6
Seismic Shear Load	Q_E : MN	1.46	1.46
Seismic Moment Load	M_E : MN	27.72	27.92
Design Shear Load	Q_{Ed} : MN	1.46	1.46
Design Moment Load	M_{Ed} : MN	27.72	27.92
Ultimate Shear Load	Q_u : MN	2.28	1.07
Ultimate Moment Load	M_u : MN	31.06	14.59
Safety Factor in Vertical Loading	Q_E : MN	5.57	3.11
Safety Factor in Seismic Loading	M_E : MN	1.1	0.51

Table 1.Foundation Design: Summary of loads and safety factors

5.3 Dynamic Analysis

A series of dynamic analysis was conducted; the model base was excited by a variety of real excitation from Greece and japan with different magnitude and frequency to further examine the model comparisons.

5.3.1 Kalamata EQ Greece (1986).

As shown in *Figure 6.* The results of the dynamic excitation of the two conventionally designed models, the comparison in terms of deck acceleration is showing a slight difference in the peak acceleration along with a slight shift in the period.

The lumped mass model is showing a slight increase in foundation rotation and deck displacement compared to the Full Model.

Figure 6e shows the displacement components of the deck displacement, as in the case of conventional design the column deformation is the main contributor to the total drift.

Figure 6g Shows the column behavior, where the "lumped-mass" model appears to result in higher curvature compared to the "Full Model".

Figure 7 Shows the results of the dynamic excitation of the rocking isolated models, the comparison in terms of the deck acceleration is showing a slight variation; as the "Full Model" is showing higher vibration but no much difference in the peak values.

The lumped mass model is showing a slight increase in foundation rotation compared to the Full Model.

Figure 7e shows the displacement components of the deck displacement, as in the case of rocking isolation the Foundation rotation and uplift is the main contributor to the total drift.

5.3.2 Lefkada EQ Greece (2003).

As shown in *Figure 8.* The results of the dynamic excitation of the two conventionally designed models, the comparison in terms of deck acceleration is showing a slight difference in the peak acceleration.

The lumped mass model is showing a slight increase in foundation rotation and deck displacement compared to the Full Model and higher residual deck displacement towards the end of the excitation.

Figure 8e shows the displacement components of the deck displacement, as in the case of conventional design the column deformation is the main contributor to the total drift.

Figure 8g shows the column inelastic behavior. Where the two models are showing a very slight variation in behavior.

Figure 9 Shows the results of the dynamic excitation of the rocking isolated models, the comparison in terms of the deck acceleration is showing a slight variation; as the "Full Model" is showing higher vibration with slight difference in the peak values.

The lumped mass model is showing a slight increase in foundation rotation compared to the Full Model.

Figure 9f shows the deck displacement of the two models; where there is a slight increase in values of the "Full Model" compared to the "Lumped-mass Model" especially towards the end of the excitation.

5.3.3 JMA-OOO Kobe Japan (1995).

As shown in *Figure 10.* The results of the dynamic excitation of the two conventionally designed models, the comparison in terms of deck acceleration is not showing a significant difference in the peak acceleration.

The lumped mass model is not showing an increase in foundation rotation or settlement compared to the Full Model. While the "Full Model" shows higher deck displacement compared to the "Lumped-mass Model".

Figure 10g shows the column inelastic behavior. The two models is showing a very slight variation in behavior where the column goes well beyond yielding.

As shown in *Figure 11.* The results of the dynamic excitation of the two Rocking isolation designed models, the comparison in terms of deck acceleration is showing a slight difference in the peak acceleration along with a shift in the period.

The lumped mass model is showing a slight increase in foundation rotation compared to the Full Model.

Figure 11f shows the deck displacement of the two models; where there is a slight decrease in values of the "Full Model" compared to the "Lumped-mass Model" especially towards the end of the excitation.

Figure 11e shows the displacement components of the deck displacement, as in the case of Rocking Isolation design the Foundation rotation the main contributor to the total drift.

5.3.4 Northridge Rinaldi EQ (1994).

Figure 12 Shows the results of the dynamic excitation of the Conventional models, the comparison in terms of the deck acceleration is showing a slight variation; as the "Full Model" is showing a much higher vibration but no much difference in the peak values.

The lumped mass model is not showing an increase in foundation rotation or settlement compared to the Full Model. While the "Full Model" shows higher deck displacement compared to the "Lumped-mass Model" with higher rate of failure of the column.

Figure 11g Shows the column behavior, where the "lumped-mass" model appears to result in higher curvature compared to the "Full Model".

Figure 13 Shows the results of the dynamic excitation of the Rocking models, the comparison in terms of the deck acceleration is showing a slight variation; as the "Full Model" is showing a much higher vibration which results in difference of the peak values.

The lumped-mass model is showing a slight increase in foundation rotation and deck displacement compared to the Full Model.

Figure 13e shows the displacement components of the deck displacement, as in the case of Rocking Isolation design the Foundation rotation the main contributor to the total drift.

Figure 8g shows the column inelastic behavior. Where in the case of the rocking isolation design the EQ intensity is redirected away from the column to the soil-foundation interface and the column section doesn't suffer high straining actions.

Chapter 5

Figures

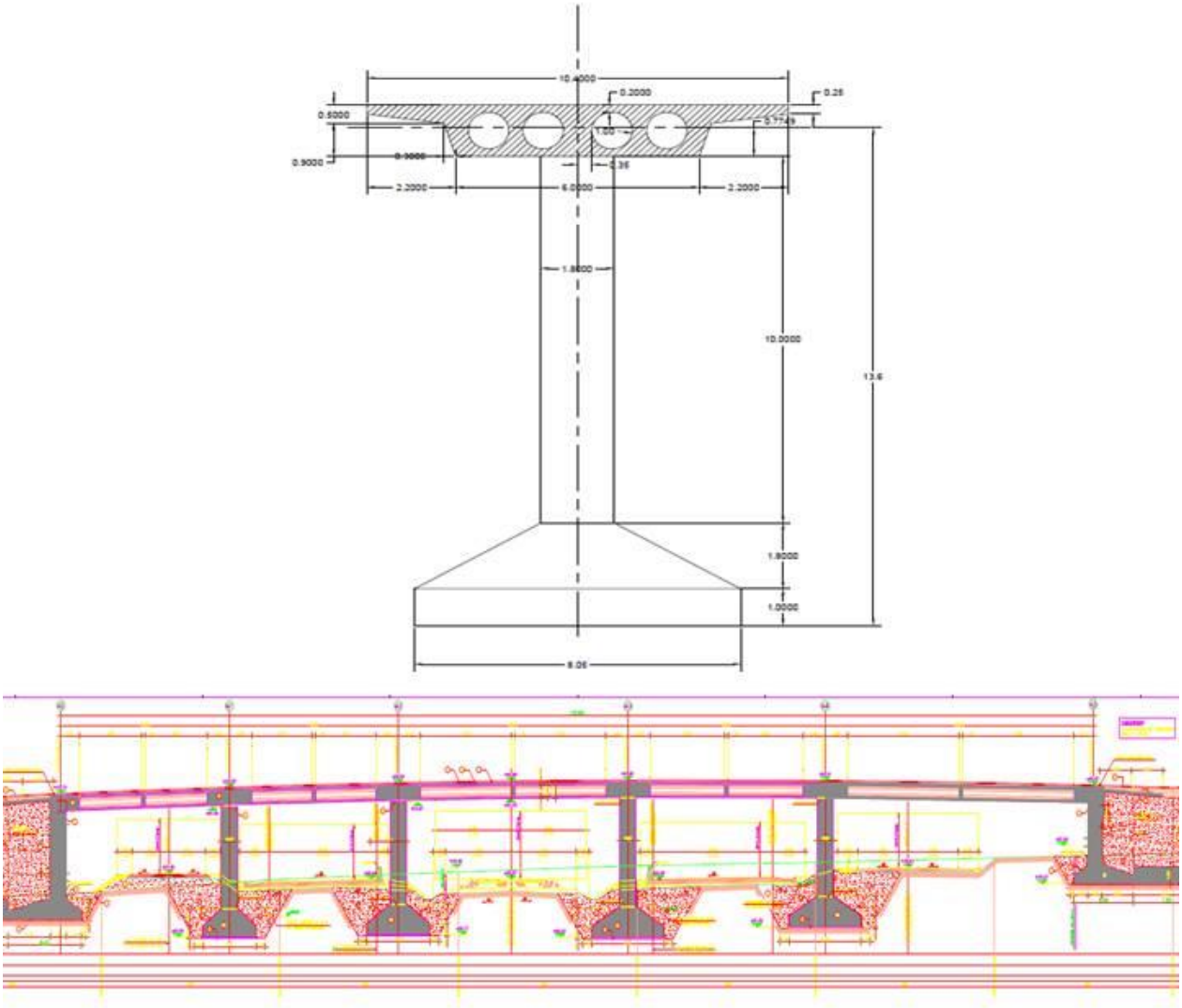

Figure 5.1 Bridge Model "TE-23 "Overall Dimensions.

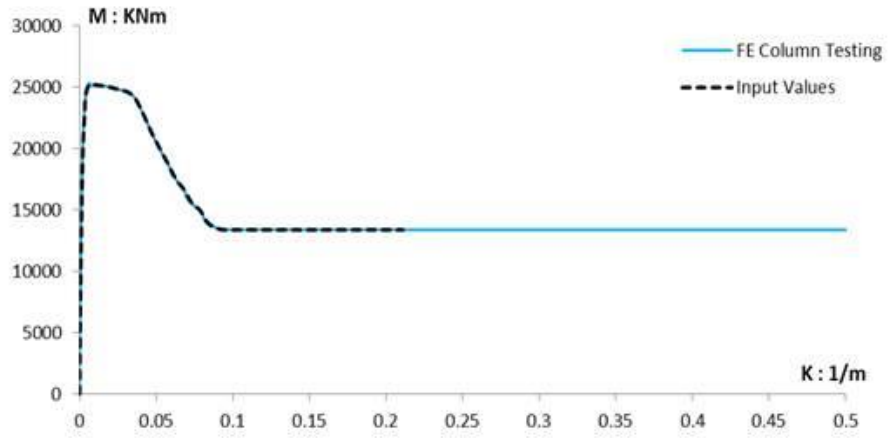

Figure 5.2 Pier Column inelastic behavior: Moment - Curvature.

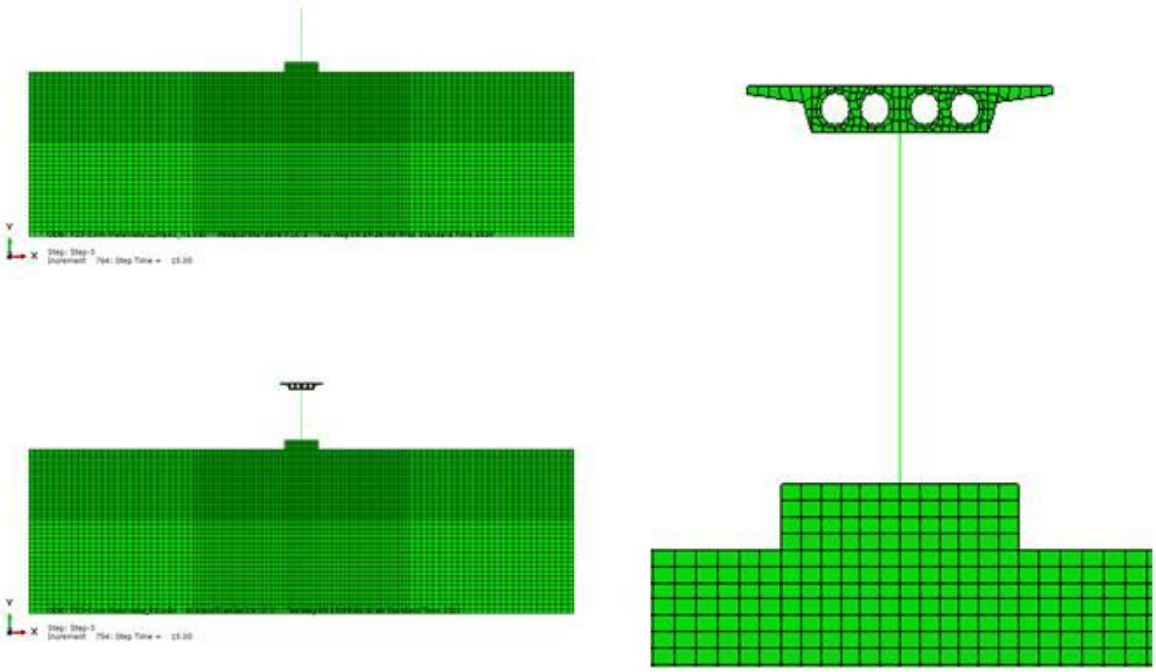

Figure 5.3 a) Conventional Design Models and deck geometry.

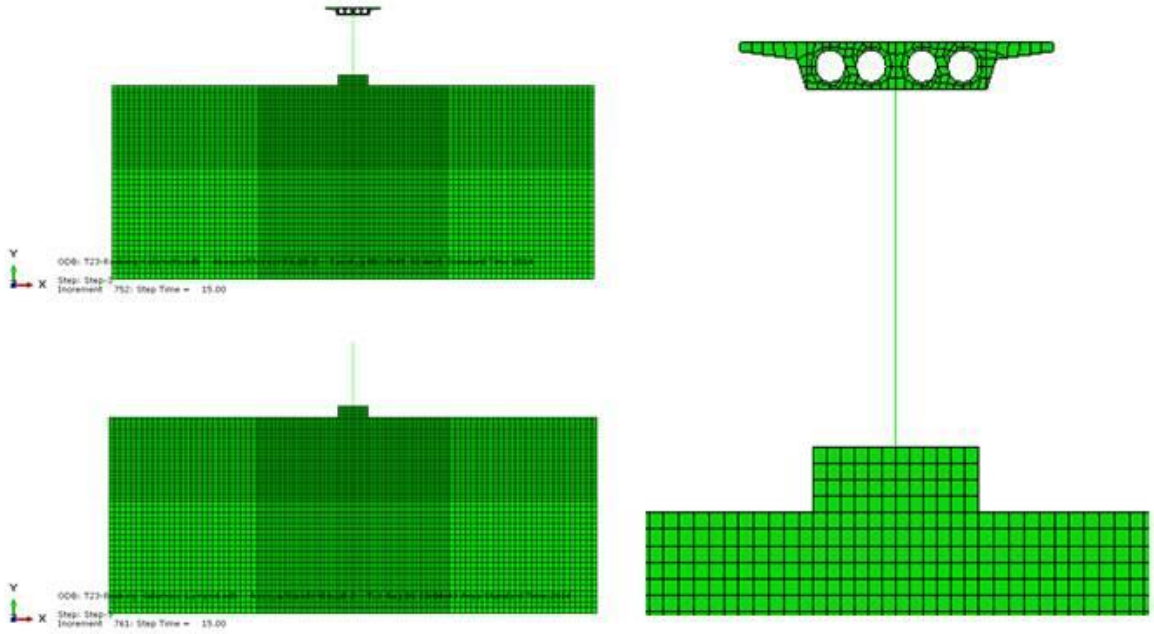

Figure 5.3 b) Rocking Isolation design Models and deck geometry.

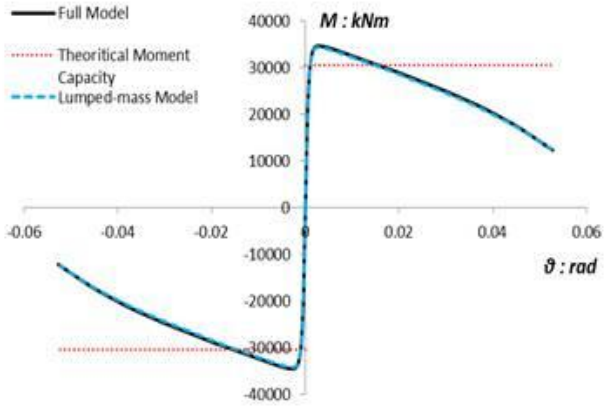

a) Conventional design Models.

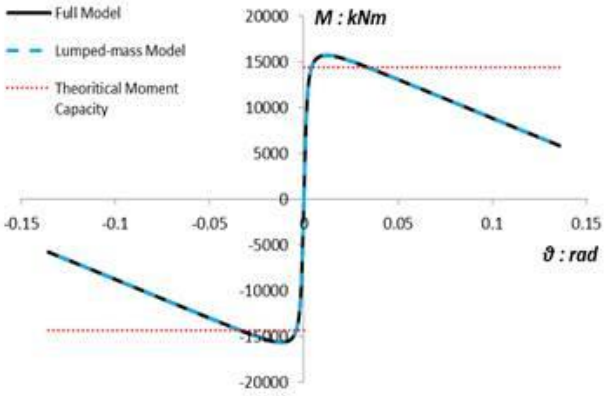

b) Rocking Isolation Models.

Figure 5.4 Push-over Result: Moment rotation and comparison with theoretical flexural capacity.

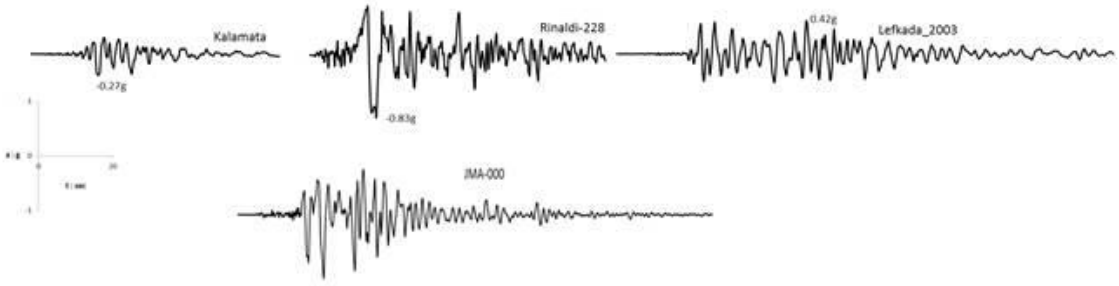

Figure 5.5 Real Earthquake Records used in the analysis.

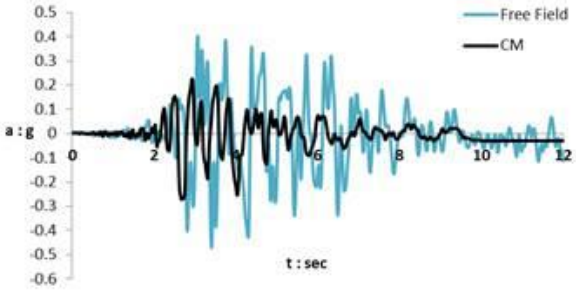

a) "Freefield" & "Center of mass" Acceleration-Time.

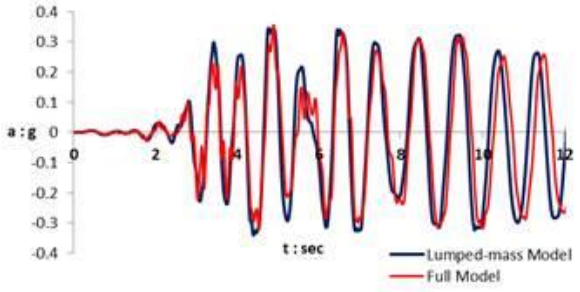

b) Deck Acceleration - Time.

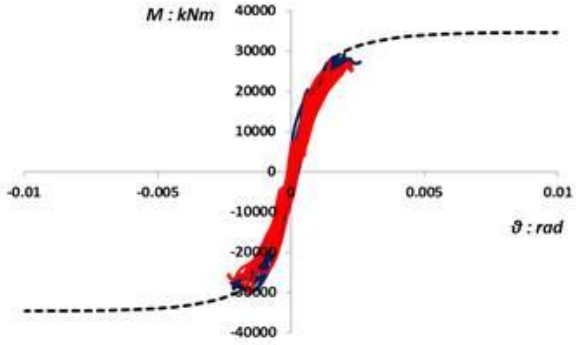

c) Moment – Foundation Rotation.

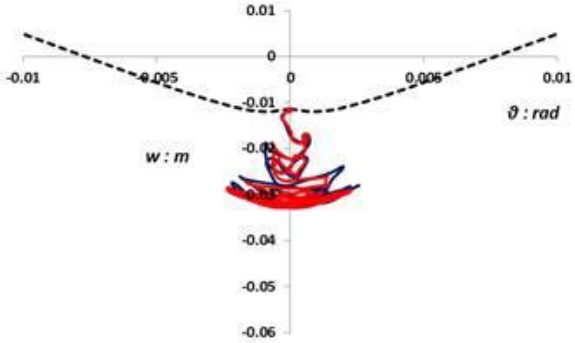

d) Settlement – Foundation Rotation.

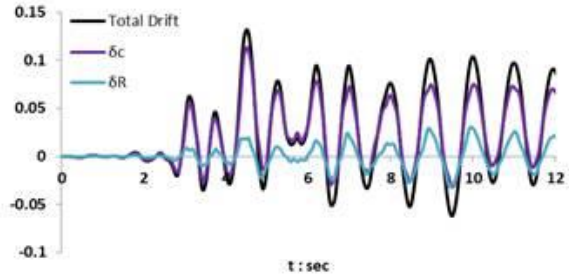

e) Displacement Components of the system.

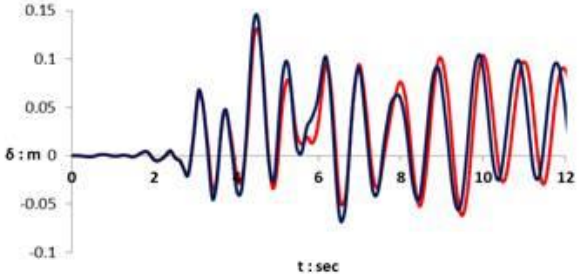

f) Deck Displacement - Time.

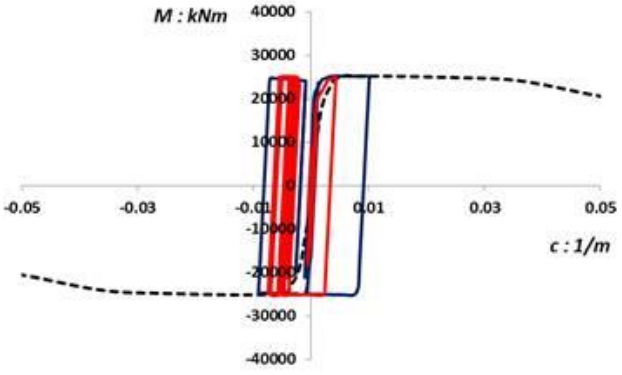

g) Pier Section Flexural Moment - Curvature.

Figure 5.6 Dynamic Results of the Conventionally designed models subjected to Kalamata EQ.

a) "Freefield" & "Center of mass" Acceleration-Time.

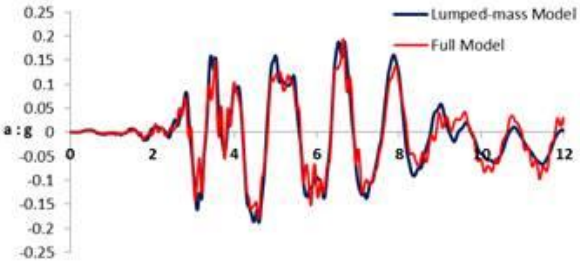

b) Deck Acceleration - Time.

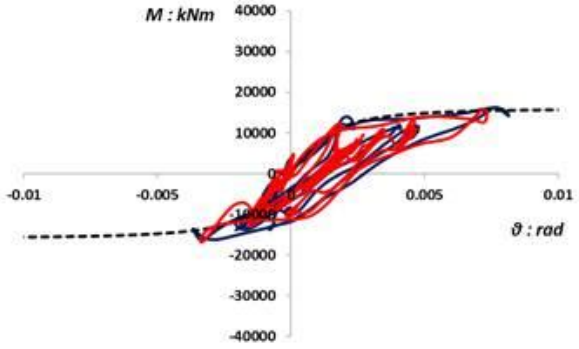

c) Moment – Foundation Rotation.

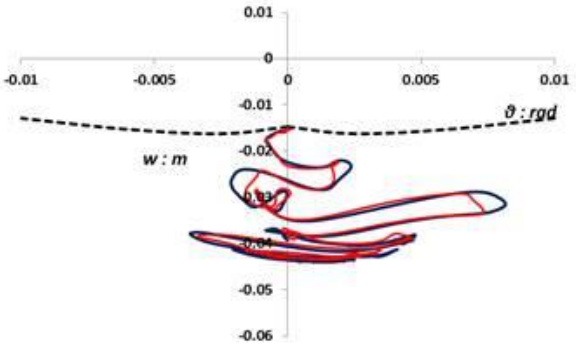

d) Settlement – Foundation Rotation.

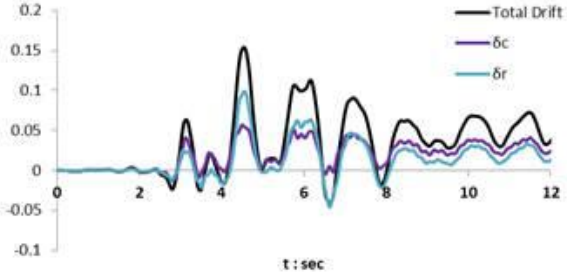

e) Displacement Components of the system.

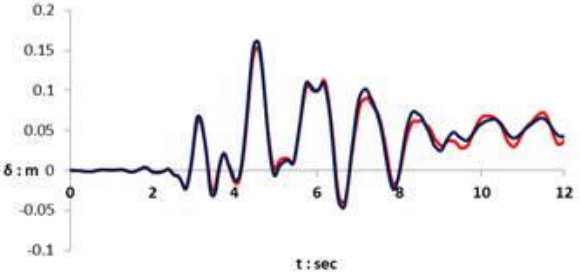

f) Deck Displacement - Time.

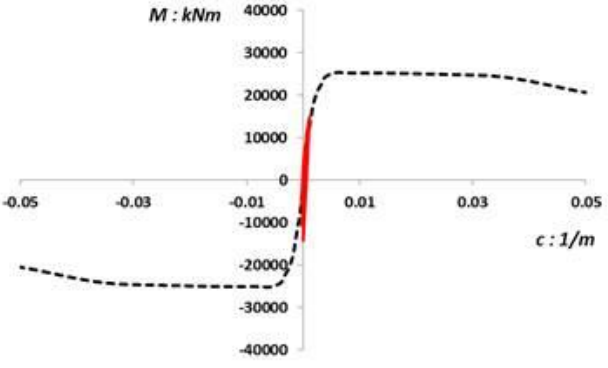

g) Pier Section Flexural Moment - Curvature.

Figure 5.7 Dynamic Results of the Rocking Isolation designed models subjected to Kalamata EQ.

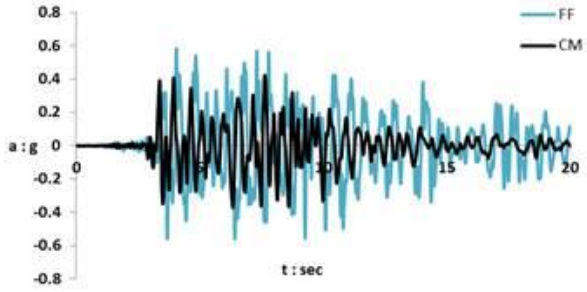

a) "Freefield" & "Center of mass" Acceleration-Time.

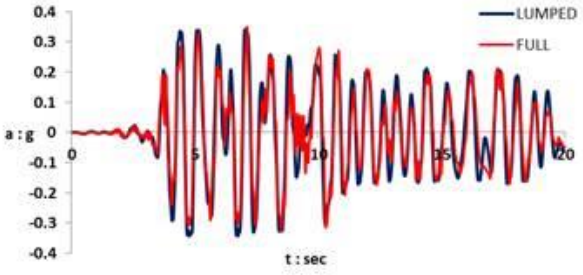

b) Deck Acceleration - Time.

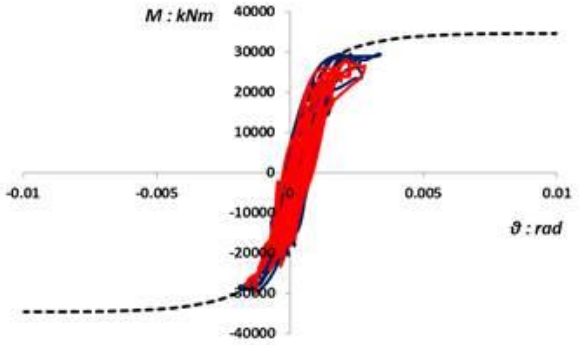

c) Moment – Foundation Rotation.

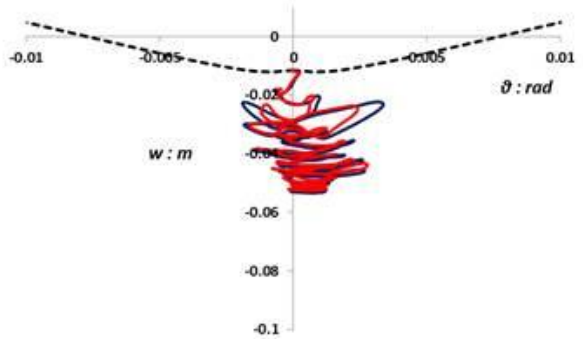

d) Settlement – Foundation Rotation.

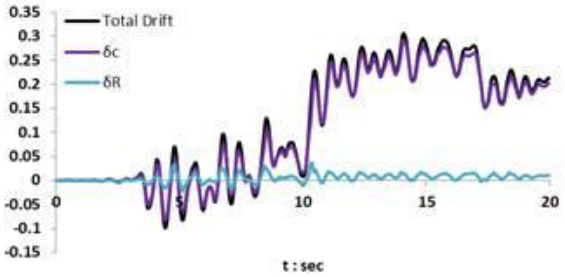

e) Displacement Components of the system.

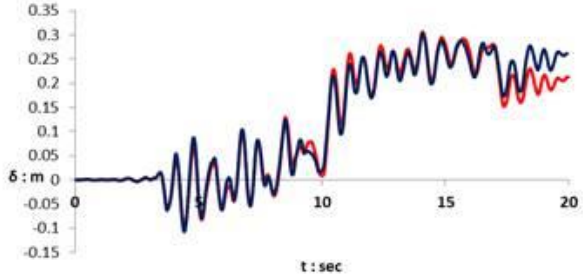

f) Deck Displacement - Time.

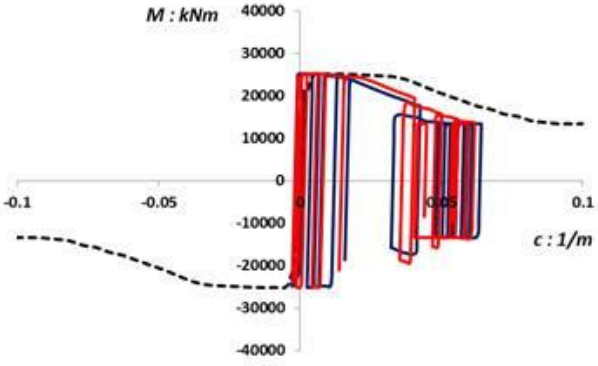

g) Pier Section Flexural Moment - Curvature.

Figure 5.8 Dynamic Results of the Conventionally designed models subjected to Lefkada EQ.

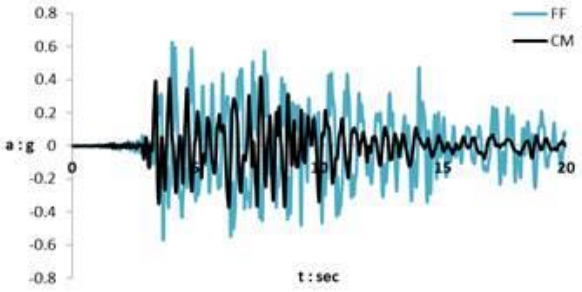

a) "Freefield" & "Center of mass" Acceleration-Time.

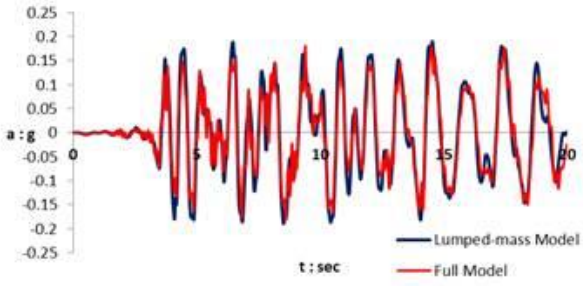

b) Deck Acceleration - Time.

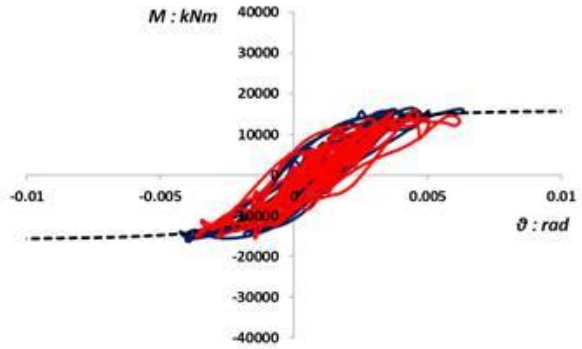

c) Moment – Foundation Rotation.

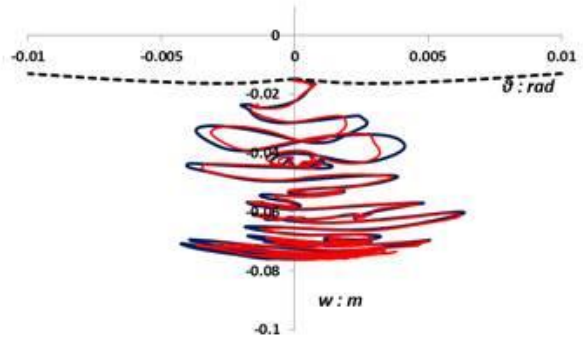

d) Settlement – Foundation Rotation.

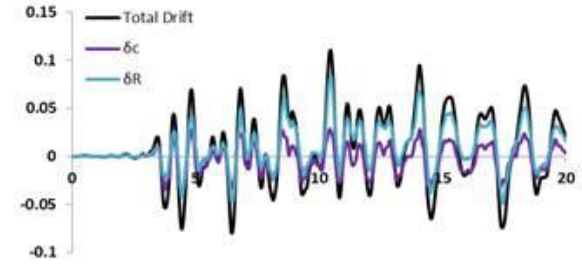

e) Displacement Components of the system.

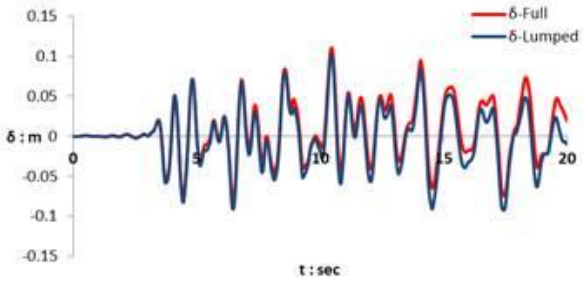

f) Deck Displacement - Time.

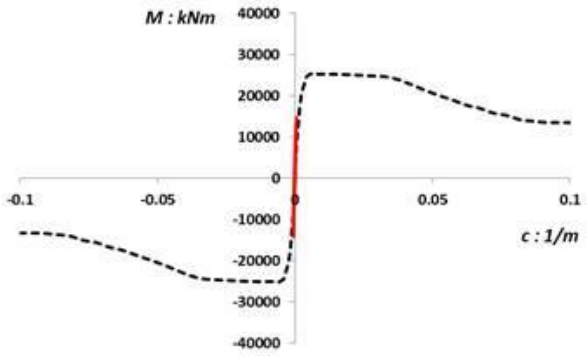

g) Pier Section Flexural Moment - Curvature.

Figure 5.9 Dynamic Results of the Rocking Isolation designed models subjected to Lefkada EQ.

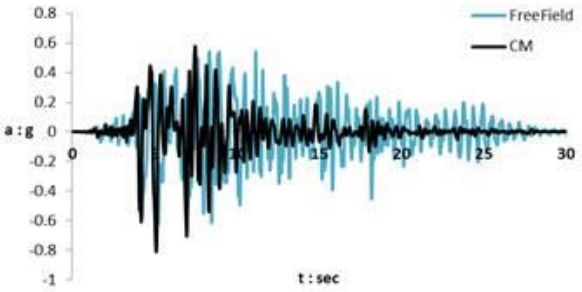

a) "Freefield" & "Center of mass" Acceleration-Time.

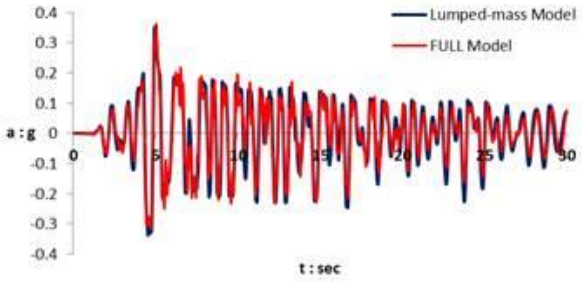

b) Deck Acceleration - Time.

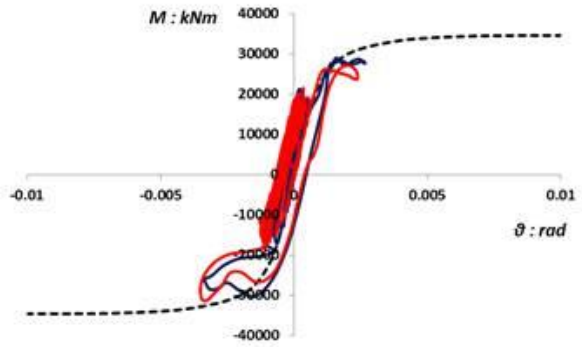

c) Moment – Foundation Rotation.

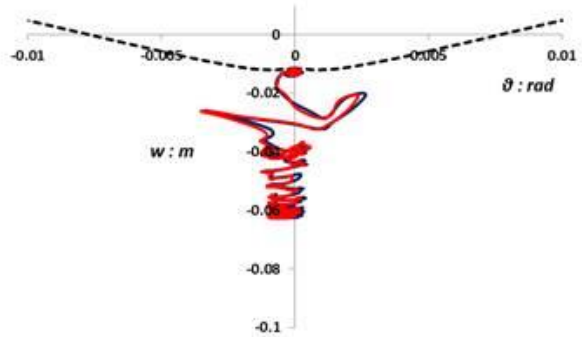

d) Settlement – Foundation Rotation.

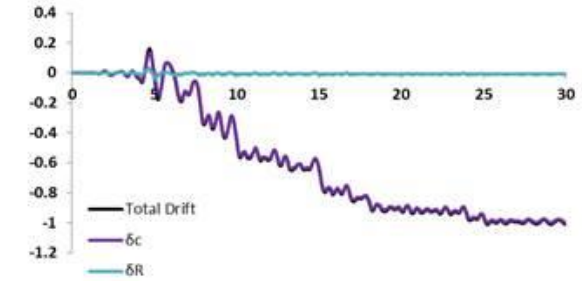

e) Displacement Components of the system.

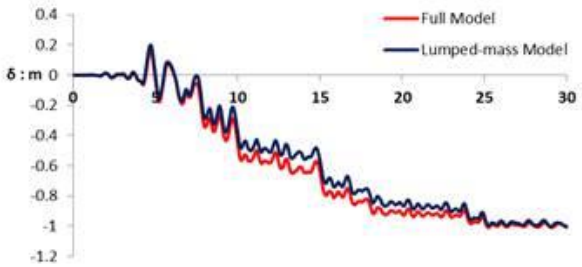

f) Deck Displacement - Time.

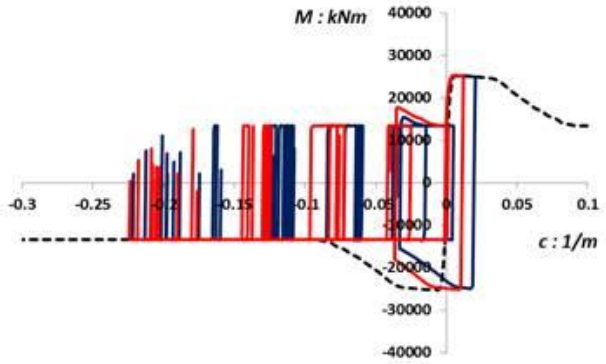

g) Pier Section Flexural Moment - Curvature.

Figure 5.10 Dynamic Results of the Conventionally designed models subjected to Kobe JMA 000 EQ.

a) "Freefield" & "Center of mass" Acceleration-Time.

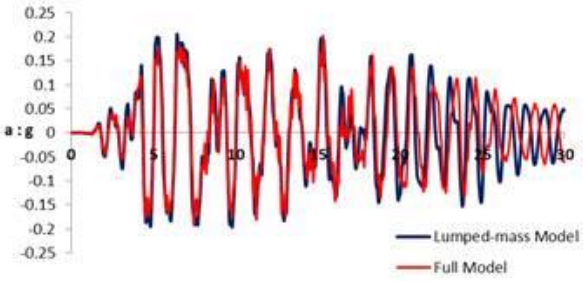

b) Deck Acceleration - Time.

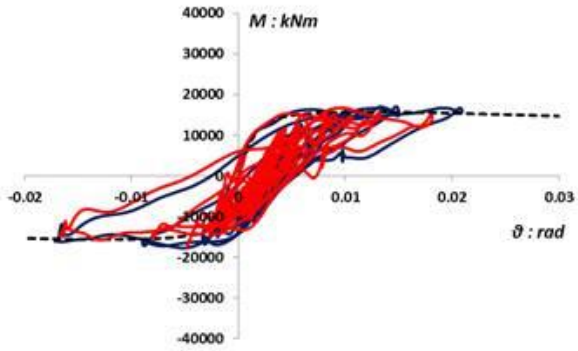

c) Moment – Foundation Rotation.

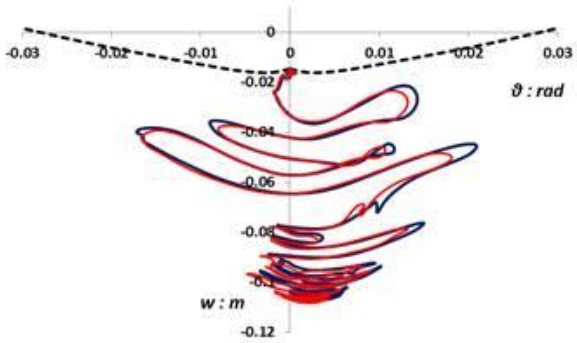

d) Settlement – Foundation Rotation.

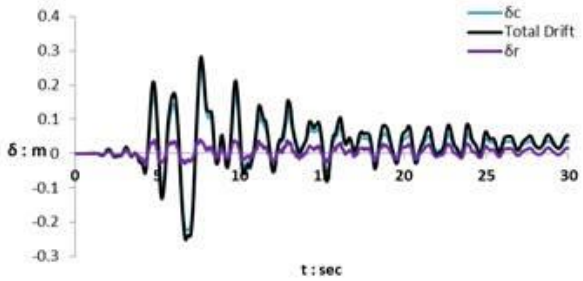

e) Displacement Components of the system.

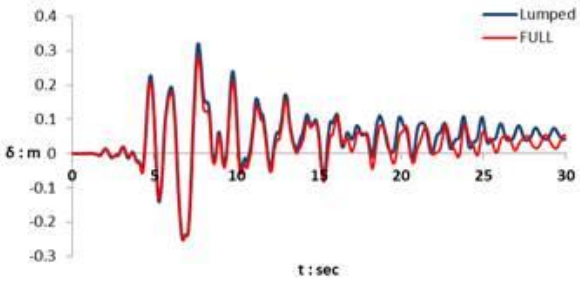

f) Deck Displacement - Time.

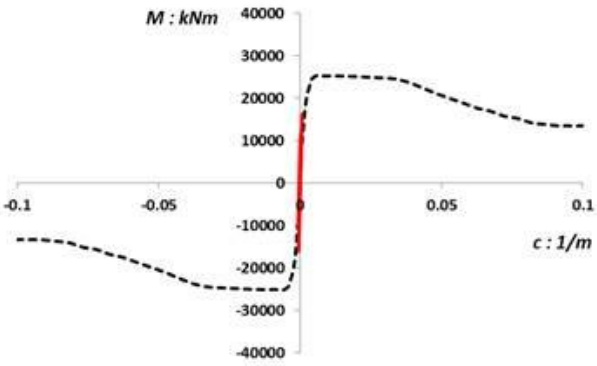

g) Pier Section Flexural Moment - Curvature.

Figure 5.11 Dynamic Results of the Rocking Isolation designed models subjected to Kobe JMA 000 EQ.

a) "Freefield" & "Center of mass" Acceleration-Time.

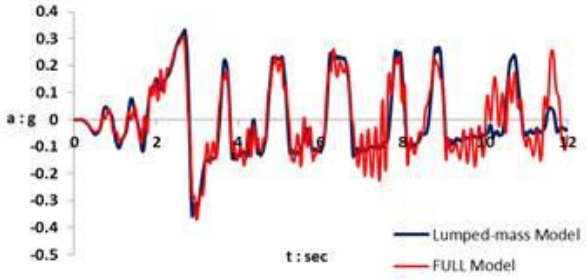

b) Deck Acceleration - Time.

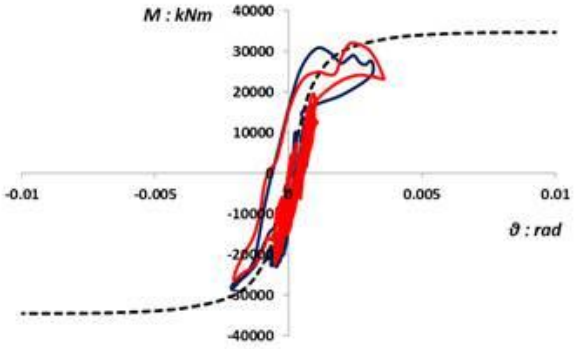

c) Moment – Foundation Rotation.

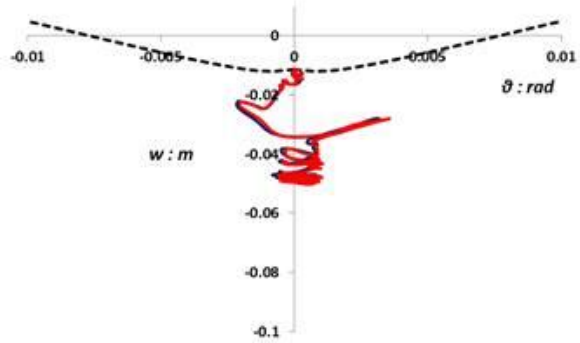

d) Settlement – Foundation Rotation.

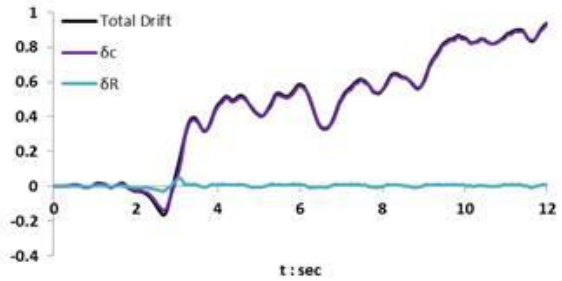

e) Displacement Components of the system.

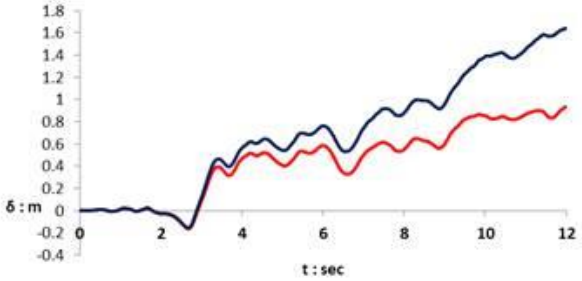

f) Deck Displacement - Time.

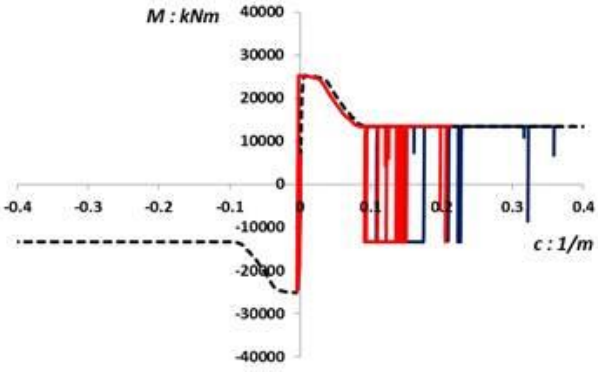

g) Pier Section Flexural Moment - Curvature.

Figure 5.12 Dynamic Results of the Conventionally designed models subjected to Northridge Rinaldi EQ.

a) "Freefield" & "Center of mass" Acceleration-Time.

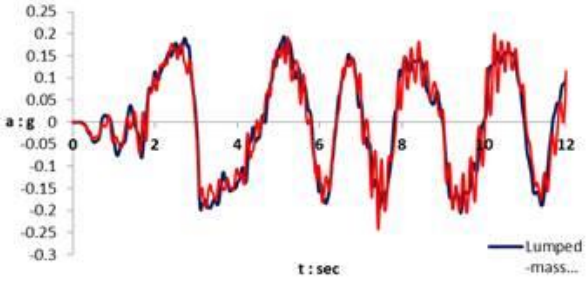

b) Deck Acceleration - Time.

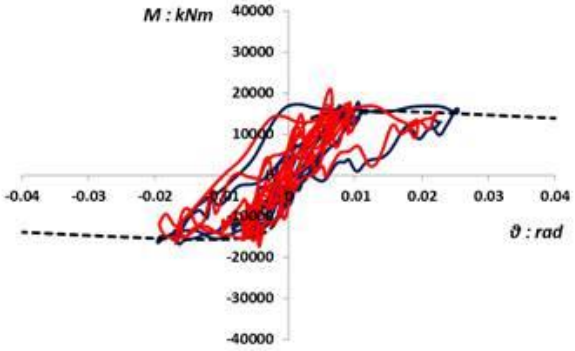

c) Moment – Foundation Rotation.

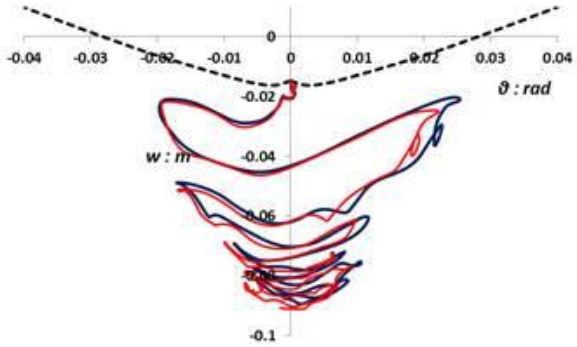

d) Settlement – Foundation Rotation.

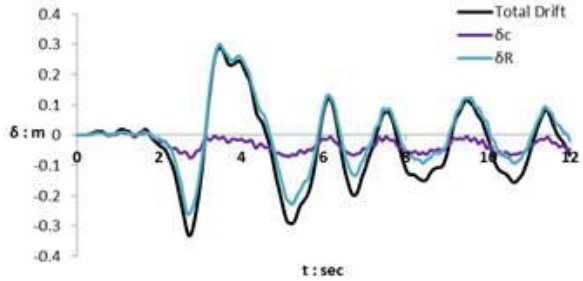

e) Displacement Components of the system.

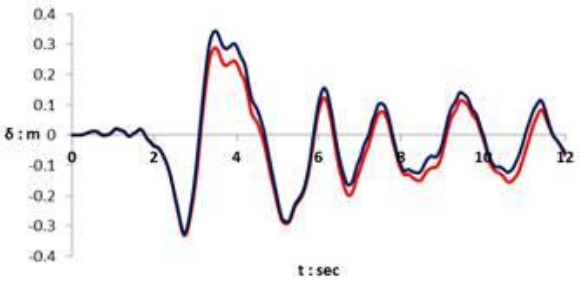

f) Deck Displacement - Time.

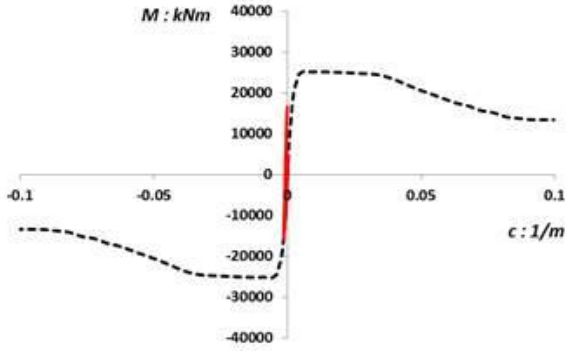

g) Pier Section Flexural Moment - Curvature.

Figure 5.13 Dynamic Results of the Rocking Isolation designed models subjected to Northridge Rinaldi EQ.

CHAPTER 6

CASE STUDY OF FREEWAY CROSSING "ELEFSINAS - WEST REGIONAL Ave. YMITTOU" BRIDGE MODEL TE-20

6.1 Introduction

Based on the study of the previous chapters and in an effort to examine the rotational effect further more on realistic bridge geometries. In this chapter, a bridge model will be examined typical to a Bridge Crossing "ELEFSINAS - WEST REGIONAL Ave. YMITTOU", which is a five span 93 m crossing bridge with a varying span length and pier height. The section under study is the mid pier which centers the longest spans and the larger in height.

The Bridge dimensions and layout are shown in *Figure 1*. The deck is box type girder supported by a single column Pier, The Bridge Pier is supported by a shallow rectangular foundation. It should be noted that comparing with the mode studied in the previous chapter, this bridge has a much larger mass despite being slightly shorter in deck height.

6.2 FE Model Setup

A 2-D nonlinear finite element modeling is conducted using ABAQUS. The geometry of this bridge, which represent a tall (h=12.5 m) highway bridge pier carrying a deck with total dead load (Q = 875 Mgm) supported by a square (B X B) shallow foundation. The 2 m circular section pier (cross sectional area A_c = 3.14 m^2) was simulated with 2-dimensional inelastic beam elements assigned the geometric and stiffness properties of the concrete section (E = 70 GPa, γ = 25 kN/m^3 , Transverse shear stiffness = 27019375 kN/m^2) and inelastic behavior as shown in *Figure 2*. Given the relatively high position of the lumped mass, second order (P – δ) effects are important and were therefore taken into account.

The soil was modelled with 4-node bilinear continuum elements CPE4. Representing the following properties (ρ = 1.6 Mg/m^3, S_u = 150 kPa, E = 270000 kPa, v = 0.3).The same element type (CPE4), but with the assumption of linear elastic behavior, was used for the footing. The soil – foundation interface was modelled using special contact elements, which allow sliding and uplifting to take pace being governed by a hard contact law and Coulomb's friction law in the normal and tangential direction respectively.

Four models were tested , the first two represent the conventional capacity design concept where the large foundation (B = 8.1 m) which follows the current code provisions ensuring minimum displacements of the soil-foundation interface under the design earthquake where the seismic actions on the foundation (Q_{Ed}, M_{Ed}) are substantially magnified (by as much as 40% in this case) in comparison to the actual loads at the column base to avoid nonlinear response and accumulation of plastic deformations ant the column base, The factor of safety (FS_v) is greater than one under the expected seismic action. The only difference between these first two models is the modeling of the upper deck geometry in the first model it is modeled as a lumped mass with no physical dimensions, While the other model the deck geometry is modelled as a box girder which will represent the case where the rotational inertia comes into action. *Figure 3a.*

The next two models will represent the alternative design philosophy of rocking isolation. Where the footing dimensions is smaller (B = 5.5 m) which represents a factor of safety (FS_v) < 1 under the design seismic conditions. *Figure 3b.*

Table 1 summarizes the design of the two foundation alternatives listing the actual loads and the design actions, the bearing capacity in pure vertical loading and in combined seismic loading, and the corresponding factors of safety for static vertical loads (FS_v) and seismic lateral loading (FS_E).

It is important to note that in this chapter, the damping effect of the deck elements in the FE models was taken out to further focus on the rotational inertia effect and since that the damping effect of the presence of the deck elements was consistent in the earlier analysis.

Property	*Unit*	*Conventional*	*Rocking*
Breadth	B : m	8.1	5.5
Total Vertical Load	N : MN	12.6	10.89
Seismic Shear Load	Q_E : MN	1.97	1.97
Seismic Moment Load	M_E : MN	24.67	24.67
Design Shear Load	Q_{Ed} : MN	1.97	1.97
Design Moment Load	M_{Ed} : MN	24.67	24.67
Ultimate Shear Load	Q_u : MN	2.87	1.28
Ultimate Moment Load	M_u : MN	35.8	15.9
Safety Factor in Vertical Loading	Q_E : MN	4.6	2.46
Safety Factor in Seismic Loading	M_E : MN	1.45	0.65

Table 1.Foundation Design: Summary of loads and safety factors

6.3 Dynamic Analysis

A series of dynamic analysis (*Figure 5*) was conducted; the model base was excited by a variety of real excitation from Greece and japan with different magnitude and frequency to further examine the model comparisons.

6.3.1 Kalamata EQ Greece (1986).

As shown in *Figure 6.* The results of the dynamic excitation of the two conventionally designed models, the comparison in terms of deck acceleration is showing a slight difference in the peak acceleration along with a slight shift in the period.

The lumped mass model is not showing difference in foundation rotation or Settlement compared to the Full Model. However in terms of deck displacement the “Lumped-mass” Model is showing higher values compared to the “Full Model”.

Figure 6e shows the displacement components of the deck displacement, as in the case of conventional design the column deformation is the main contributor to the total drift.

Figure 6g Shows the column behavior, where the “lumped-mass” model appears to result in higher curvature compared to the “Full Model”.

Figure 7 Shows the results of the dynamic excitation of the rocking isolated models, the comparison in terms of the deck acceleration is showing a slight variation; as the “Full Model” is showing higher vibration but no much difference in the peak values

The lumped mass model is showing a slight increase in foundation rotation compared to the Full Model.

Figure 7h shows the deck rotation in both conventional design and rocking isolation, where as expected the rocking models leaves some residual rotation due to soil plastification.

6.3.2 Aegion EQ Greece (1995).

As shown in *Figure 8.* The results of the dynamic excitation of the two conventionally designed models, the comparison in terms of deck acceleration is showing a slight difference in the peak acceleration along with a slight shift in the period.

The lumped mass model is not showing difference in foundation rotation or Settlement compared to the Full Model. However in terms of deck displacement the "Full Model" Model is showing slightly higher values compared to the "Lumped-mass" Model.

Figure 8e shows the displacement components of the deck displacement, as in the case of conventional design the column deformation is the main contributor to the total drift.

Figure 8g Shows the column behavior, where the "lumped-mass" model appears to result in slightly higher curvature compared to the "Full Model".

Figure 9 Shows the results of the dynamic excitation of the rocking isolated models, the comparison in terms of the deck acceleration is showing a slight variation; where the Full Model is showing higher peak values.

The lumped mass model is showing a slight increase in foundation rotation compared to the Full Model.

Figure 9h shows the deck rotation in both conventional design and rocking isolation, where as expected the rocking models leaves some residual rotation due to soil plastification.

6.3.3 Sepolia EQ Greece (1999).

As shown in *Figure 10.* The results of the dynamic excitation of the two conventionally designed models, the comparison in terms of deck acceleration is showing a difference in the peak acceleration; where the “Lumped-mass” model is showing higher peak values compared to the “Full” model.

The lumped mass model is not showing difference in foundation rotation or Settlement compared to the Full Model.

Figure 10e shows the displacement components of the deck displacement, as in the case of conventional design the column deformation is the main contributor to the total drift.

Figure 11 Shows the results of the dynamic excitation of the rocking isolated models, the comparison in terms of the deck acceleration is showing a slight variation; as the “Full Model” is showing higher vibration but no much difference in the peak values

The lumped mass model is not showing difference in foundation rotation or Settlement compared to the Full Model.

Figure 11e shows the displacement components of the deck displacement, as in the case of Rocking Isolation design the Foundation rotation is the main contributor to the total drift.

Figure 11h shows the deck rotation in both conventional design and rocking isolation, where as expected the rocking models leaves some residual rotation due to soil plastification.

6.3.4 Duzce EQ Italy (1999).

As shown in *Figure 12.* The results of the dynamic excitation of the two conventionally designed models, the comparison in terms of deck acceleration is showing a slight difference in the peak acceleration.

The lumped mass model is not showing difference in foundation rotation or Settlement compared to the Full Model. However in the case of deck displacement the Lumped-mass model is showing a much higher displacement.

Figure 12g Shows the column behavior, where the "lumped-mass" model appears to result in higher curvature compared to the "Full Model".

Figure 13 Shows the results of the dynamic excitation of the rocking isolated models, the comparison in terms of the deck acceleration is showing not much variation in terms of peak values.

The lumped mass model is showing a slight increase in foundation rotation, settlement and deck displacement compared to the Full Model.

Figure 13h shows the deck rotation in both conventional design and rocking isolation, where as expected the rocking models leaves some residual rotation due to soil plastification.

6.3.5 Lefkada EQ Greece (2003).

As shown in *Figure 14.* The results of the dynamic excitation of the two conventionally designed models, the comparison in terms of deck acceleration is showing a slight difference in the peak acceleration. However the lumped-mass model is showing higher rate of failure late in the excitation.

The lumped mass model is showing a slight increase in foundation rotation and deck displacement compared to the Full Model. While in the case of deck displacement the Lumped-mass model shows higher rate into failure compared to the Full model.

Figure 14g Shows the column behavior, where the "lumped-mass" model appears to result in higher curvature compared to the "Full Model".

Figure 15 Shows the results of the dynamic excitation of the rocking isolated models, the comparison in terms of the deck acceleration is showing a slight variation; as the "Full Model" is showing higher vibration but no much difference in the peak values.

Figure 15f shows the deck displacement of the two models; where there is a slight increase in values of the "Full Model" compared to the "Lumped-mass Model" especially towards the end of the excitation.

Figure 15e shows the displacement components of the deck displacement, as in the case of rocking isolation the Foundation rotation and uplift is the main contributor to the total drift.

6.3.6 JMA-OOO Kobe Japan (1995).

Shown in *Figure 16* are the results of the dynamic excitation of the two conventionally designed models. The comparison in terms of deck acceleration is not showing a significant difference.

Compared to the previous bridge model, the model under study in this chapter failed early which can be explained by the higher overall mass of the bridge in this case compared to the previous.

In this case of a very strong motion, the concept of Rocking Isolation really proves its advantages, while the conventionally designed model failed, the rocking isolated one sustains the motions while compensating in higher soil plastification and residual drift.

As shown in *Figure 17.* The results of the dynamic excitation of the two Rocking isolation designed models, the comparison in terms of deck acceleration is showing a slight difference in the peak acceleration.

The lumped mass model is showing a slight increase in foundation rotation, settlement and deck displacement compared to the Full Model.

Figure 17h shows the deck rotation in both cases of conventional design and rocking isolation where the first failed while the rocking model survived the strong motion.

6.3.7 Northridge Rinaldi EQ (1994).

Shown in *Figure 18* are the results of the dynamic excitation of the two conventionally designed models. The comparison in terms of deck acceleration is not showing a significant difference.

Compared to the previous bridge model, the model under study in this chapter failed early which can be explained by the higher overall mass of the bridge in this case compared to the previous.

In this case of a very strong motion, the concept of Rocking Isolation proves yet again its advantages, while the conventionally designed model failed, the rocking isolated one sustains the motions while compensating in higher soil plastification and residual drift.

Figure 19 Shows the results of the dynamic excitation of the Rocking models, the comparison in terms of the deck acceleration is showing a slight variation; as the "Full Model" is showing higher vibration.

The lumped-mass model is showing a slight increase in foundation rotation and deck displacement compared to the Full Model.

Figure 19e shows the displacement components of the deck displacement, as in the case of Rocking Isolation design the Foundation rotation the main contributor to the total drift.

Figure 19h shows the deck rotation in both cases of conventional design and rocking isolation where the first failed while the rocking model survived the strong motion.

Chapter 6

Figures

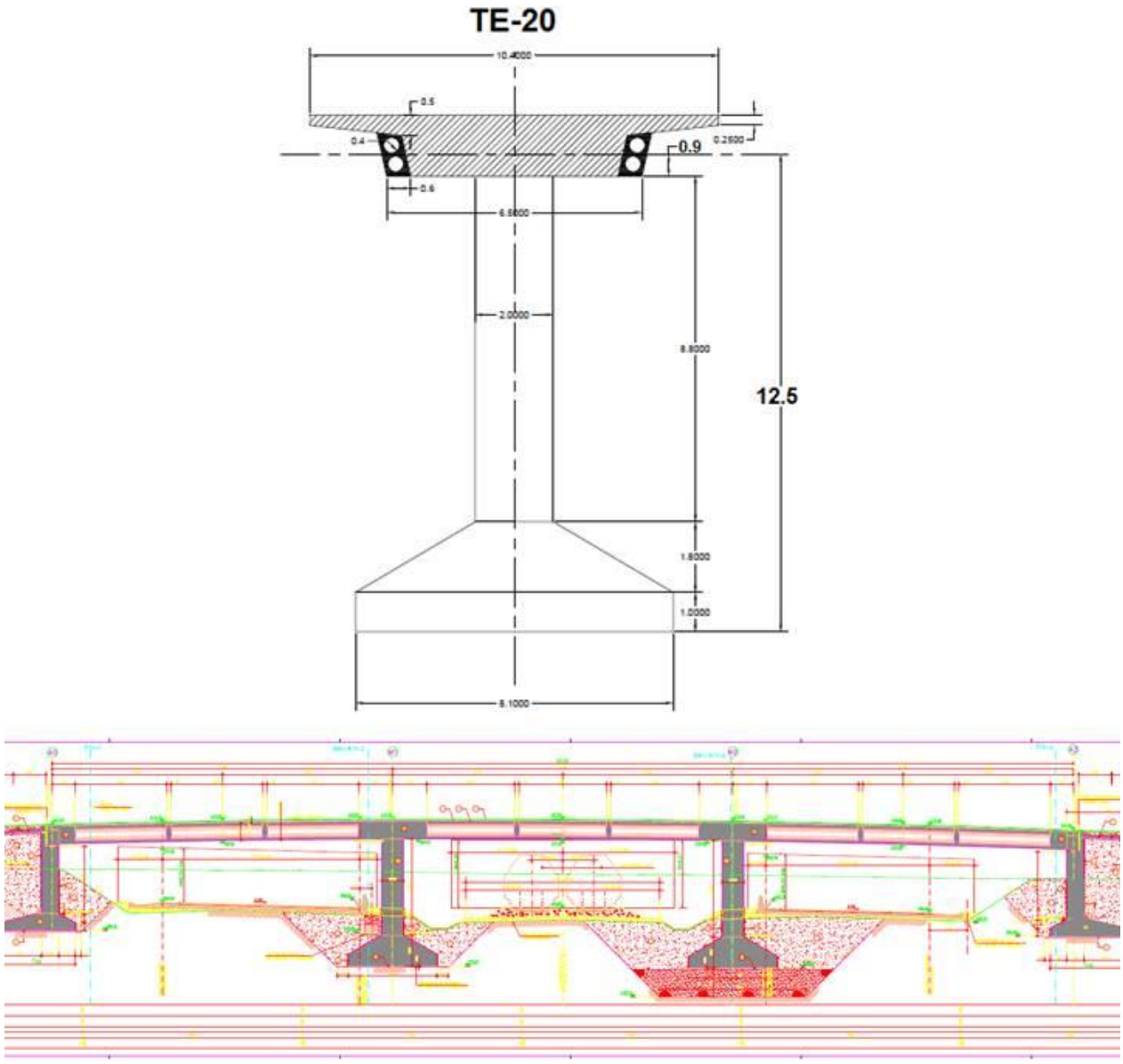

Figure 6.1 Bridge Model "TE-23 "Overall Dimensions.

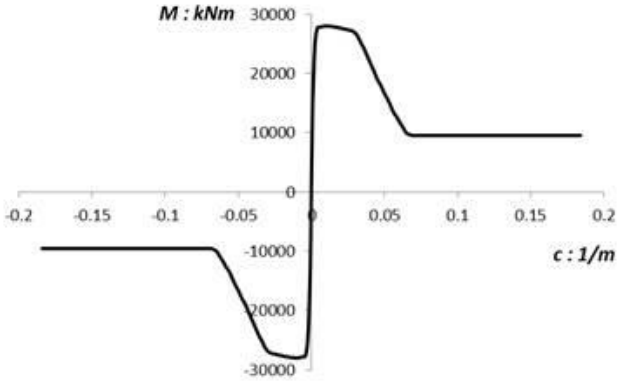

Figure 6.2 Pier Column inelastic behavior: Moment - Curvature.

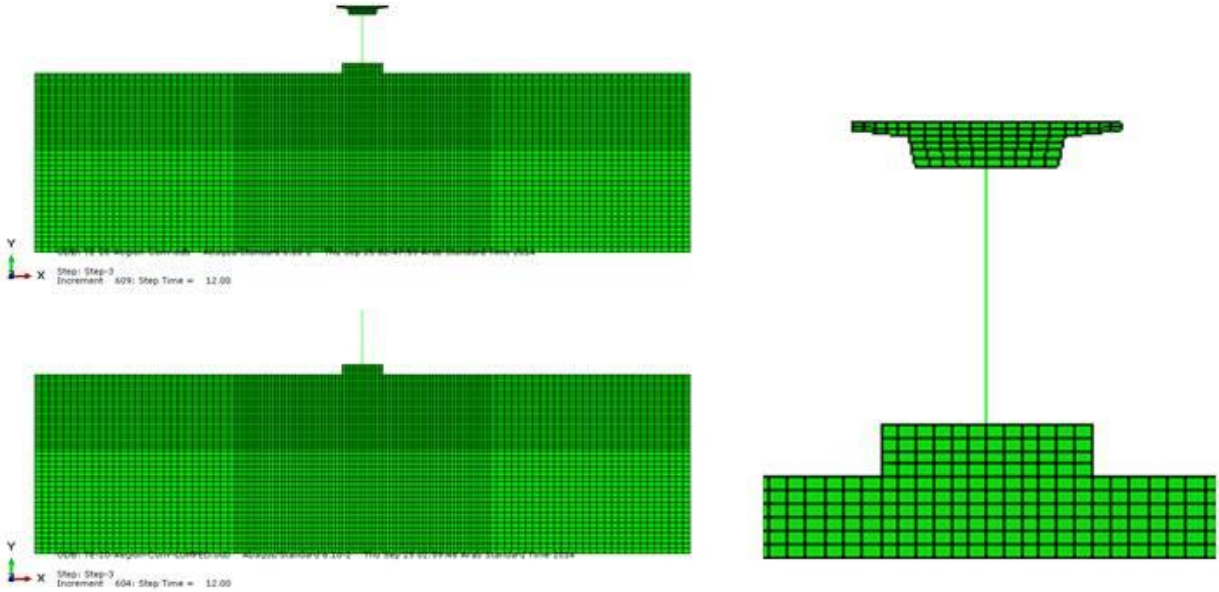

Figure 6.3 a) Conventional Design Models and deck geometry.

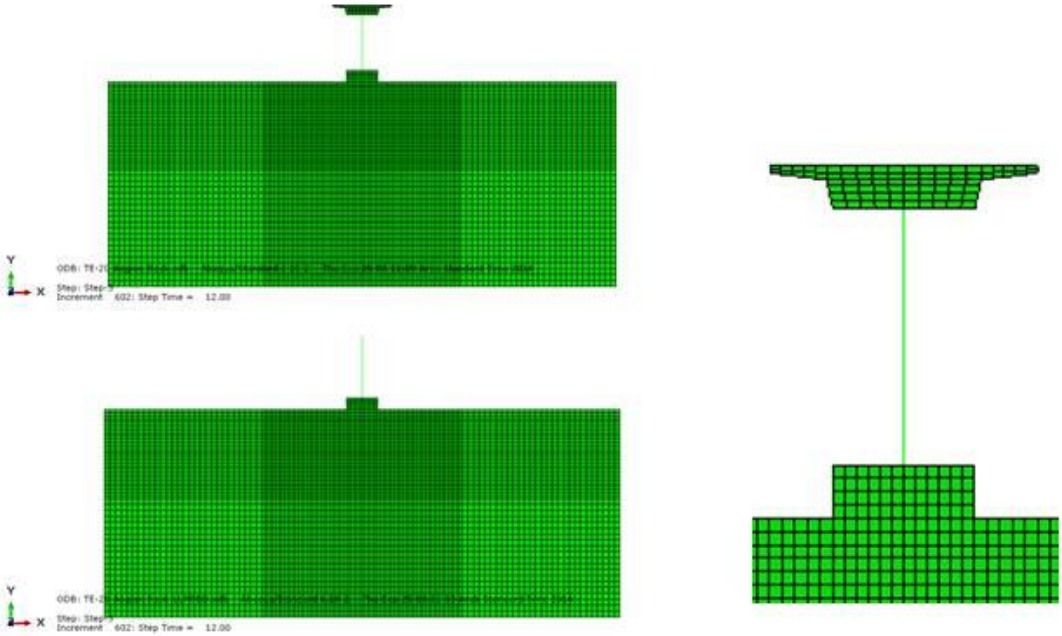

Figure 6.3 b) Rocking Isolation design Models and deck geometry.

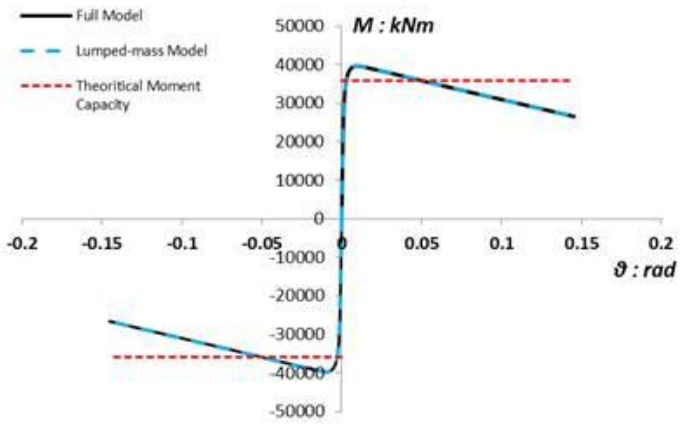

a) Conventional design Models.

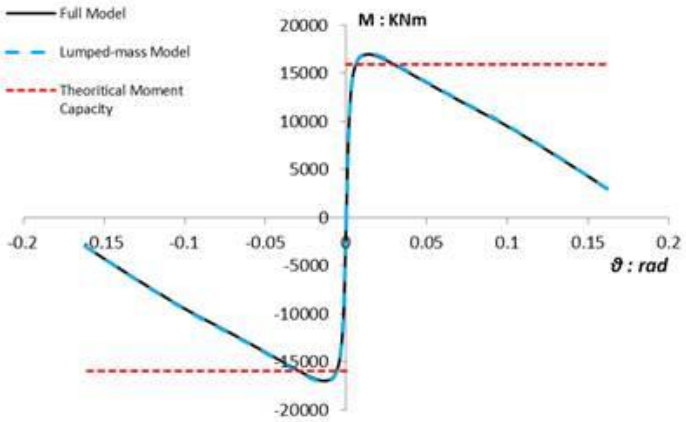

b) Rocking Isolation Models.

Figure 6.4 Push-over Result: Moment rotation and comparison with theoretical flexural capacity.

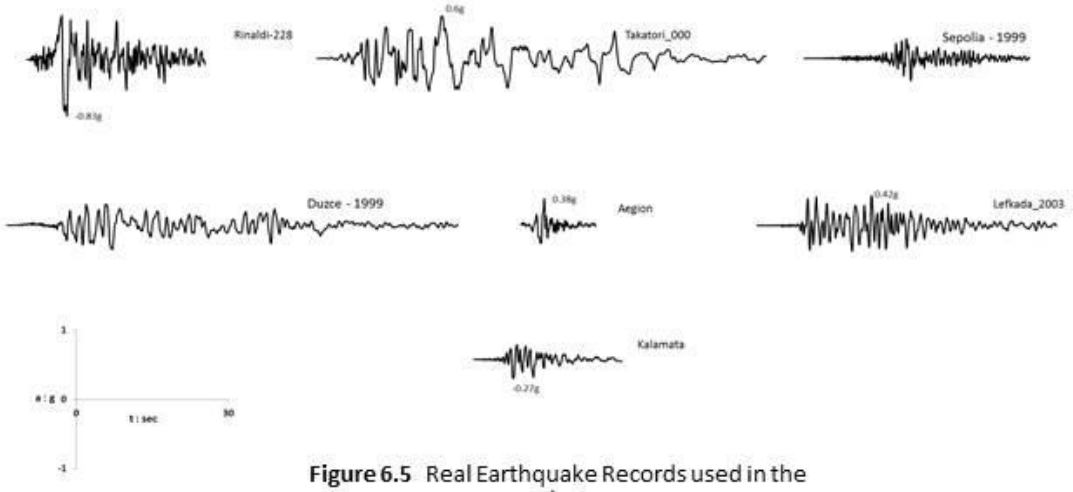

Figure 6.5 Real Earthquake Records used in the analysis.

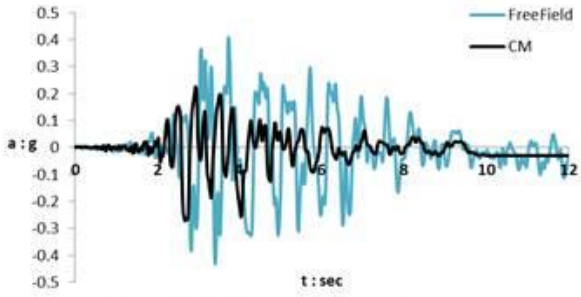

a) "Freefield" & "Center of mass" Acceleration-Time.

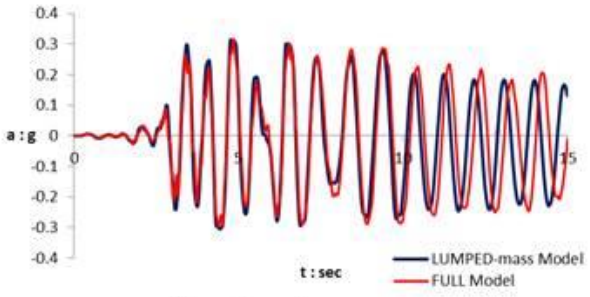

b) Deck Acceleration - Time.

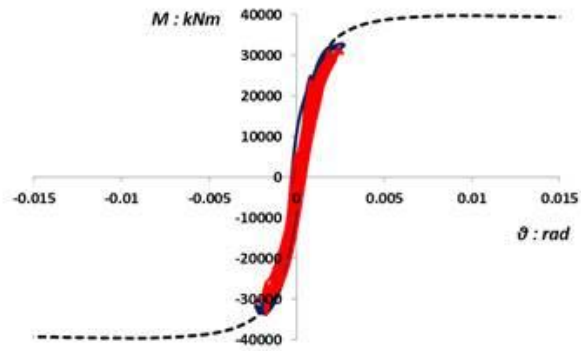

c) Moment – Foundation Rotation.

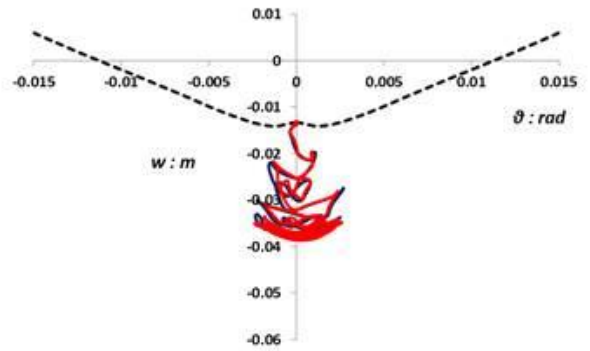

d) Settlement – Foundation Rotation.

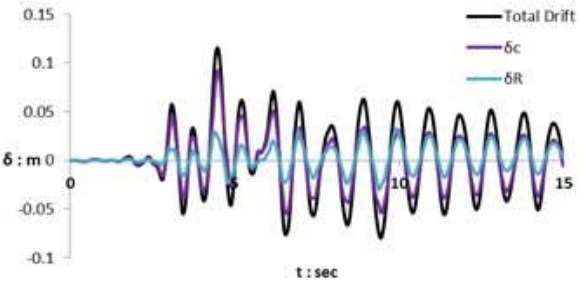

e) Displacement Components of the system.

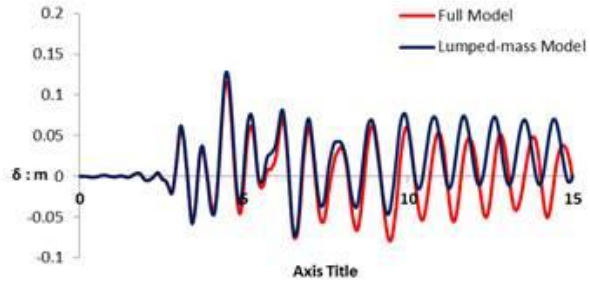

f) Deck Displacement - Time.

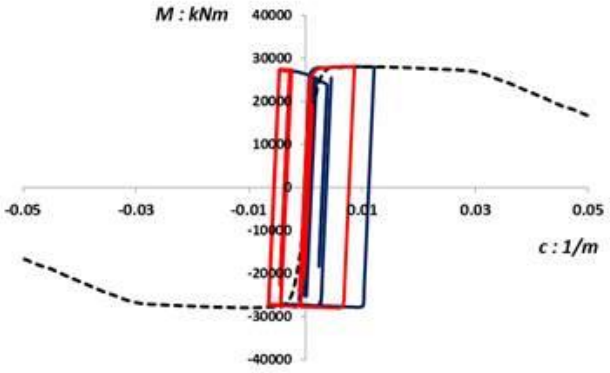

g) Pier Section Flexural Moment - Curvature.

Figure 6.6 Dynamic Results of the Conventionally designed models subjected to Kalamata EQ.

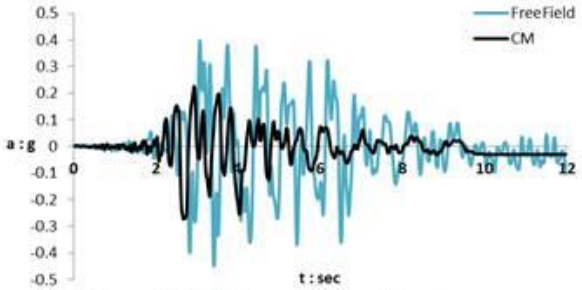

a) "Freefield" & "Center of mass" Acceleration-Time.

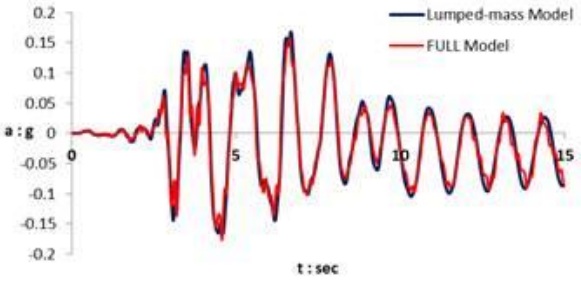

b) Deck Acceleration - Time.

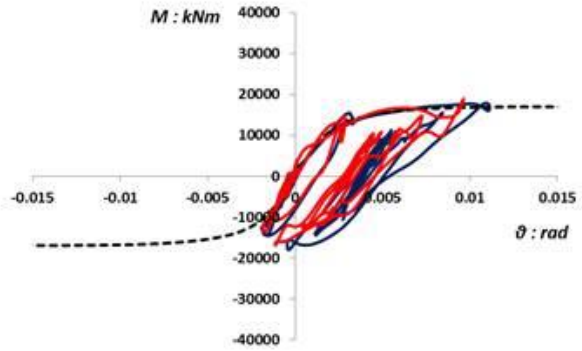

c) Moment – Foundation Rotation.

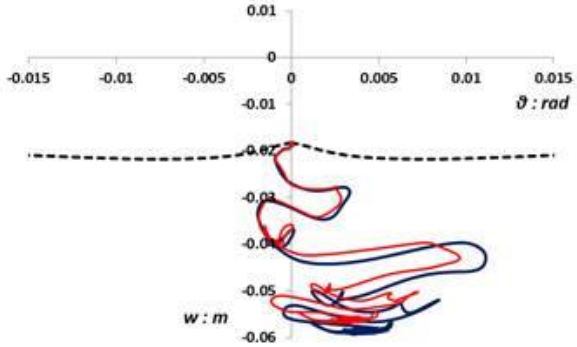

d) Settlement – Foundation Rotation.

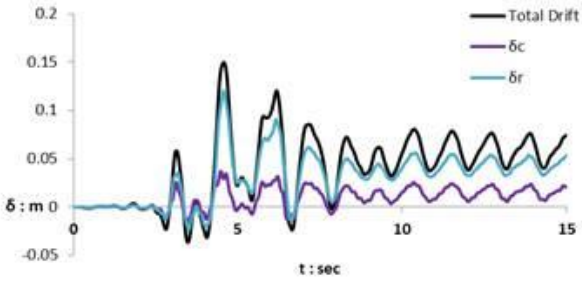

e) Displacement Components of the system.

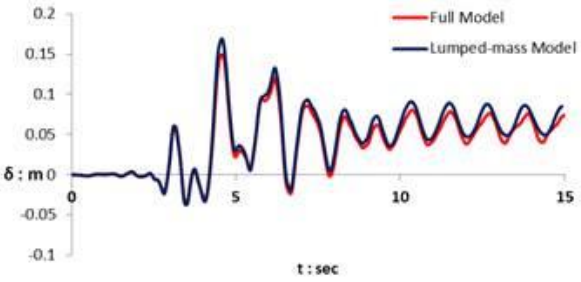

f) Deck Displacement - Time.

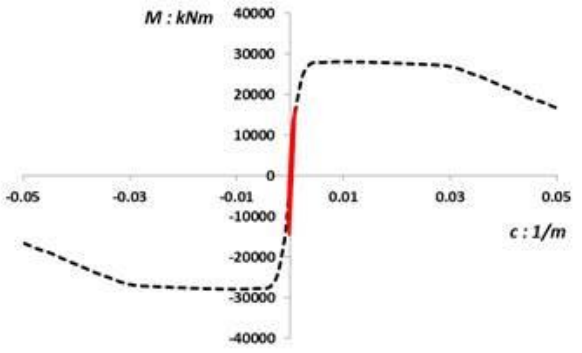

g) Pier Section Flexural Moment - Curvature.

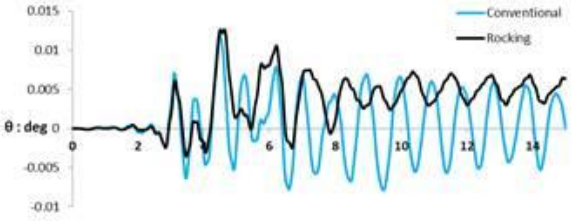

h) Deck Rotation of the "Full Models - time.

Figure 6.7 Dynamic Results of the Rocking Isolation designed models subjected to Kalamata EQ.

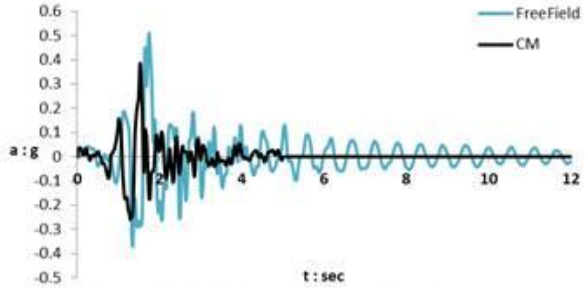

a) "Freefield" & "Center of mass" Acceleration-Time.

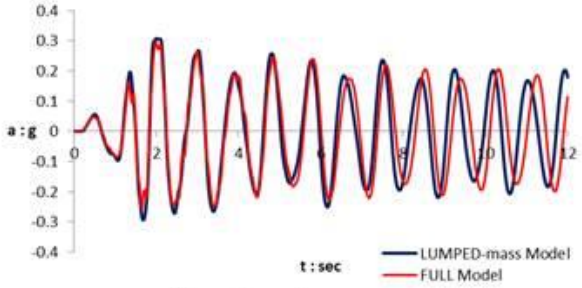

b) Deck Acceleration - Time.

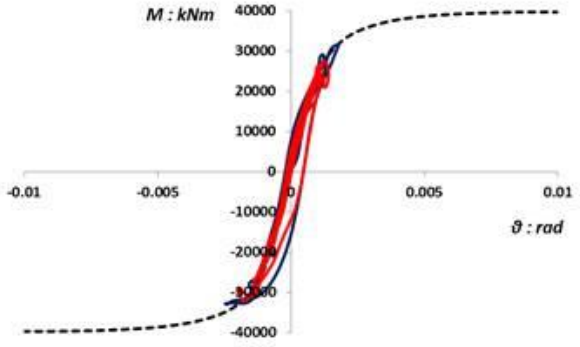

c) Moment – Foundation Rotation.

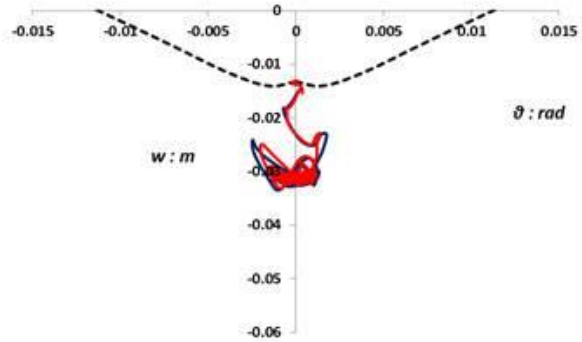

d) Settlement – Foundation Rotation.

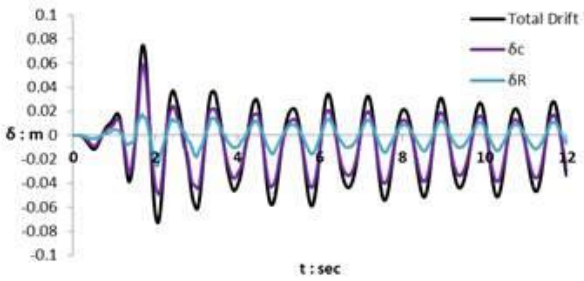

e) Displacement Components of the system.

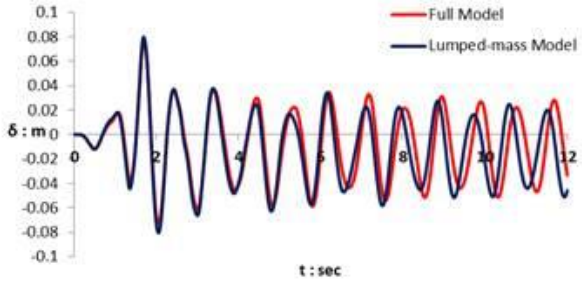

f) Deck Displacement - Time.

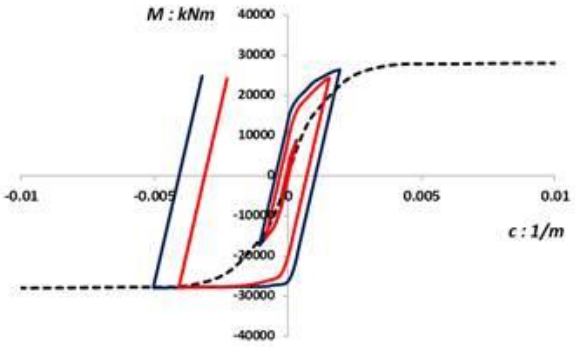

g) Pier Section Flexural Moment - Curvature.

Figure 6.8 Dynamic Results of the Conventionally designed models subjected to Ageion EQ.

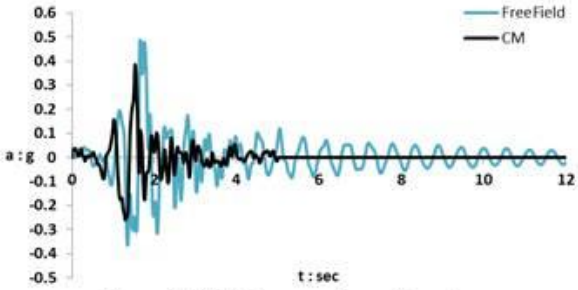

a) "Freefield" & "Center of mass" Acceleration-Time.

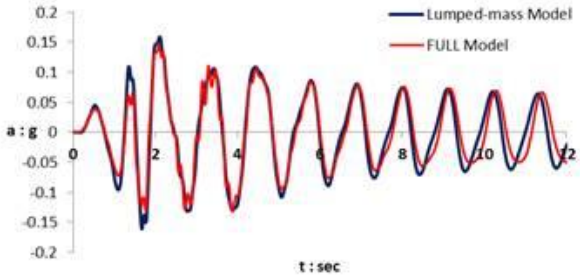

b) Deck Acceleration - Time.

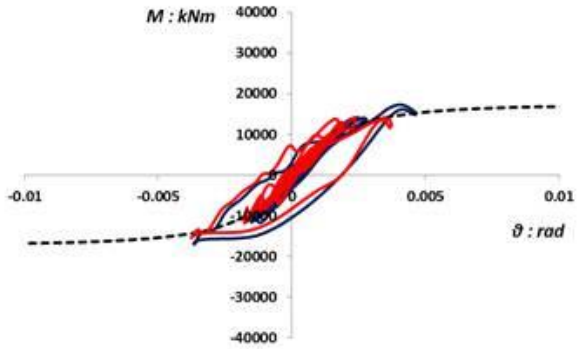

c) Moment – Foundation Rotation.

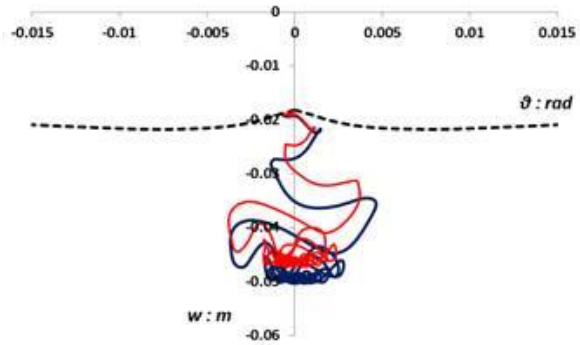

d) Settlement – Foundation Rotation.

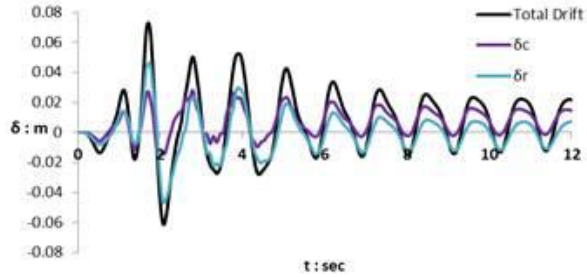

e) Displacement Components of the system.

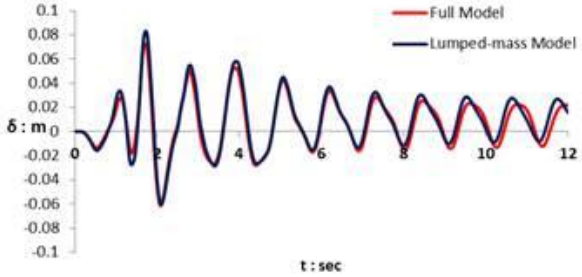

f) Deck Displacement - Time.

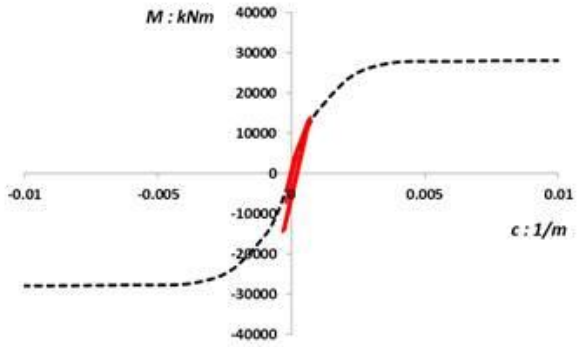

g) Pier Section Flexural Moment - Curvature.

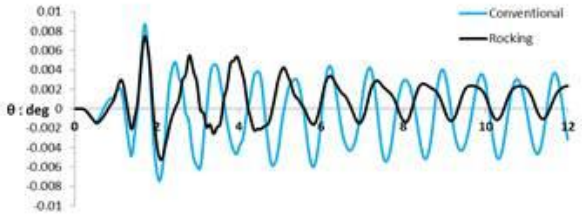

h) Deck Rotation of the "Full Models - time.

Figure 6.9 Dynamic Results of the Rocking Isolation designed models subjected to Aegion EQ.

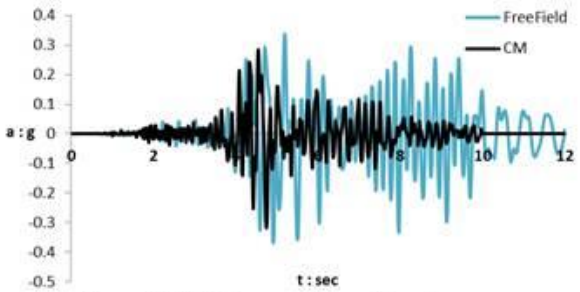

a) "Freefield" & "Center of mass" Acceleration-Time.

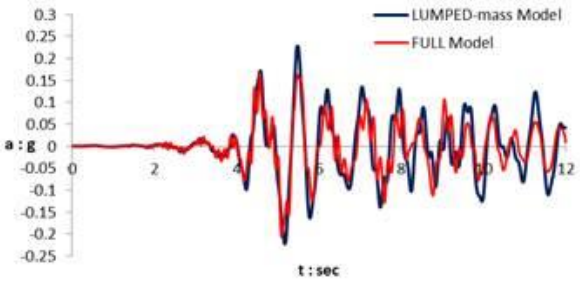

b) Deck Acceleration - Time.

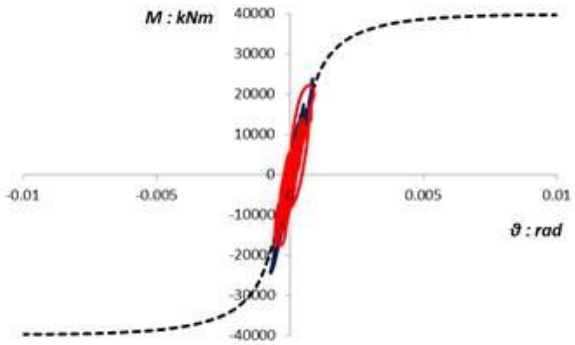

c) Moment – Foundation Rotation.

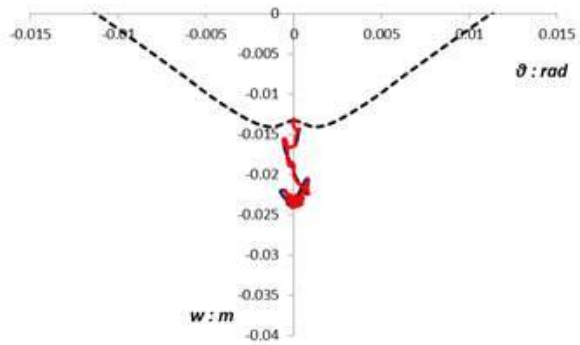

d) Settlement – Foundation Rotation.

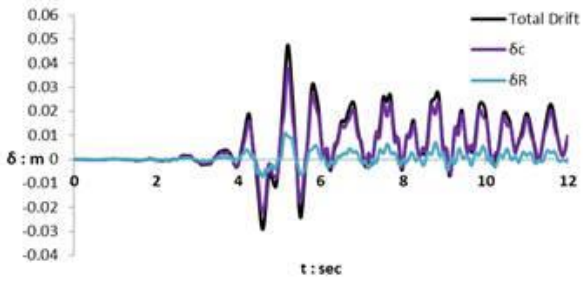

e) Displacement Components of the system.

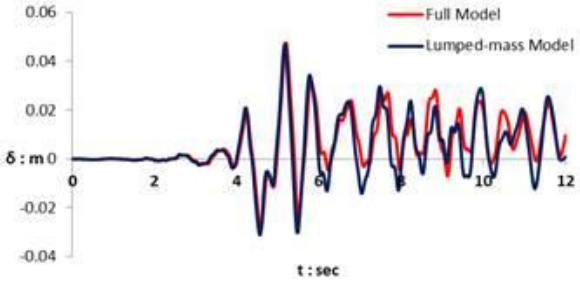

f) Deck Displacement - Time.

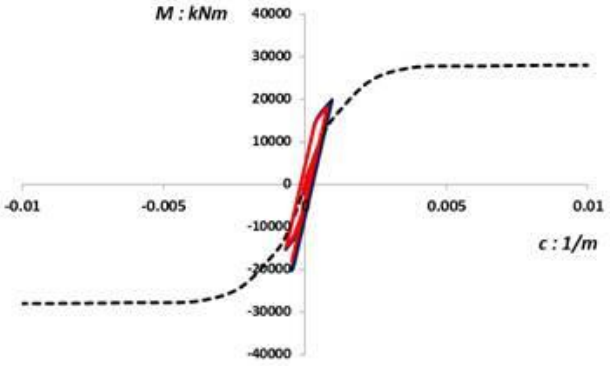

g) Pier Section Flexural Moment - Curvature.

Figure 6.10 Dynamic Results of the Conventionally designed models subjected to Sepolia EQ.

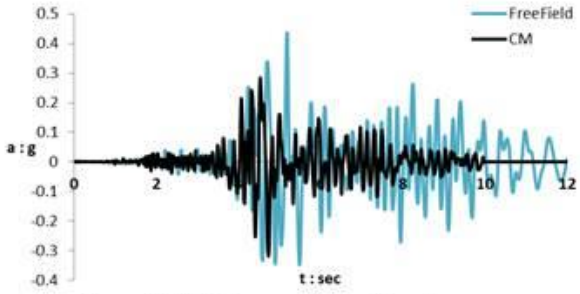

a) "Freefield" & "Center of mass" Acceleration-Time.

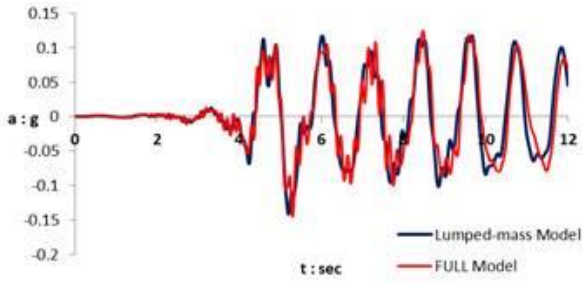

b) Deck Acceleration - Time.

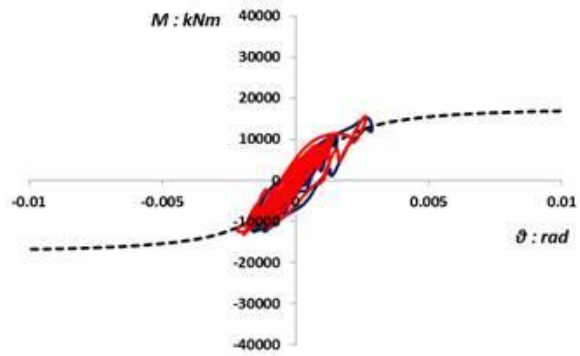

c) Moment – Foundation Rotation.

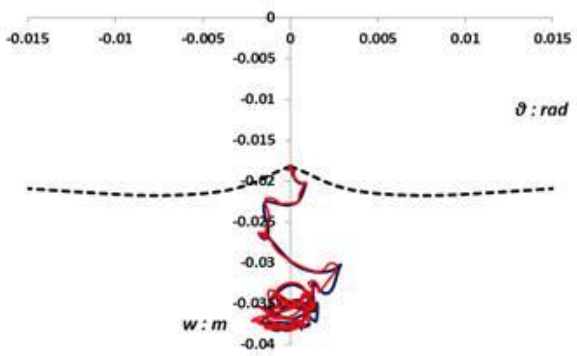

d) Settlement – Foundation Rotation.

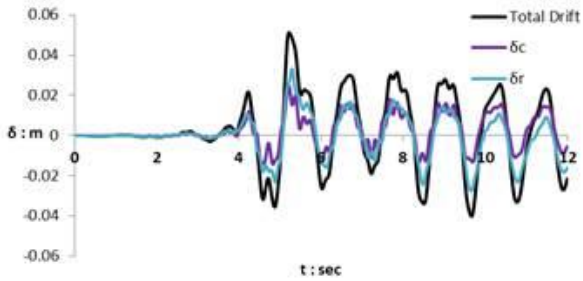

e) Displacement Components of the system.

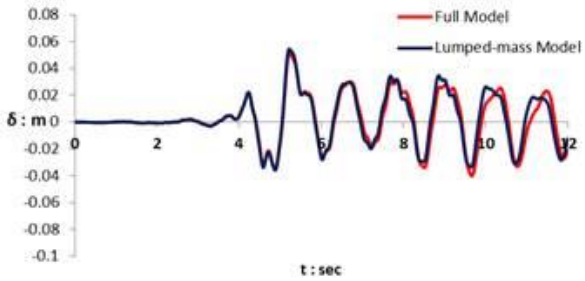

f) Deck Displacement - Time.

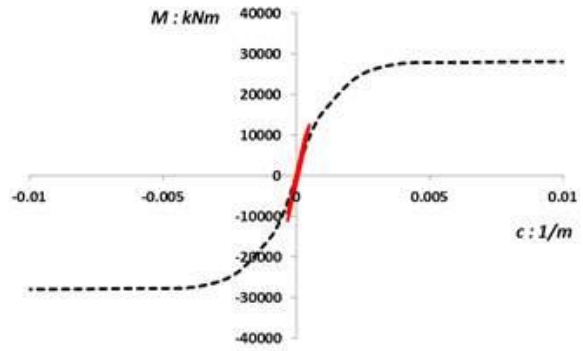

g) Pier Section Flexural Moment - Curvature.

h) Deck Rotation of the "Full Models - time.

Figure 6.11 Dynamic Results of the Rocking Isolation designed models subjected to Sepolia EQ.

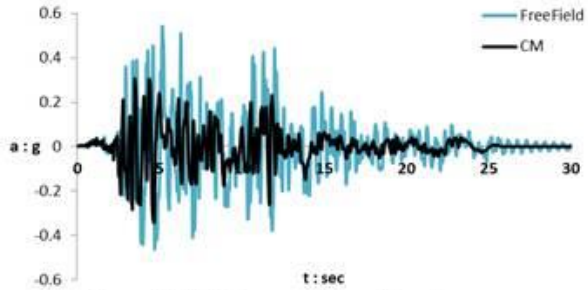

a) "Freefield" & "Center of mass" Acceleration-Time.

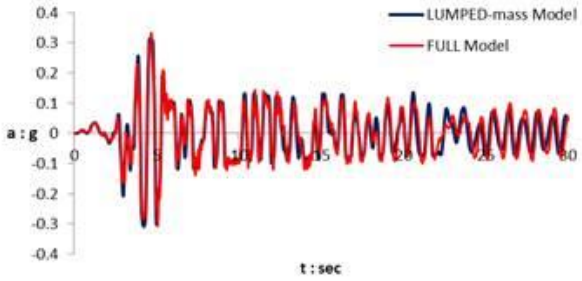

b) Deck Acceleration - Time.

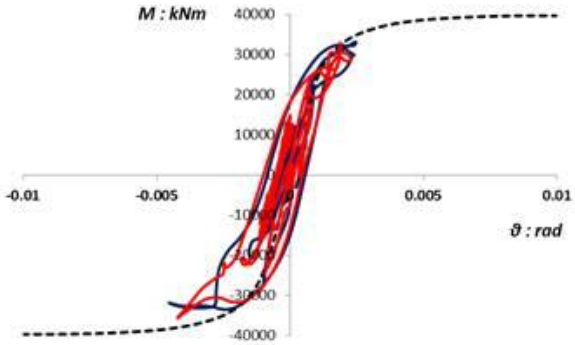

c) Moment – Foundation Rotation.

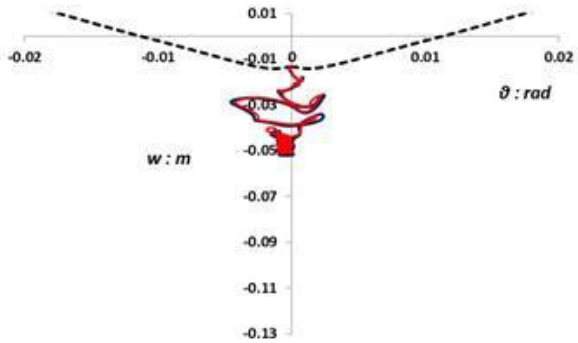

d) Settlement – Foundation Rotation.

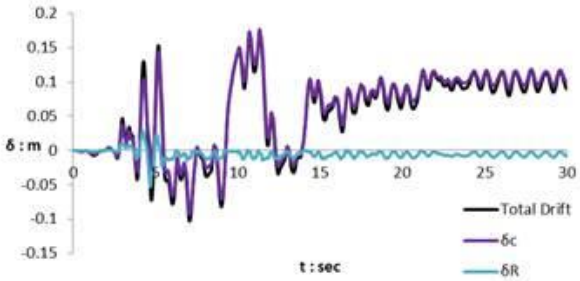

e) Displacement Components of the system.

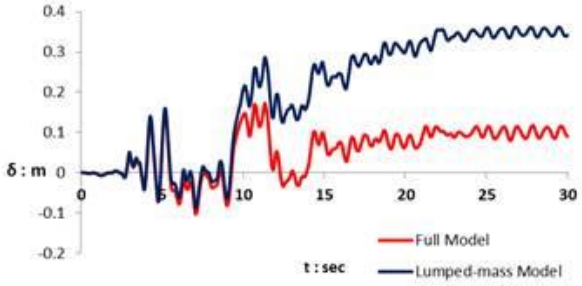

f) Deck Displacement - Time.

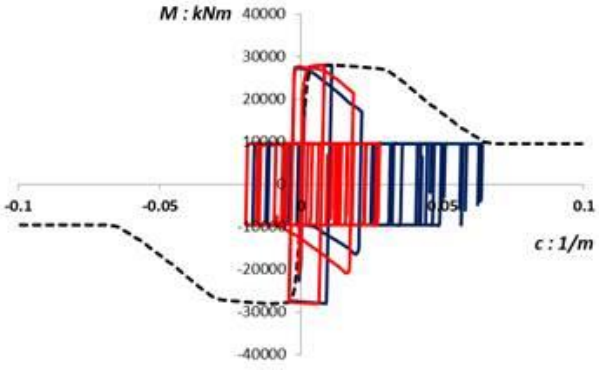

g) Pier Section Flexural Moment - Curvature.

Figure 6.12 Dynamic Results of the Conventionally designed models subjected to Duzce EQ.

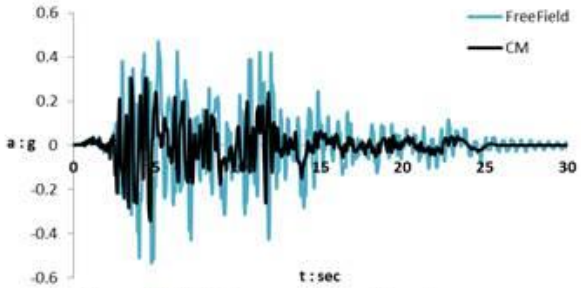

a) "Freefield" & "Center of mass" Acceleration-Time.

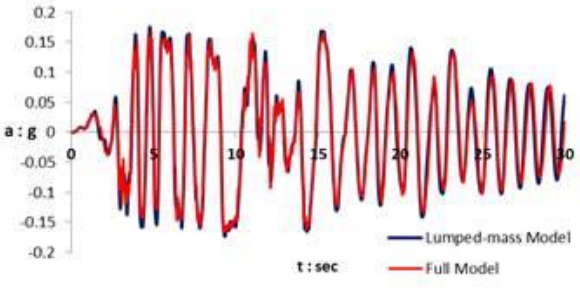

b) Deck Acceleration - Time.

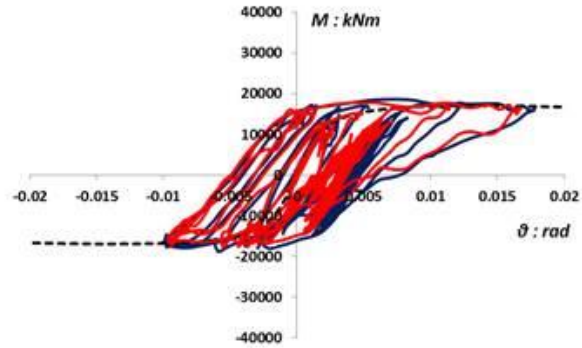

c) Moment – Foundation Rotation.

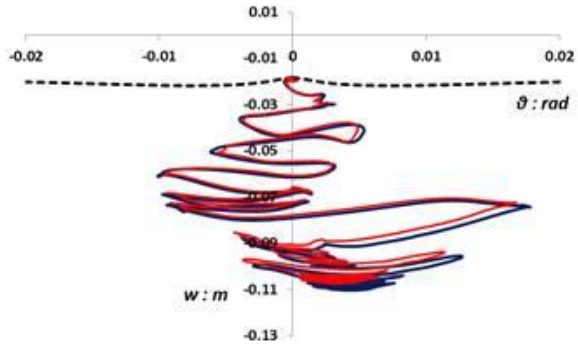

d) Settlement – Foundation Rotation.

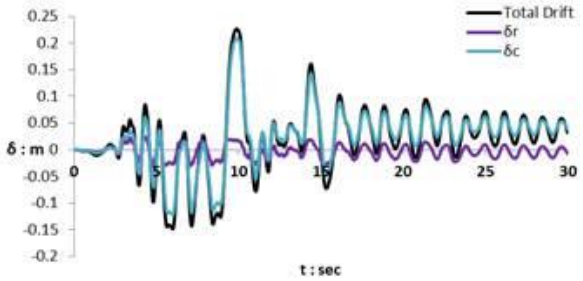

e) Displacement Components of the system.

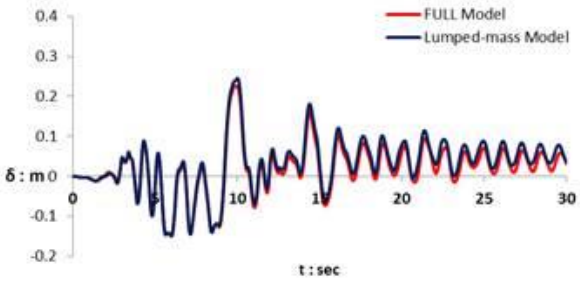

f) Deck Displacement - Time.

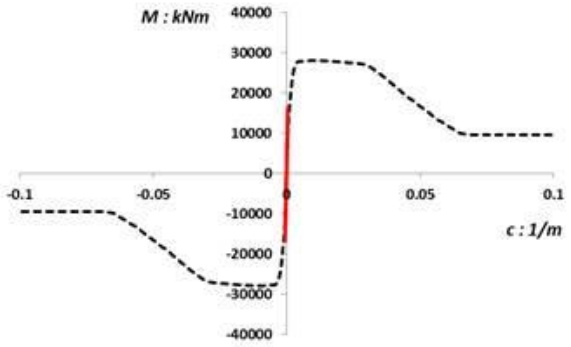

g) Pier Section Flexural Moment - Curvature.

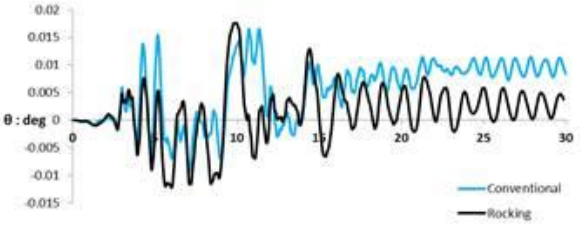

h) Deck Rotation of the "Full Models - time.

Figure 6.13 Dynamic Results of the Rocking Isolation designed models subjected to Duzce EQ.

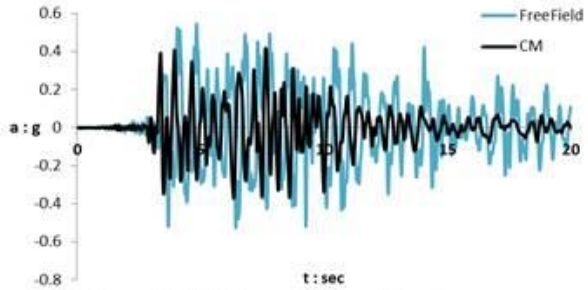

a) "Freefield" & "Center of mass" Acceleration-Time.

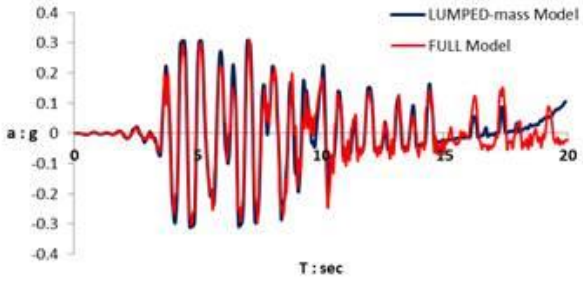

b) Deck Acceleration - Time.

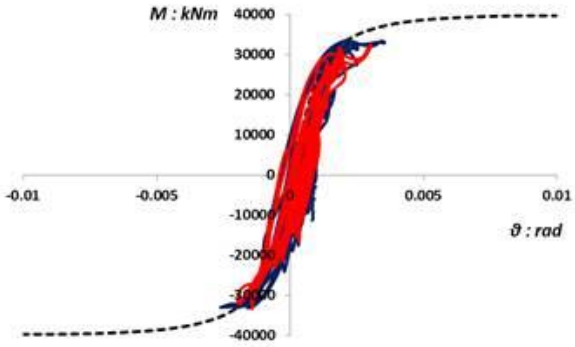

c) Moment – Foundation Rotation.

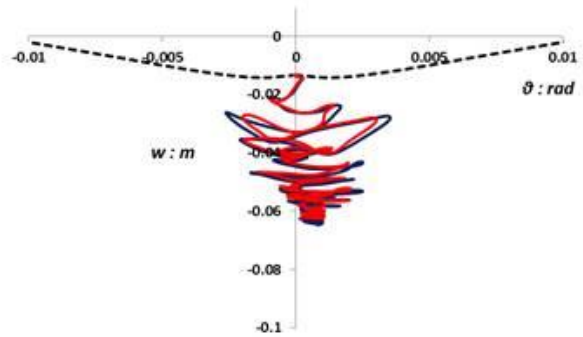

d) Settlement – Foundation Rotation.

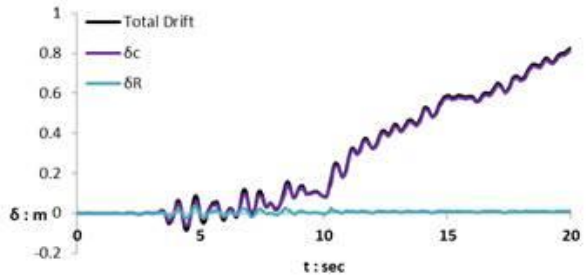

e) Displacement Components of the system.

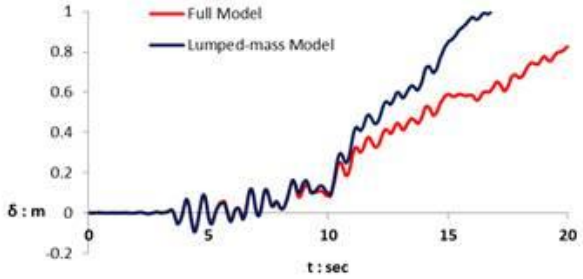

f) Deck Displacement - Time.

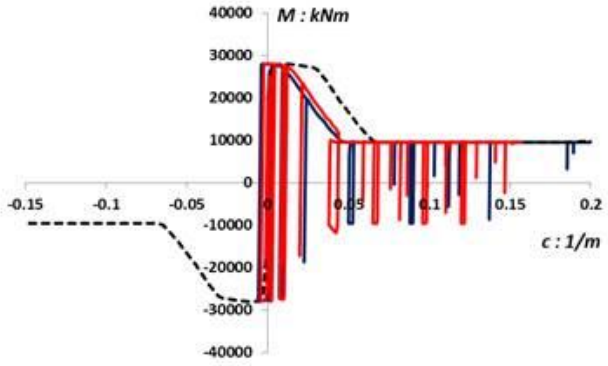

g) Pier Section Flexural Moment - Curvature.

Figure 6.14 Dynamic Results of the Conventionally designed models subjected to Lefkada EQ.

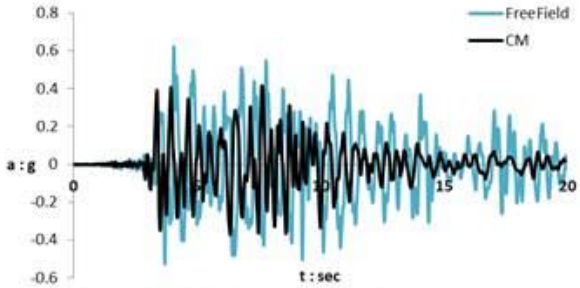

a) "Freefield" & "Center of mass" Acceleration-Time.

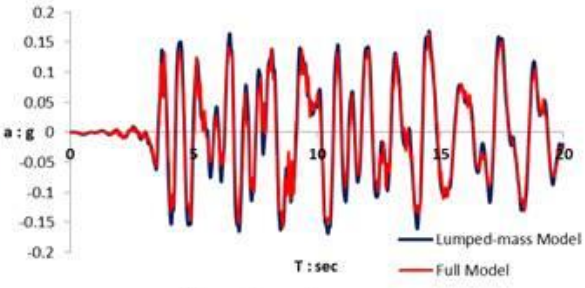

b) Deck Acceleration - Time.

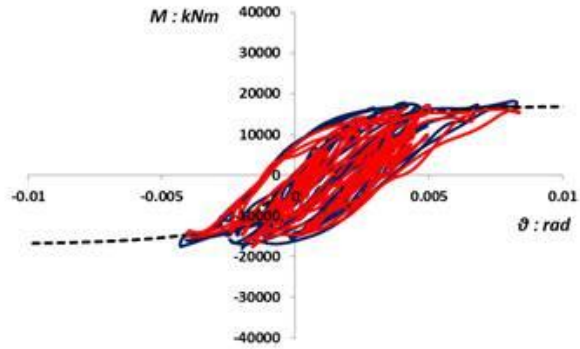

c) Moment – Foundation Rotation.

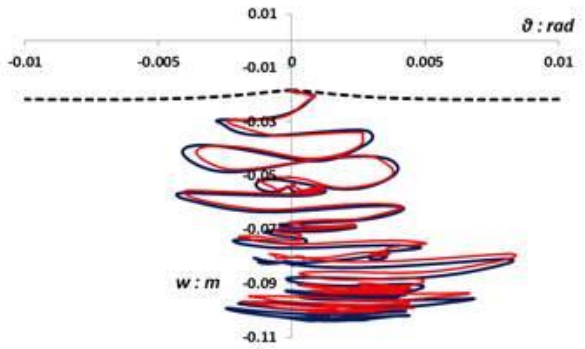

d) Settlement – Foundation Rotation.

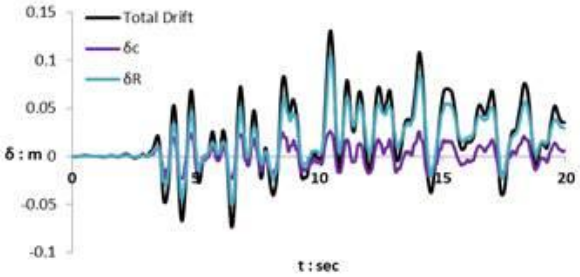

e) Displacement Components of the system.

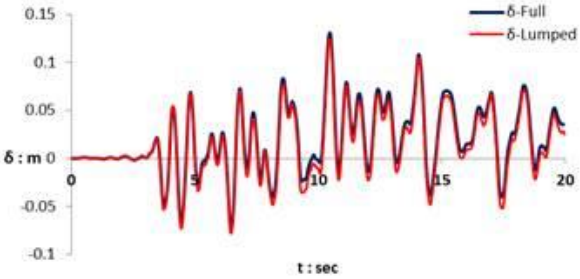

f) Deck Displacement - Time.

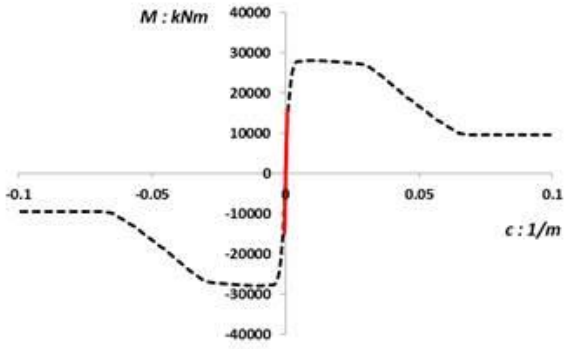

g) Pier Section Flexural Moment - Curvature.

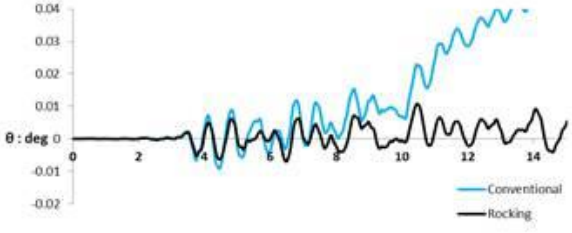

h) Deck Rotation of the "Full Models - time.

Figure 6.15 Dynamic Results of the Rocking Isolation designed models subjected to Lefkada EQ.

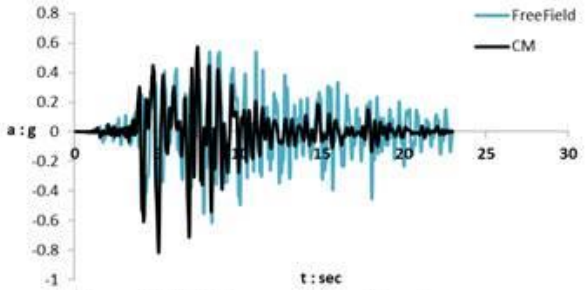

a) "Freefield" & "Center of mass" Acceleration-Time.

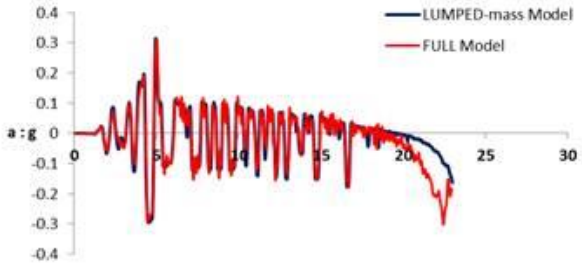

b) Deck Acceleration - Time.

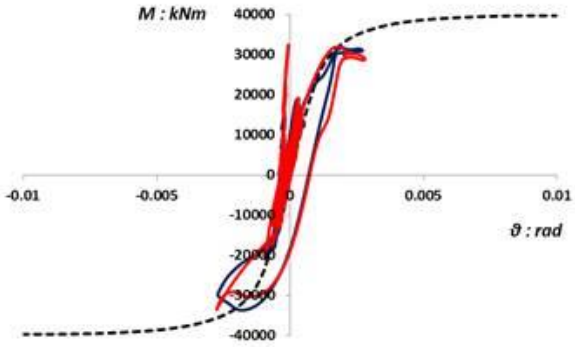

c) Moment – Foundation Rotation.

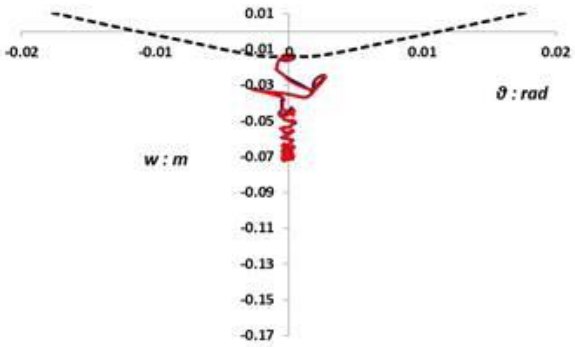

d) Settlement – Foundation Rotation.

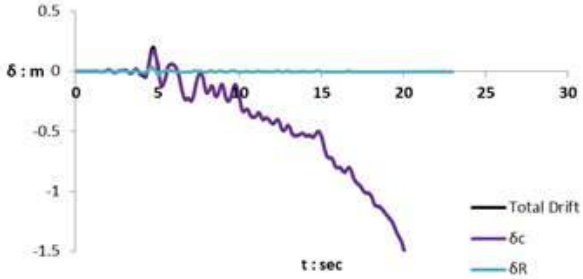

e) Displacement Components of the system.

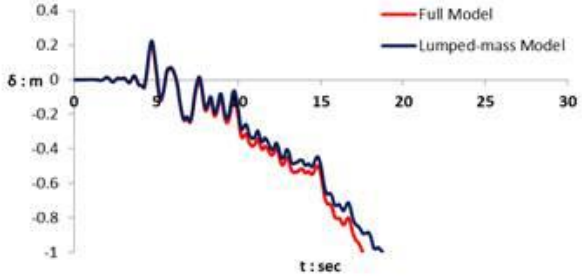

f) Deck Displacement - Time.

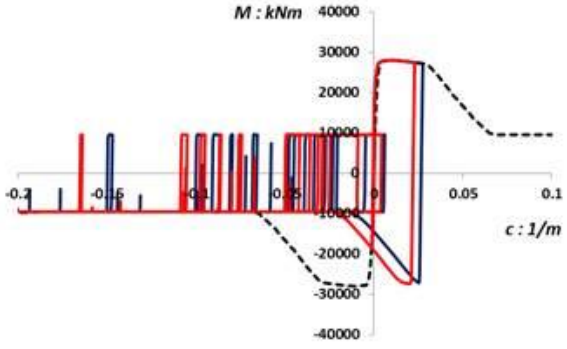

g) Pier Section Flexural Moment - Curvature.

Figure 6.16 Dynamic Results of the Conventionally designed models subjected to Kobe JMA-000 EQ.

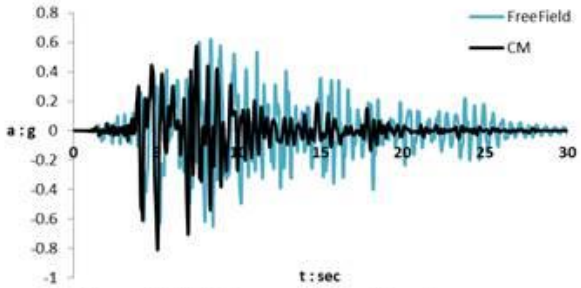

a) "Freefield" & "Center of mass" Acceleration-Time.

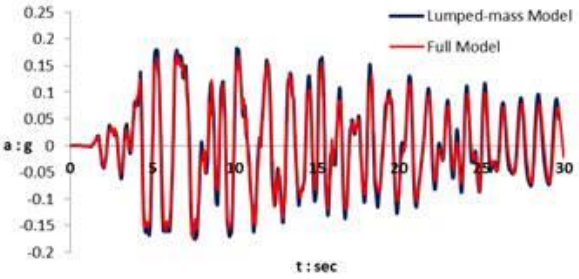

b) Deck Acceleration - Time.

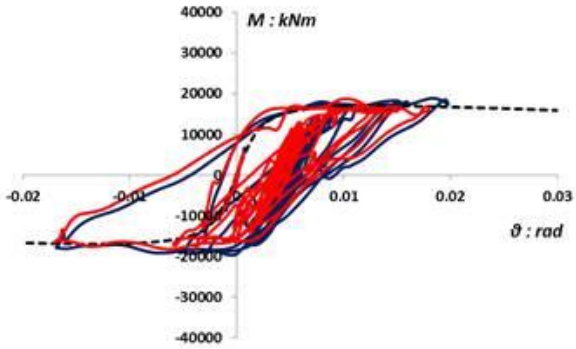

c) Moment – Foundation Rotation.

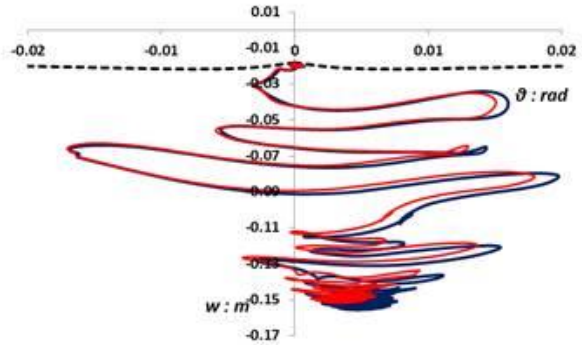

d) Settlement – Foundation Rotation.

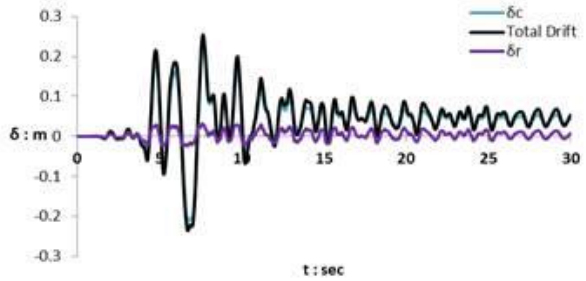

e) Displacement Components of the system.

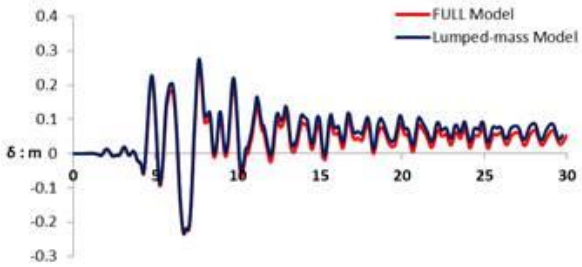

f) Deck Displacement - Time.

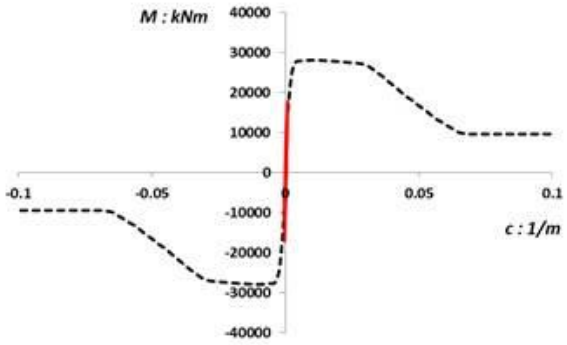

g) Pier Section Flexural Moment - Curvature.

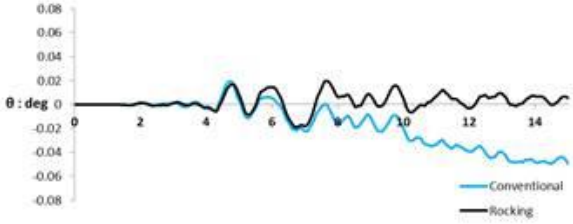

h) Deck Rotation of the "Full Models - time.

Figure 6.17 Dynamic Results of the Rocking Isolation designed models subjected to Kobe JMA-000 EQ.

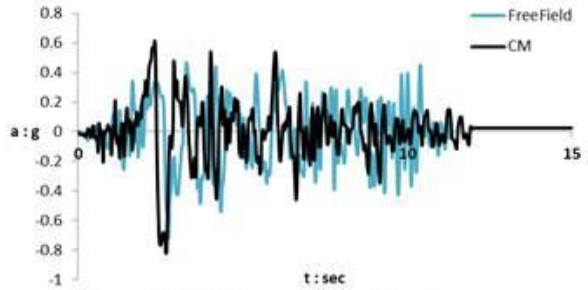

a) "Freefield" & "Center of mass" Acceleration-Time.

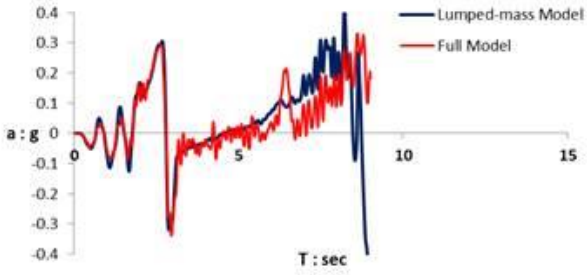

b) Deck Acceleration - Time.

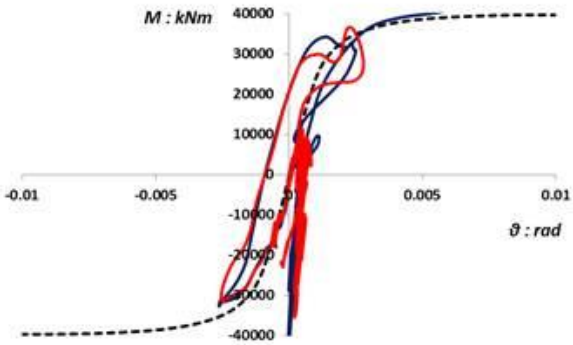

c) Moment – Foundation Rotation.

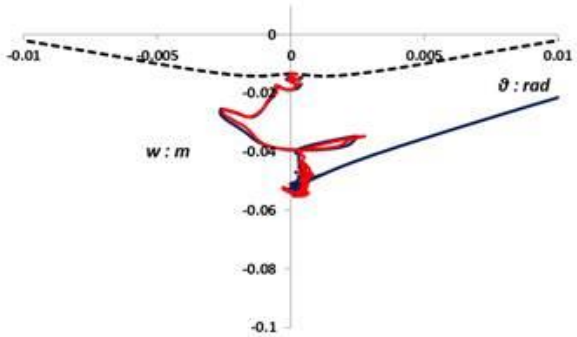

d) Settlement – Foundation Rotation.

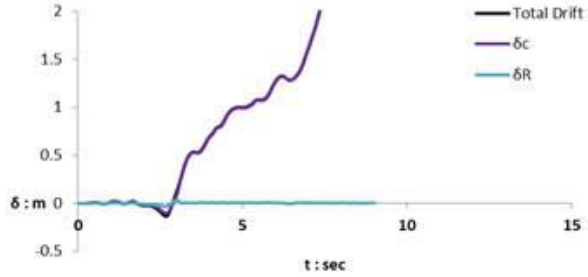

e) Displacement Components of the system.

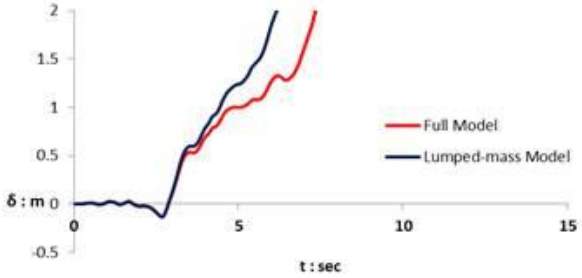

f) Deck Displacement - Time.

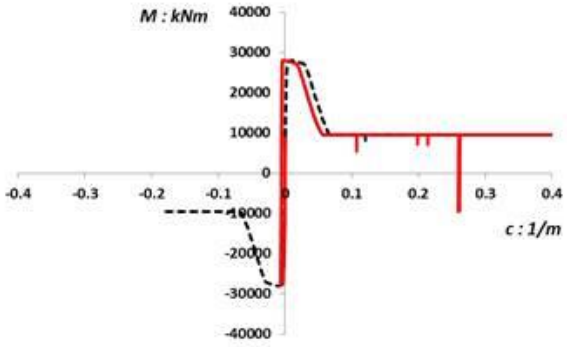

g) Pier Section Flexural Moment - Curvature.

Figure 6.18 Dynamic Results of the Conventionally designed models subjected to Northridge Rinaldi EQ.

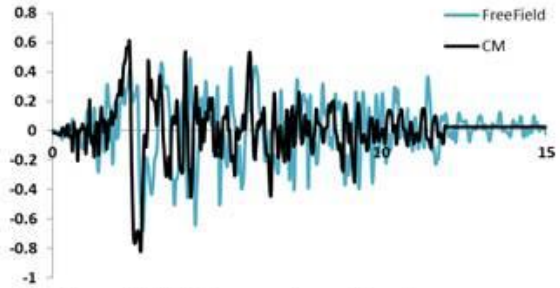

a) "Freefield" & "Center of mass" Acceleration-Time.

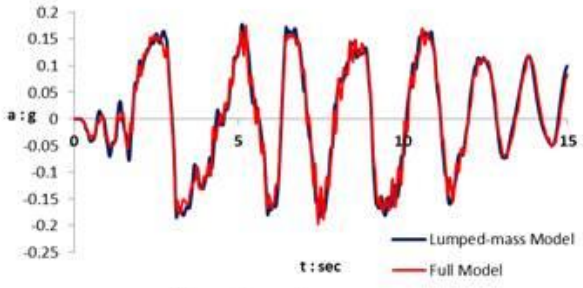

b) Deck Acceleration - Time.

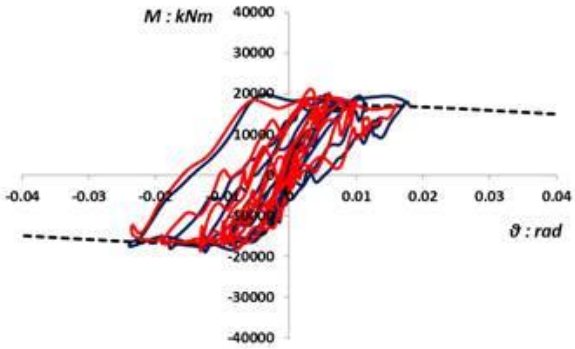

c) Moment – Foundation Rotation.

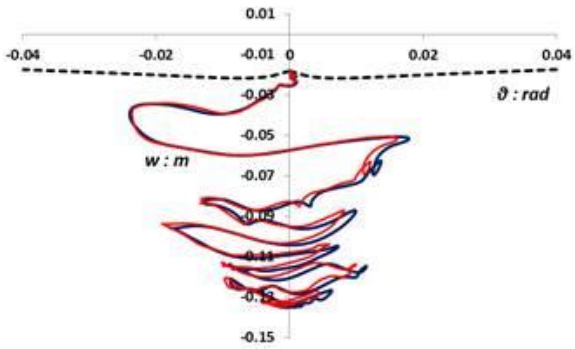

d) Settlement – Foundation Rotation.

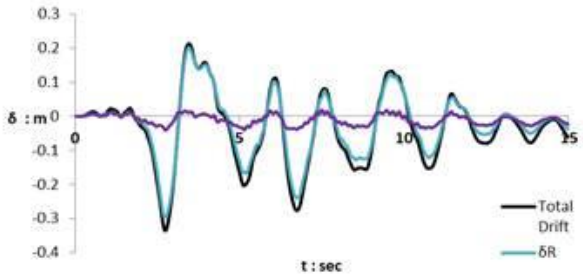

e) Displacement Components of the system.

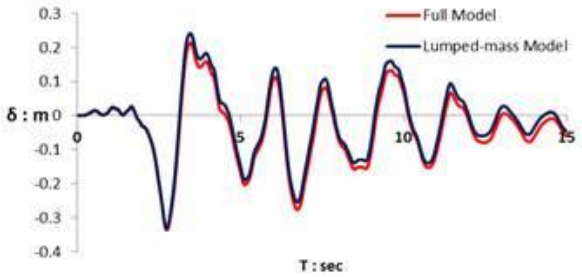

f) Deck Displacement - Time.

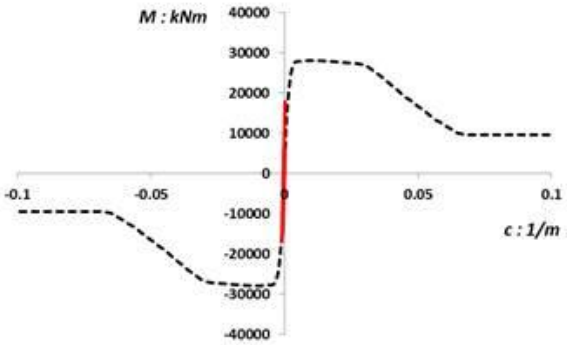

g) Pier Section Flexural Moment - Curvature.

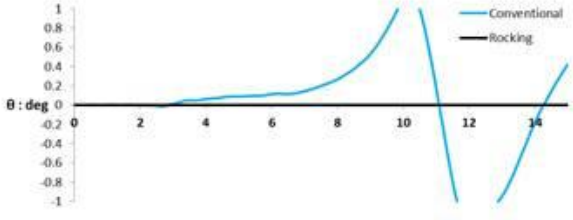

h) Deck Rotation of the "Full Models - time.

Figure 6.19 Dynamic Results of the Rocking Isolation designed models subjected to Northridge Rinaldi EQ.

Conclusions

The key objective of the present thesis can be summarized in the following points:

- Evaluating the effect of the rotational inertia of Highway Bridge's deck on the overall seismic response of the system.
- Determining whether this effect diminish the advantages of the "Rocking Isolation" concept of redirecting the plastic deformation to the soil-foundation interface to retain the overall system from collapse.

During this study, first by examining a simplified bridge model (Model-A) in chapters (3, 4):

- Modeling the deck geometry resulted in higher damping properties in the dynamic response.
- However the results were inconsistent, the models with lumped-masses in most cases resulted with higher foundation rotation, settlement and deck displacement.

By further studying the problem on a more realistic bridge models and deck geometries, and excluding the damping properties of the deck elements (Chapters' 5, 6):

- The difference in response comparing the Models with the deck geometry and the lumped mass becomes minimal in terms of deck acceleration, foundation rotation and deck displacement.
- Most importantly it can be concluded that taking into consideration the rotational inertia of the bridge deck doesn't take away the advantages of the "Rocking Isolation" design concept, where it continues to prove it's advantages compared to the conventional design concept in protecting the structures against strong and severe excitations.

References

1. EC8. Design provisions for earthquake resistance of structures. Part5: foundations, retaining structures and geotechnical aspects. Brussels: EN, 1998–5, European Committee for Standardization; 2008.
2. Yim S.C., Chopra A.K. (1985).”Simplified earthquake analysis structures with foundation uplift” *Journal of Structural Engineering*, ASCE,
3. Apostolou M., Gazetas G., Grini E. (2007). "Seismic response of slender rigid structures with foundation uplift" *Soil Dynamics and Earthquake Engineering*.
4. Drosos V., Georgarakos P., Loli M., Zarzouras O., Anastasopoulos I., Gazetas G. (2012). “Soil–Foundation–Structure Interaction with Mobilization of Bearing Capacity: An Experimental Study,” Journal of Geotechnical and Geoenvironmental Engineering, ASCE, Vol. 138(11).
5. Anastasopoulos I., Gazetas G., Loli M., Apostolou M., Gerolymos N. (2010). “Soil failure can be used for seismic protection of structures,” Bulletin of Earthquake Engineering.
6. Hung H., Liu K., Ho T., and Chang K. (2011). “An experimental study on the rocking response of bridge piers with spread footing foundations,” Earthquake Engineering & Structural Dynamics,
7. Anastasopoulos I., Loli M., Georgarakos T., and Drosos V. (2013b), “Shaking Table Testing of Rocking−isolated Bridge Pier on Sand,” Journal of Earthquake Engineering,
8. Anastasopoulos I., Gelagoti F., Kourkoulis R., Gazetas G. (2011). “Simplified Constitutive model for Simulation of Cyclic Response of Shallow Foundations: Validation against Laboratory Tests,” Journal of Geotechnical and Geoenvironmental Engineering, ASCE, Vol. 137(12),
9. Gazetas G., Anastasopoloulos I., Garini E. (2014). “Geotechnical design with apparent seismic safety factors well-below 1” *Soil Dynamics and Earthquake Engineering.*
10. Gazetas G., Anastasopoloulos I., Adamidis O., Kontoroupi Th. (2013). “Nonlinear rocking stiffness of foundations” *Soil Dynamics and Earthquake Engineering*.

11. Loli M., Knappett J.M., Brown M.J., Anastasopoulos I., & Gazetas G. (2014).”Centrifuge Modeling of Rocking-Isolated Inelastic RC Bridge Piers”, Earthquake Engineering &Structural Dynamics, DOI : 10.1002/eqe.2451
12. Gourvenec, S. (2007).” Shape effects on the capacity of rectangular footings under general loading”. *Ge´otechnique* 57, No. 8, 637–646
13. Loli M., Anastasopoulos I., Knappett J.A., Brown M.J. (2014). “Use of Ricker wavelet ground motions as an alternative to pushover testing”. *Proc. 8th International Conference on Physical Modelling in Geotechnics*, ICPMG’14, Perth, Australia, January 14–17, 2014; 1073–1078.